Expanding substrate scope of sequence-regulating polyhydroxyalkanoate synthase for block copolymer synthesis

A Dissertation for the Degree of Doctor of Engineering

PHAN THI HIEN

Graduate School of Chemical Sciences and Engineering

Hokkaido University

September 2023

Table of content

Chapter 1.

General Introduction

1.1. Polyhydroxyalkanoates (PHAs)

Polyhydroxyalkanoates (PHAs) are biobased and biodegradable polymers as storage sources inside many bacteria under a lack of nutrition conditions and excess carbon sources.[1] PHAs share similar physical properties such as tensile strength and stiffness with plastic derived from petroleum.[2] In the attempt to finding a solution the decrease the effect of plastic on natural environment, PHAs has emerged as a potential strategy. Figure 1-1 show the general chemical structure of PHA which has which has a three-carbon main chain, zero to the nine-carbon side chain, and an asterisk denotes chiral center of the PHA-building block at asymmetric carbon that generates almost isotactic or (*R*)-PHA.

Depending on the total number of carbon atoms within a PHA monomer, PHAs are categorized into three groups short-chain-length or SCL units with 3 – 5 carbon atoms, and medium-chain-length or MCL units with 6 – 12 carbon atoms and SCL-MCL PHA has wide carbon atom range from 3 to 4 carbons.[2]

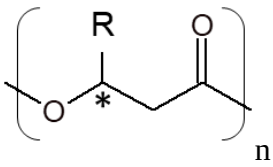

Figure 1-1. Structure of natural PHAs. R: alkyl group

A representative of the SCL-PHA category is poly(3-hydroxybutyrate) [P(3HB)] well known to be produced by *Ralstonia eutropha* bacteria and had long-term studies from other research groups.[3] Since then, much research has revolved around the issue of how to increase polymer accumulation and improve the inherent inflexibility and physical properties of this homopolymer by using specified approaches such as *in vitro* and *in vivo* as described previously. Consistent with this, studies on SCL-MCL-PHA which are

synthesized by copolymerization of different monomer units infer rational properties such as lower brittle and higher elongation were investigated.[4] Poly(3-hydroxybutyrate-*co*-3-hydroxyhexanoate) [P(3HB-*co*-3HHx)] emerged as commercial-plastic namely PHBH as a such representation.[5] Therefore, enhancing polymer production and quality of this specific material has much attention.

1.2. PHA biosynthesis

1.2.1. Polyhydroxyalkanoate synthases

PHA synthase (or PhaC) is a key enzyme in PHAs biosynthesis and it contributed to regulating the monomer constituent in polymer structure.[6] PhaC synthase is classified into four main classes based on substrate specificity and their structure in which class I, class II, class III, and class IV as shown in Table 1-1.[7] Class I PhaCs are typically capable of polymerizing SCL monomers. Class II PhaCs typically catalyze reactions of MCL-substrates.[8] On the other hand, for synthesis of copolymer SCL-MCL-PHA, class I PHA synthase from different bacteria strains, for example, *Ralstonia eutropha* showed the possibility of incorporating MCL-monomers into PHA such as 3- hydroxy hexanoate 3HHx, 3-hydroxyoctanoate 3HO, and 3-hydroxydodecanoate 3HD, as previous reports.[9, 10] Besides, some other strains showed the same ability namely *Aeromonas caviae*, *Rhodospirillum rubrum*, *Rhodocylus gelatinosus*, *Rhodococcus ruber* as reported previously.[4] These significant outcomes motivated generating modified enzymes in which the ability to incorporate MCL-units into PHA and accumulation of MCL-composition in SCL-MCL-PHA polymer has extended.

Table 1-1. Class of PHA synthase

Class	Subunits	Representative species	Substrate
I	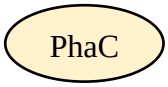 ~60 -73 kDa	*Cupriavidus necator* *Sinorhizobium melioti* *Burkholderia* sp.	$3HA_{scl}$-CoA (~C3-C5) $4HA_{scl}$-CoA, $5HA_{scl}$-CoA,
II	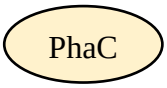 ~60 – 65 kDa	*Pseudomonas aeruginosa* *P. putida*	$3HA_{mcl}$-CoA (~ ≥C5)
III	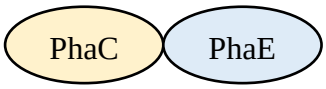	*Allochromatium vinosum* *Thiocapsa pfennigii* *Synechocystis* sp. PCC6803	$3HA_{scl}$-CoA ($3HA_{mcl}$-CoA [~C6-C8], $4HA_{scl}$-CoA, $5HA_{scl}$-CoA)
IV	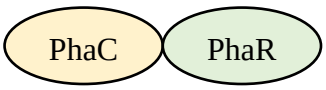 (~40 kDa) (~20 kDa)	*Bacillus megaterium* *Bacillus* sp. INT005	$3HA_{scl}$-CoA

1.2.2. General PHA biosynthesis pathway from various carbon sources

PHA can be produced by microorganisms from a number of carbon sources, including simple sugars, fatty acids found in plant oils, alkanes, and cheap, complex waste effluents like beet/cane molasses. Based on the kinds of monomers that are absorbed by PHA, it has been shown that various metabolic processes are involved in the synthesis of these monomers. There are two basic categories of bacteria that manufacture PHA, based on the monomer composition of the PHA made by various wild-type bacteria. While *R. eutropha* represents one group, the *Pseudomonads* represent the second main kind of PHA production. Figure 1-2 lists the several metabolic procedures that are known to supply monomer units for PHA synthesis.[4]

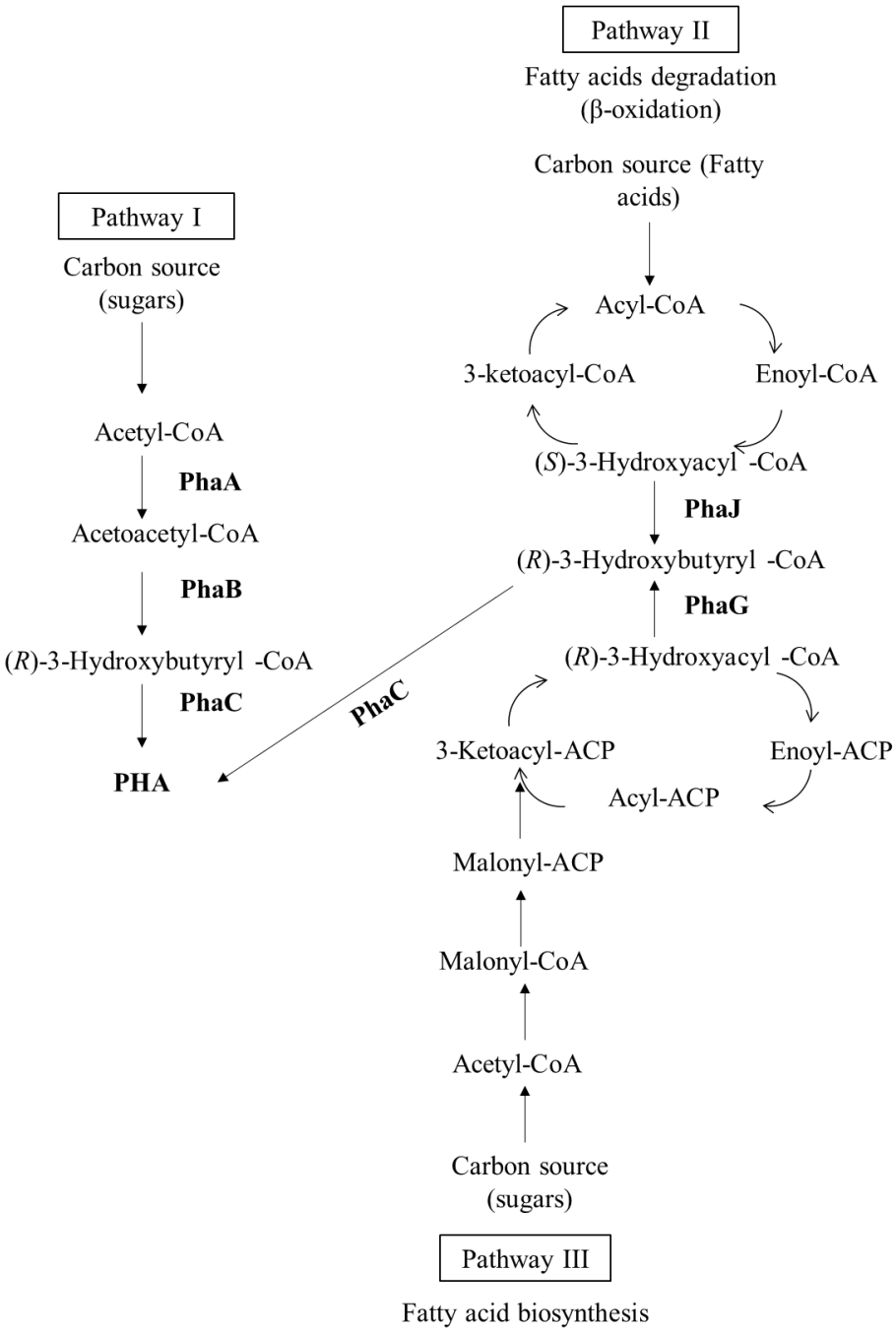

Figure 1-2. Metabolic pathways for P(3HB) biosynthesis. PhaA, β-ketothiolase; PhaB, NADPH-dependent acetoacetyl-CoA reductase; PhaC, PHA synthase; PhaG, 3-hydroxyacyl-ACP-CoA transferase; PhaJ, (*R*)-enoyl-CoA hydratase;

1.3. Physical properties of PHA

The PHA inclusions inside bacteria cell are now understood to be mostly amorphous, [11] but it acts very crystalline polyester after extraction from cell by organic solvent like chloroform. P(3HB) is one of the most common PHA, like petroleum-based plastic, P(3HB) is thermoplastic as shown in (Table 1-2).[4] However, its high crystallinity (70 °C) and low fracture elongation of 5%, resulting in a hard material. In addition, since the glass transition temperature is below room temperature, secondary crystallization occurs over time after formation, and there is also a disadvantage that it becomes a hard material.

Homopolymer P(3HB) has brittle properties, but its copolymers have improved physical properties. In contrast to crystalline SCL-PHAs, MCL-PHAs are amorphous. MCL-PHAs have soft, low T_m, low glass transition temperature (T_g), low tensile strength, and high elongation at break elastomeric characteristics. Therefore, SCL- and MCL-PHA combined have better thermal and mechanical properties than PHA homopolymers. MCL units such as 3HHx monomer is an example. P(3HB-*co*-25 mol%3HHx has lower thermal property 52 °C (Table 1-2) than P(3HB) (180 °C). The larger alkyl side chain of 3HHx prevents it from crystallizing in the 3HB lattice.[12] The thermal and physical characteristics of the resulting PHAs will depend on the monomers added to PHA polymers.

Table 1-2. Thermal properties of some biosynthesized polymers

Polymer	Melting temperature, T_m (°C)	Glass-transition temperature, T_g (°C)
P(3HB)	180	4
P(3HB-*co*-71% 3HV)	83	213
P(3HB-*co*-25mol%3HHx)	52	– 4
P(4HB)	53	248
MCL-PHA	45 – 54	–240 to –25
Polystyrene	240	100
Polypropylene	176	– 10

3HB, 3-hydroxybutyrate; 3HV, 3-hydroxyvalerate; 4HB, 4-hydroxybutyrate; MCL-PHA, PHA with mainly medium-chain-length monomers ranging from C_{6-12}

1.4. Genetic engineering strategies used for PHA biosynthesis

There are many attempts to find useful PhaCs and to create beneficial PhaC mutants by means of screening, evolutionary engineering approach[13] or structure/function relationship approach.[2, 4, 14, 15] In which, recombinant *C. necator* harboring class I PhaC synthase was reported successful in incorporating MCL component in its copolymer.[4] Another example come from the first achievement of class I $PhaC_{Ac}$ from *A. cavie* in synthesizing copolymer SCL-MCL PHA.[16] Furthermore, participation of at least two mutations in the same region on PhaC synthase bring outstanding effect on the accumulation of PHA, this was proven via some representative including mutants such as S325T/Q481K mutant PhaC1Ps, N149S/D171G mutant PhaCAc. [17, 18 19] Recently, Tsuge

et al., proposed that beneficial mutations in $PhaC_{Ac}$ from *Aeromonas caviae* were obtained from the alignment unknown sequence structure of PhaC and the known sequence structure of $PhaC_{Re}$.[20, 21] Their valuable results are reliable evidence reinforced in understanding how PhaC synthase work.

Following *in vitro* engineering evolution approach, previous study reported the chimeric synthase $PhaC_{AR}$ which possess synergic effects of both class I $PhaC_{Re}$ (strong activity toward SCL-substrate (*R*)-3HB-CoA) and class I $PhaC_{Ac}$ (broad substrate specificity). [22, 23]. $PhaC_{AR}$ composed N-terminal moiety of $PhaC_{Ac}$ from *Aeromonas caviae* strain and C-terminal moiety of $PhaC_{Re}$ from *Ralstonina eutropha* (or *Curpriavidus necator*) strain.[22] From this discovery, it has expected that further investigation using $PhaC_{AR}$ in synthesizing variety of copolymer has advantageous properties based on natural P(3HB). Indeed, generating a mutant library from parental synthase is a strategy aimed to reinforce the reserve region of PhaC.[22]

1.5. The aim of this thesis

The aim of this study is to examine the engineering of sequence-regulating polyhydroxyalkanoate (PHA) synthase to broaden its substrate range and produce novel block PHA copolymers using the engineered enzymes.

Sequence-regulating polyhydroxyalkanoate (PHA) synthase $PhaC_{AR}$ is a unique enzyme that spontaneously synthesizes block copolymers from the mixture of substrates. Block copolymers composed of segments with distinct properties can exert useful and characteristic physical properties. For example, poly(2-hydroxybutyrate)-*b*-poly(3-hydroxybutyrate) P(2HB)-*b*-P(3HB) exhibited elasticity, whereas P(2HB-*ran*-3HB) is stretchable but not elastic. In addition, $PhaC_{AR}$ has possessed broad substrate scopes that recognize artificial monomer 2-hydroxyacyl (2HA)-coenzyme A (CoA), SCL monomer, and weak activity toward medium-chain-length (MCL, $C_{6–12}$) monomer. Previously, the

directed evolution of $PhaC_{AR}$ was performed to increase its activity toward 3-hydroxyhexanoyl (3HHx)-CoA (MCL monomer), and the beneficial mutations N149D (ND), F314L, and T319I have been achieved. Based on these finding, I investigated the site-directed saturation mutagenesis at position 314, which is adjacent to the catalytic center C315. In chapter 2, the goal is the site-directed mutagenesis of $PhaC_{AR}$ to enhance the activity toward a MCL substrate 3-hydroxyhexanoyl-CoA. I also focused on to expand the range of molecular design of PHA block copolymers. In chapter 3, PLA segment attempted to be introduced to generate new types of PHA-PLA block copolymer. To incorporate larger monomer substrate such as 3-hydroxyoctanoate (C8) is thought to be effective to improve the flexibility of PHA. Accordingly developed directed evolution system of $PhaC_{AR}$ in order to obtain the new enzyme capable of recognizing 3-hydroxyoctanoyl-CoA that was shown in chapter 4. Overall, my goal was to expand the substrate scope of $PhaC_{AR}$ toward the biosynthesis of brand-new MCL-SCL block copolymers.

1.6. References

(1) Zher Neoh, S.; Fey Chek, M.; Tiang Tan, H.; Linares-Pastén, J. A.; Nandakumar, A.; Hakoshima, T.; Sudesh, K. Polyhydroxyalkanoate synthase (PhaC): The key enzyme for biopolyester synthesis. *Current Research in Biotechnology* **2022**, *4*, 87-101. DOI: 10.1016/j.crbiot.2022.01.002.

(2) Nomura, C. T.; Taguchi, S. PHA synthase engineering toward superbiocatalysts for custom-made biopolymers. *Appl Microbiol Biotechnol* **2007**, *73* (5), 969-979. DOI: 10.1007/s00253-006-0566-4.

(3) Lemoigne, M. Products of dehydration and of polymerization of β-hydroxybutyric acid. *Bull Soc Chem Biol* **1926**, *8*, 770-782.

(4) Sudesh, K.; Abe, H.; Doi, Y. Synthesis, structure and properties of polyhydroxyalkanoates: biological polyesters. *Progress in Polymer Science* **2000**, *25* (10), 1503-1555. DOI: 10.1016/S0079-6700(00)00035-6.

(5) Sato, S.; Maruyama, H.; Fujiki, T.; Matsumoto, K. Regulation of 3-hydroxyhexanoate composition in PHBH synthesized by recombinant *Cupriavidus necator* H16 from plant oil by using butyrate as a co-substrate. *J Biosci Bioeng* **2015**, *120* (3), 246-251. DOI: 10.1016/j.jbiosc.2015.01.016.

(6) Stubbe, J.; Tian, J. Polyhydroxyalkanoate (PHA) hemeostasis: the role of PHA synthase. *Nat Prod Rep* **2003**, *20* (5), 445-457. DOI: 10.1039/b209687k.

(7) Rehm, B. H. Biogenesis of microbial polyhydroxyalkanoate granules: a platform technology for the production of tailor-made bioparticles. *Curr Issues Mol Biol* **2007**, *9* (1), 41-62. From NLM.

(8) Rehm, B. H. Polyester synthases: natural catalysts for plastics. *Biochem J* **2003**, *376* (Pt 1), 15-33. DOI: 10.1042/bj20031254 From NLM.

(9) Antonio, R. V.; Steinbüchel, A.; Rehm, B. H. Analysis of *in vivo* substrate specificity of the PHA synthase from *Ralstonia eutropha*: formation of novel copolyesters in recombinant *Escherichia coli*. *FEMS Microbiol Lett* **2000**, *182* (1), 111-117. DOI: 10.1111/j.1574-6968.2000.tb08883.x From NLM.

(10) Dennis, D.; McCoy, M.; Stangl, A.; Valentin, H. E.; Wu, Z. Formation of poly(3-hydroxybutyrate-*co*-3-hydroxyhexanoate) by PHA synthase from *Ralstonia eutropha*. *J Biotechnol* **1998**, *64* (2-3), 177-186. DOI: 10.1016/s0168-1656(98)00110-2 From NLM.

(11) Revol, J.-F.; Chanzy, H. D.; Deslandes, Y.; Marchessault, R. H. High-resolution electron microscopy of poly(β-hydroxybutyrate). *Polymer* **1989**, *30* (11), 1973-1976. DOI: 10.1016/0032-3861(89)90281-4.

(12) Yu, J. Chapter 23 - Microbial Production of Bioplastics from Renewable Resources. In *Bioprocessing for Value-Added Products from Renewable Resources*, Yang, S.-T. Ed.; Elsevier, 2007; pp 585-610.

(13) Taguchi, S.; Doi, Y. Evolution of polyhydroxyalkanoate (PHA) production system by "enzyme evolution": successful case studies of directed evolution. *Macromol Biosci* **2004**, *4* (3), 146-156. DOI: 10.1002/mabi.200300111.

(14) Wang, Q.; Tappel, R. C.; Zhu, C.; Nomura, C. T. Development of a new strategy for production of medium-chain-length polyhydroxyalkanoates by recombinant *Escherichia coli* via inexpensive non-fatty acid feedstocks. *Appl Environ Microbiol* **2012**, *78* (2), 519-527. DOI: 10.1128/aem.07020-11 From NLM.

(15) Nambu, Y.; Ishii-Hyakutake, M.; Harada, K.; Mizuno, S.; Tsuge, T. Expanded amino acid sequence of the PhaC box in the active center of polyhydroxyalkanoate synthases. *FEBS Lett* **2020**, *594* (4), 710-716. DOI: 10.1002/1873-3468.13651.

(16) Fukui, T.; Doi, Y. Cloning and analysis of the poly(3-hydroxybutyrate-*co*-3-hydroxyhexanoate) biosynthesis genes of *Aeromonas caviae*. *J Bacteriol* **1997**, *179* (15), 4821-4830. DOI: 10.1128/jb.179.15.4821-4830.1997 From NLM.

(17) Matsumoto, K. i.; Aoki, E.; Takase, K.; Doi, Y.; Taguchi, S. *In vivo* and *in vitro* Characterization of Ser477X Mutations in Polyhydroxyalkanoate (PHA) Synthase 1 from *Pseudomonas* sp. 61−3: Effects of Beneficial Mutations on Enzymatic Activity, Substrate Specificity, and Molecular Weight of PHA. *Biomacromolecules* **2006**, *7* (8), 2436-2442. DOI: 10.1021/bm0602029.

(18) Matsumoto, K.; Shozui, F.; Satoh, Y.; Tajima, K.; Munekata, M.; Taguchi, S. Kinetic analysis of engineered polyhydroxyalkanoate synthases with broad substrate specificity. *Polymer journal* **2009**, *41* (3), 237-240.

(19) Tsuge, T.; Watanabe, S.; Shimada, D.; Abe, H.; Doi, Y.; Taguchi, S. Combination of N149S and D171G mutations in *Aeromonas caviae* polyhydroxyalkanoate synthase and impact on polyhydroxyalkanoate biosynthesis. *FEMS Microbiol Lett* **2007**, *277* (2), 217-222. DOI: 10.1111/j.1574-6968.2007.00958.x.

(20) Kim, J.; Kim, Y. J.; Choi, S. Y.; Lee, S. Y.; Kim, K. J. Crystal structure of *Ralstonia eutropha* polyhydroxyalkanoate synthase C-terminal domain and reaction mechanisms. *Biotechnol J* **2017**, *12* (1). DOI: 10.1002/biot.201600648.

(21) Wittenborn, E. C.; Jost, M.; Wei, Y.; Stubbe, J.; Drennan, C. L. Structure of the Catalytic Domain of the Class I Polyhydroxybutyrate Synthase from *Cupriavidus necator*. *J Biol Chem* **2016**, *291* (48), 25264-25277. DOI: 10.1074/jbc.M116.756833.

(22) Matsumoto, K. i.; Takase, K.; Yamamoto, Y.; Doi, Y.; Taguchi, S. Chimeric Enzyme Composed of Polyhydroxyalkanoate (PHA) Synthases from *Ralstonia eutropha* and *Aeromonas caviae* Enhances Production of PHAs in Recombinant *Escherichia coli*. *Biomacromolecules* **2009**, *10* (4), 682-685. DOI: 10.1021/bm801386j.

(23) Matsumoto, K.; Taguchi, S. Biosynthetic polyesters consisting of 2-hydroxyalkanoic acids: current challenges and unresolved questions. *Appl Microbiol Biotechnol* **2013**, *97* (18), 8011-8021. DOI: 10.1007/s00253-013-5120-6.

Chapter 2.

Biosynthesis of 3-hydroxyhexanoate (3HHx)-based block copolymers using evolved PhaC$_{AR}$

2.1. Introduction

Block copolymerization is an effective and versatile method for giving functional materials that cannot be achieved with homopolymers.[1] Biosynthesis of PHA block copolymers, therefore, has attracted research interest. In the early trials to synthesize PHA block copolymers, researchers attempted several strategies, like changing feedstock and/or monomer precursors during production.[2] In other words, different substrates for individual blocks are added using a sequential feeding mode. The sequence of the obtained polymers, however, needs further verification because the time required to synthesize a single PHA molecule is thought to be much shorter than cultivation period;[3] thus, polymer blends rather than block copolymers could be synthesized.[4]

The discovery of sequence-regulating PHA synthase is a breakthrough in the biosynthesis of PHA block copolymers.[4] Sequence-regulating PHA synthase is capable of spontaneously synthesizing block copolymers from a mixture of monomer substrates without manipulations during polymer production. $PhaC_{AR}$, the first-discovered sequence-regulating PHA synthase, synthesizes poly(2-hydroxybutyrate)-*b*-poly(3-hydroxybutyrate) [P(2HB)-*b*-P(3HB)] in recombinant *E. coli* with supplementation of 2HB and 3HB.[4] $PhaC_{AR}$ is also characterized by the unusual substrate specificity toward 2HB-CoA. To date, only engineered PHA synthases incorporate 2HB units. The evolved class II enzyme $PhaC1_{Ps}$STQK is known to synthesize P(2HB).[5]

P(2HB)-*b*-P(3HB) is the first structure-verified PHA block copolymer. Its block sequence was verified by solvent fractionation and observation of microphase separation.[4] This polymer possesses elastomer-like properties,[6] a common characteristic of block copolymers.[7] In the copolymer, the combination of amorphous P(2HB) and crystalline P(3HB) phases, which served as soft and hard segments, respectively, contributed to the expression of elastomer-like properties. This finding indicates that PHA block

copolymers may expand PHA mechanical properties. Useful and characteristic properties of block copolymers are attributable to the distinct properties of each segment. In this regard, PHA block copolymers composed of MCL and SCL segments are attractive targets. However, a major obstacle in molecular design is presented by $PhaC_{AR}$, which has a limited ability to incorporate MCL monomers.[6]

Here, I aimed to create engineered $PhaC_{AR}$ proteins with increased activity toward an MCL substrate, 3HHx. The goal was to biosynthesize a new type of PHA, an MCL-SCL block copolymer. Directed evolution is an effective approach to create engineered PHA synthases with desired function. Previous studies have demonstrated effective methodologies for random mutant library screening and the rational protein structure design.[8, 9] Previously, random mutagenesis in the entire $PhaC_{AR}$ (including $PhaC_{Ac}$ and $PhaC_{Re}$) to explore the broad range of mutations was performed (Master theses of Masayoshi Tomoi, 2019 and Maureen Gauex, 2019). Candidates of beneficial PhaC mutants were selected using *in vivo* Nile Red plate assay.[10] This screening method is based on a positive correlation between cellular PHA content and fluorescent intensity of the colonies stained with a hydrophobic dye bound to the intracellularly accumulated PHA inclusion body.[11] Previously, the homopolymers of the target monomer have been chosen as an indicator polymer.[10] However, the method is not simply applicable to the present study because $PhaC_{AR}$ does not synthesize a homopolymer of the target monomer, P(3HHx). Thus, the screening system is designed that utilizes 3HHx-rich P(3HB-*co*-3HHx) as an indicator polymer. As a result, beneficial $PhaC_{AR}$ mutants with increased activity toward 3HHx-CoA were successfully obtained from the screening. Based on that result, my results indicated that the $PhaC_{AR}$ mutant can synthesize a new MCL-SCL PHA block copolymer, P(3HHx)-*b*-P(2HB).

2.2. Materials and Methods

2.2.1. Bacterial strains and plasmids

E. coli JM109 was the host for plasmid construction, screening, and polymer production. The plasmid pBSP$_{Re}$phaC$_{AR}$pctalkK was used in this study.[12] This plasmid contains the chimeric PHA synthase gene (*phaC*$_{AR}$), propionyl-CoA transferase gene (PCT) from *Megasphaera elsdenii*, and the MCL 3-hydroxyalkanoic acid CoA ligase gene (*alkK*) from *Pseudomonas putida*[9] under the control of the *phb* operon promoter P$_{Re}$ from *R. eutropha*.[4] The *phaC*$_{Re}$ region in *phaC*$_{AR}$ was replaced with the codon-optimized fragment for expression in *E. coli*, which was synthesized by Eurofins Scientific (Luxembourg). The modified plasmid is referred to as pBSP$_{Re}$phaC$_{AR}$(opt)pctalkK, and its sequence is shown in Appendix-I. Unless mentioned otherwise, all chemicals were purchased from Tokyo Chemical Industry (Japan), Bio-Rad Laboratories (USA), JUNSEI Chemical (Japan), or FUJIFILM Wako Pure Chemicals Corporation (Japan).

2.2.2. Construction of a site-directed saturation mutagenesis library

Site-directed saturation mutagenesis at position 314 was performed by overlap extension PCR using pBSP$_{Re}$phaC$_{AR}$(opt)pctalkK as the template and following primers: F1: 5′-AACTTCCTTGCCACCAATCC-3′; R1: 5′-TCATGCCTTGGCTTTGAC-3′; F314X_F: 5′-CGGTCAGGATAAAATCAATGTTCTGGGTNNNTGTGTTGGTGGC-3′; F314X_R: 5′-ACCCAGAACATTGATTTTATCCTGACCG-3′. Underlined bases correspond to the 314th amino acid residue replaced by the following codons individually to introduce site-directed saturation mutagenesis; A (GCG), C (TGC), D (GAT), E (GAA), F (TTT), G (GGC), H (CAT), I (ATT), K (AAA), L (CTT), M (ATG), N (AAC), P (CCG), Q (CAG), R (CGC), S (AGC), T (ACC), V (GTG), W (TGG), and Y (TAT).

Mutated fragments and pBSP$_{Re}$phaC$_{AR}$(opt)pctalkK were digested with *Bgl*II and *Sfi*I before ligation to obtain a mutant library.

2.2.3. Culture conditions

To select the beneficial mutant candidates of *phaC$_{AR}$*, the mutant gene library was introduced into *E. coli* JM109. Cells were grown on agar plates of Luria–Bertani (LB) medium containing 5 g/L yeast extract, 10 g/L tryptone, 10 g/L NaCl, 2 wt% glucose, 0.5 mg/L Nile Red, 100 mg/L ampicillin, 1.0 g/L sodium (*R*,*S*)-3-hydroxybutyrate (3HB-Na), 2.5 g/L sodium (*R*,*S*)-3-hydroxyhexanoate (3HHx-Na), and 15 g/L agar. Beneficial mutant candidates were selected on the basis of the fluorescent intensity of colonies.[13] 3HHx-Na was prepared from ethyl 3HHx as previously reported.[14]

P(3HB-*co*-3HHx) production by the selected mutant candidates was investigated using the liquid medium with the same composition (without Nile Red and agar). P(3HB) and P(3HHx) were also produced with the supplementation of 3HB-Na and 3HHx-Na as sole precursors, respectively. *E. coli* JM109 harboring pBSP$_{Re}$PhaC$_{AR}$pctalkK, pBSP$_{Re}$PhaC$_{AR}$(opt)pctalkK, or their mutated derivatives were cultivated in 1.5 mL medium in a test tube at 30 °C for 48 h. Polymer production and monomer composition were determined via gas chromatography (GC) as described previously.[15] For nuclear magnetic resonance (NMR) analysis of P(3HB-*co*-3HHx), the cells were cultured in 100 mL medium containing 2.5 g/L 3HB-Na and 1.0 g/L 3HHx-Na in 500-mL shake flasks with reciprocal shaking at 120 rpm at 30 °C for 48 h. Polymers were extracted with chloroform at 60 °C for 48 h and purified via polymer precipitation by adding excess methanol. The purification step was repeated twice. ^{13}C NMR of the extracted polymer was analyzed in $CDCl_3$ as described previously.[16]

For producing P(2HB), P(3HHx), and P(2HB-*co*-3HHx) at the flask scale, the cells harboring pBSP$_{Re}$PhaC$_{AR}$(opt)pctalkK or its derivative were cultivated in 100 mL

medium containing 2.5 g/L (*R*,*S*)-2HB-Na and/or 1.0 g/L 3HHx-Na in 500-mL shake flasks with reciprocal shaking at 120 rpm at 30 °C for 50 h. The precursors were added at 2 h after inoculation. Polymers were extracted as described above. Polymer production was determined by weight. Monomer composition was determined using ^{1}H NMR.

2.2.5. Immunoblot analysis

Cells harboring pBSP$_{Re}$PhaC$_{AR}$(opt)pctalkK and its derivative were cultivated in 1.5 mL LB medium containing 100 mg/L ampicillin at 30 °C for 14 h and harvested via centrifugation (15,300 *g*, 3 min, 4 °C). The cells were resuspended in 0.2 mL 20 mM lysis buffer (pH 7.5)[17] and disrupted by sonication on ice for 10 min. After centrifugation (15,300 *g*, 3 min, 4 °C), the obtained supernatant was referred to as crude extract. Crude extract protein concentration was determined using Bradford assay.[18] Immunoblot analysis was performed following reported methodology using anti-PhaC$_{Re}$ antibody as the primary antibody.[19]

2.2.6. Preparation of CoA thioesters and enzyme activity assay

(*R*,*S*)-3-Hydroxybutyryl-CoA (3HB-CoA) was synthesized from (*R*,*S*)-3-hydroxybutyric acid. The CoA thioesters were prepared using a modified method[20] as follows: 1,1′-carbonyldiimidazole (42.2 mg) was dissolved in 2 mL dry tetrahydrofuran (THF). (*R*,*S*)-3-Hydroxybutyric acid (109 mg) was then added, and the mixture was incubated for 30 min with stirring at room temperature (~25 °C). CoA (40 mg) (Oriental Yeast, Tokyo, Japan) was dissolved in 1 mL of 0.5 M $NaHCO_3$ (pH 7.4), and the solution was combined with the THF solution and incubated for 12 h with stirring on ice. The reaction mixture was diluted with 9 mL of 0.5 M $NaHCO_3$. After acidification using formic acid to pH ~ 3, THF was evaporated *in vacuo*. 3HB-CoA was purified using a

preparative high-performance liquid chromatography equipped with a reverse-phase column (ODS-80Ts, TOSOH, Japan) using 5 mM ammonium acetate (pH 5.5) and acetonitrile as mobile phases. The fractions containing 3HB-CoA were collected, and acetonitrile was evaporated *in vacuo*. The synthesis of 3HB-CoA was confirmed by LC-electrospray ionization-mass spectroscopy (LC-ESI-MS) (LCMS2020, Shimadzu, Japan). The concentration of 3HB-CoA was determined by the absorbance at 259 nm using a molar attenuation coefficient of $1.64 \times 10^4\ M^{-1}\ cm^{-1}$. (*R*,*S*)-3-Hydroxyhexanoyl-CoA (3HHx-CoA) was synthesized in the same manner using 162 mg sodium (*R*,*S*)-3-hydroxyhexanoate.

An *in vitro* enzyme activity assay was conducted using crude extract and CoA thioesters prepared as described above. For 3HB-CoA, the reaction mixture (62 µL) contained 65 ng/µL crude extract, 2.1 mM 3HB-CoA, and 1.1 µg/µL bovine serum albumin (BSA) in 40 mM potassium phosphate buffer (pH 7.4). For 3HHx-CoA, the reaction mixture (75 µL) contains 400 ng/µL crude extract, 1.7 mM 3HHx-CoA, and 0.9 µg/µL BSA in the same buffer. The reaction was performed in a 96-well microplate. After addition of crude extract to initiate the reaction, 60 µL 1% trichloroacetic acid was periodically added for quenching. The reaction solution was filtered via centrifugation (12,000 *g*, 10 min, 4 °C) using filtering microplates with 0.45 µm pore size (Cytiva, USA). An aliquot of 100 µL filtrate was transferred to a new microplate and 60 mL of 1 mM 5,5′-dithiobis (2-nitrobenzoic acid) (DTNB) (Merck, Germany) was added. Released free CoA was quantified by measuring absorbance at 412 nm. One unit of enzyme activity is defined as the amount required to catalyze the transformation of 1 µmol substrate in 1 min.[21]

2.2.7. Solvent fractionation of polymers

To distinguish block copolymer from polymer blend, purified polymer samples were fractionated into two fractions depending on their solubility in organic solvents.[22, 23] Approximately 8 mg of purified polymer sample was dissolved in 0.5 mL THF in a test tube with a screw cap by heating at 60 °C for 10 min. After cooling down to room temperature, the solution was combined with 6 mL cyclohexane and incubated at 18 °C for 1 h. The precipitant collected on a PTFE filter membrane (pore size 0.1 µm) is referred to as the insoluble fraction. The flow-through fraction is referred to as the soluble fraction. The components in both insoluble and soluble fractions were recovered in $CDCl_3$ and analyzed using ^1H NMR. The same experiment was conducted using a polymer blend composed of two homopolymers P(2HB) and P(3HHx).

2.2.8. Protein structure prediction

Five structural models of $PhaC_{AR}$ were predicted using the Google collaborative notebook for AlphaFold2 prediction (https://colab.research.google.com/github/sokrypton/ColabFold/blob/main/AlphaFold2.ipynb). Model 1 is used for interpretation because it had the highest confidence score. The per-residue confidence score provided by AlphaFold2 (named pLDDT[1]) was above 80% for 85% of the residues. The hydrophobicity of the residues was calculated based on the hydrophobicity scale defined by Eisenberg et al.[24]

2.3. Results

2.3.1. Exploration of beneficial mutations in the $PhaC_{Ac}$ region

The metabolic pathway used in this study is shown in Figure 2-1. P(3HB-*co*-3HHx) was used as an indicator polymer because $PhaC_{AR}$ does not synthesize P(3HHx) homopolymer. The copolymer possesses a random sequence based on ^{13}C NMR (Figure S2-1, Appendix—III). Supplementation of 1.0 g/L 3HB-Na and 2.5 g/L 3HHx-Na enabled the synthesis of P(3HB-*co*-3HHx) with approximately 50 mol% 3HHx (Table 2-1) (Master thesis Masayoshi Tomoi, 2019). This synthesis of the 3HHx-rich P(3HB-*co*-3HHx) allowed to isolate candidates having enhanced capacity to incorporate 3HHx units.

First, the random mutant library of the N-terminal region of the $phaC_{AR}$ (the $phaC_{Ac}$ region) was subjected to screening. *E. coli* expressing enzymes in the metabolic pathway in Figure 2-1 was grown on Nile red plates. Six colonies with stronger fluorescence, which can be expected to produce greater amount of 3HHx-rich P(3HB-*co*-3HHx) were selected from approximately 1,000 colonies. The selected $phaC_{AR}$ mutants contained either N149D or H121Y mutation. The liquid culture using the isolated mutants indicated that N149D was particularly effective at enhancing 3HHx incorporation (Table 2-1) (Masayoshi Tomoi, 2019, Master thesis)

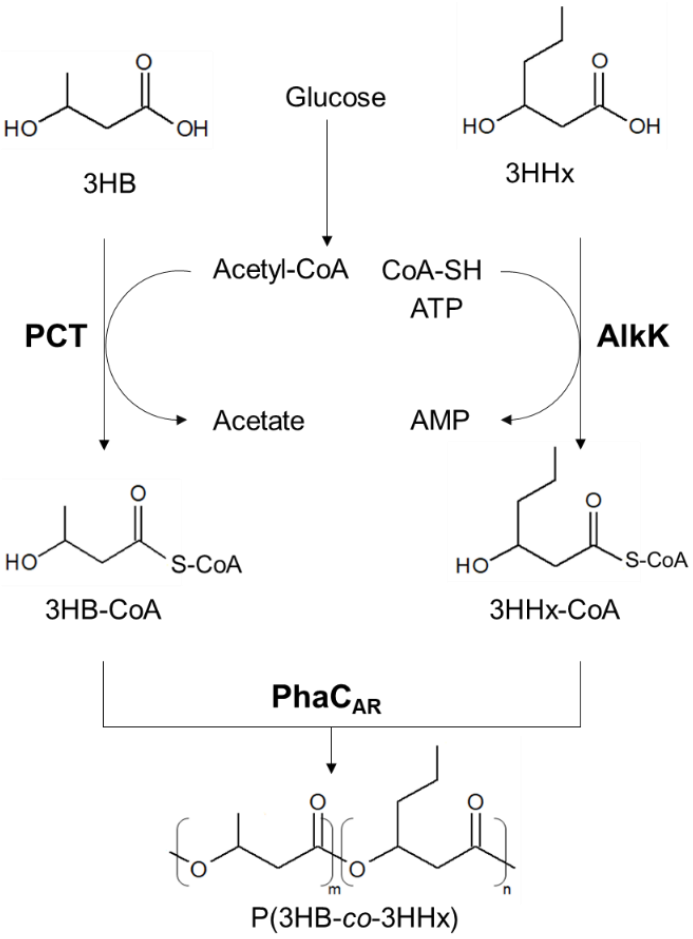

Figure 2-1. Metabolic pathway used in the study. The monomer precursors, 3HB and 3HHx, are supplemented into the medium. PCT and AlkK serve as monomer supplying routes for 3HB-CoA and 3HHx-CoA, respectively.

Table 2-1. The effects of mutations in the $PhaC_{Ac}$ region in $PhaC_{AR}$ on the production of P(3HB-*co*-3HHx).

$PhaC_{AR}$ mutants	Cell dry weight (g/L)	Polymer content (wt%)	Monomer composition (mol%)	
			3HB	3HHx
Parent	1.5 ± 0.0	22.5 ± 2.4	47.6 ± 0.7	52.4 ± 0.7
H121Y	1.5 ± 0.2	26.1 ± 1.6	43.6 ± 0.4	56.4 ± 0.4
N149D	1.5 ± 0.1	36.6 ± 3.3	37.9 ± 1.5	62.1 ± 1.5

Note: Cells harboring $pBSP_{Re}phaC_{AR}$pctalkK and its derivatives were used for polymer production. Data are presented as mean ± standard deviation of the biological triplicate.

All the data of Table 2-1 are collected from previous study (Master thesis of Masayoshi Tomoi, 2019)

2.3.2. Exploration of beneficial mutations in the $PhaC_{Re}$ region

Next, the random mutant library of the C-terminal region of *phaC*$_{AR}$ (the *phaC*$_{Re}$ region) was screened. Error-prone PCR amplification of the region was unsuccessful, presumably due to its high G/C content (67%). Codon usage in the *phaC*$_{Re}$ region was therefore optimized for expression in *E. coli*, and the G/C content was reduced to 50%. From approximately 2,000 colonies, three candidates (T319I/G430S, V454D/I509V, and F314L) exhibiting strong fluorescence were isolated (Master thesis of Maureen Guex, 2019). To verify the effect of single mutations on targeted enzyme activity, 3HHx-CoA, a pairwise mutant T319I/G430S was separated to single mutant T319I and G430S. Due to the lack of specific restriction enzymes between mutations, the other double mutant

V454D/I509V was difficult to divide into single ones. These mutants were reproduced for polymer production via liquid culture based on the culture conditions that determined from previous study (Master thesis of Maureen Guex, 2019) and the result has been shown in Table 2. The selected mutations increased PHA production, 3HHx fraction, or both (Table 2). Among the analyzed mutants, F314L exhibited the highest 3HHx fraction (62.6 mol%), suggesting that the position plays an important role in substrate recognition. Indeed, this residue is adjacent to the catalytic center residue Cys315, which corresponds to Cys319 in $PhaC_{Re}$. On the basis of this results, the mutation at position 314 was subjected to further investigation

Table 2-2. The effects of mutations in the $PhaC_{Re}$ region in $PhaC_{AR}$ on the production of P(3HB-*co*-3HHx).

$PhaC_{AR}$ mutants	Cell dry weight (g/L)	Polymer content (wt%)	Monomer composition (mol%)	
			3HB	3HHx
Parent	1.9 ± 0.1	46.2 ± 1.4	58.4 ± 0.9	41.6 ± 0.9
F314L	2.6 ± 0.1	49.7 ± 0.9	37.4 ± 0.7	62.6 ± 0.7
T319I/G430S	2.4 ± 0.0	46.8 ± 1.2	48.1 ± 0.9	51.9 ± 0.9
T319I	2.2 ± 0.0	44.1 ± 2.3	49.4 ± 1.4	50.6 ± 1.4
G430S	1.8 ± 0.2	50.5 ± 1.6	56.0 ± 0.5	44.0 ± 0.5
V454D/ I509V	2.2 ± 0.1	53.6 ± 1.0	47.1 ± 0.2	52.9 ± 0.2

Note: Cells harboring $pBSP_{Re}phaC_{AR}$(opt)pctalkK and its derivatives were used for polymer production. Data are presented as mean ± standard deviation of the biological triplicate.

2.3.3. Saturation mutagenesis at position 314

Site-directed saturation mutagenesis at position 314 was conducted. The 19 mutant genes and the parent *phaC*$_{AR}$ gene were individually expressed in *E. coli* to test their capacity to produce P(3HB-*co*-3HHx) (Figure 2-2A). As a result, various functional groups were acceptable at this position. F314H, F314L, F314M, and F314Q exhibited particularly high (1.4 to 1.5-fold) polymer production compared with the parent PhaC$_{AR}$. Substitutions with K, N, P, and R, however, considerably decreased polymer production. Surprisingly, all mutants exhibited a higher 3HHx fraction than the parent enzyme. In addition, many of the mutants displayed 1.4 to 2.0-fold higher accumulation of 3HHx units than the parent enzyme. In contrast, most mutants produced a reduced amount of P(3HB) homopolymer (Figure 2-2B). These results suggest that the residue at position 314 contributes to substrate specificity of the enzyme.

Parent PhaC$_{AR}$ is incapable of synthesizing P(3HHx) homopolymer in *E. coli*. The enhanced 3HHx incorporation capacity of the isolated mutants motivated me to test their ability to synthesize P(3HHx). *E. coli* individually expressing the saturation mutants was cultivated with supplementation of 3HHx as a sole precursor. As a result, many mutants produced P(3HHx) homopolymer (Figure 2-2C). The P(3HHx) production was comparable (approximately 0.6-fold) with that of P(3HB).

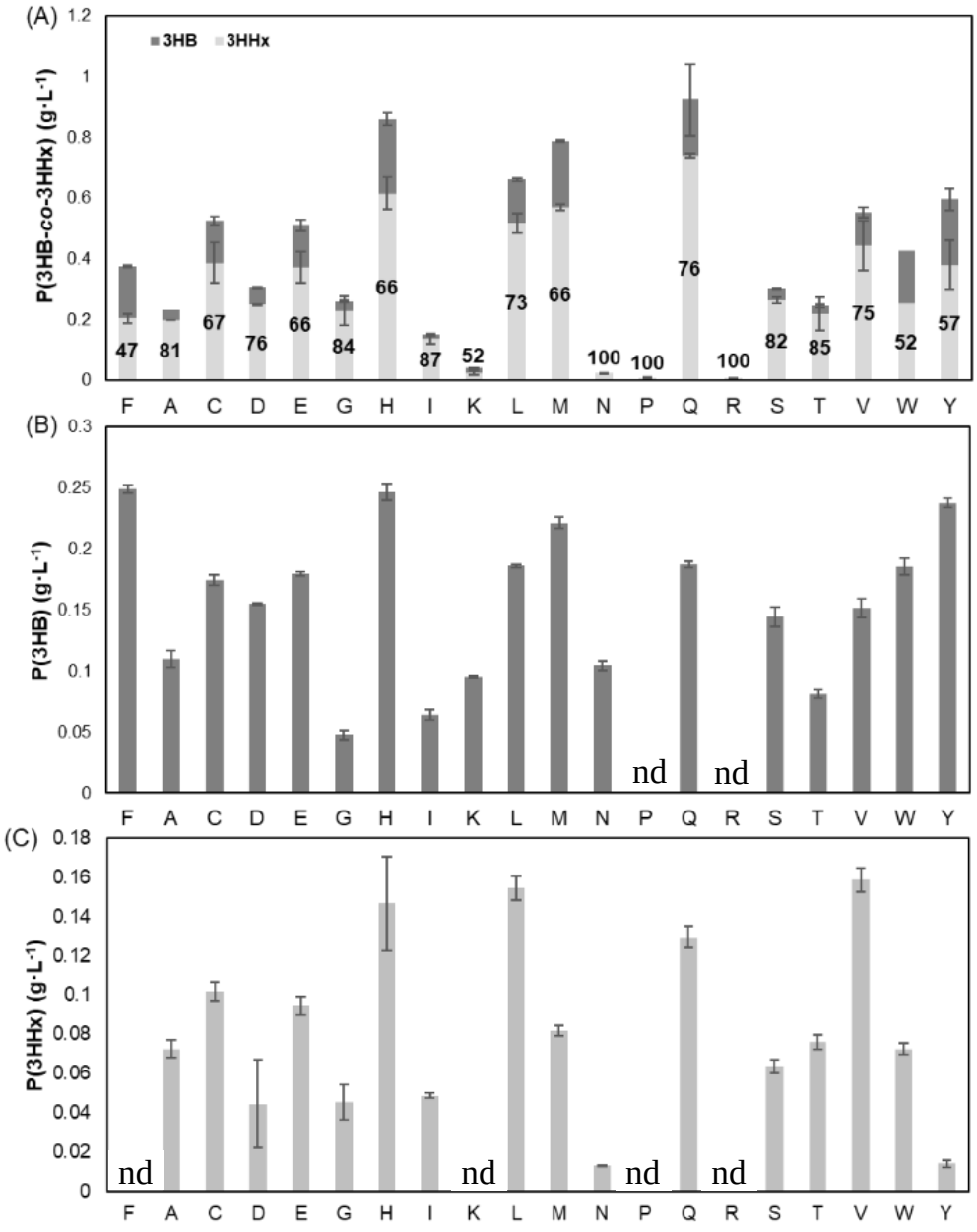

Figure 2-2. Copolymer and homopolymers production by saturation mutants at position 314. X-axis indicates amino acid residues at position 314 (F is the parent enzyme), and Y-axis indicates polymer production. (A) P(3HB-*co*-3HHx) copolymer production, (B) P(3HB) homopolymer production, and (C) P(3HHx) homopolymer production. Dark grey bar, 3HB; and light grey bar, 3HHx. The numbers at the center of the gray bars in panel (A) indicate the 3HHx fraction (mol%). Data are presented as mean ± standard deviation of the biological triplicate. nd, not detected.

2.3.4. Immunoblotting analysis

To examine expression levels of the PhaC$_{AR}$ F314X mutants, immunoblot analysis was conducted using the crude cell extracts and the anti-PhaC$_{Re}$ antibody (Figure 2-3). The expression levels of F314P and F314R significantly decreased, which accounted for the low polymer production of these mutants (Figure 2-2). For the other mutants, expression levels were comparable or slightly lower than that of the parental enzyme. These results demonstrated that the enhanced incorporation of 3HHx units by mutated PhaC$_{AR}$ was likely due to their increased activity toward 3HHx-CoA rather than elevated expression levels of the protein.

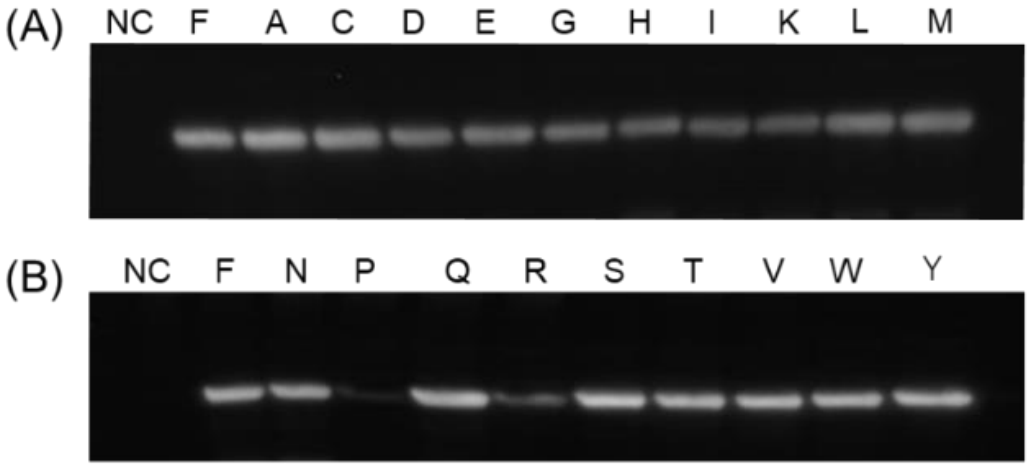

Figure 2-3. Immunoblot analysis of saturation mutations at position 314 in PhaC$_{AR}$ using crude cell extracts and the anti-PhaC$_{Re}$ antibody. NC, negative control (the crude extract of *E. coli* harboring the empty plasmid, pUC18); single letters indicate the F314X substitutions. The full membrane image is shown in Figure S2-2 in Appendix-III.

2.3.5. Enzyme activity assay

Enzyme activity and substrate specificity were evaluated via *in vitro* analysis. The F314H mutant was chosen because of its high P(3HHx) and P(3HB) production capacity (Figure 2-2C). I found that both the parent and F314H enzymes exhibited clear consumption of 3HB-CoA (Figure 2-4A). The activity of the parent enzyme to 3HB-CoA was 2.4-fold higher than that of F314H (Figure 2-4C). In contrast, the parent enzyme exhibited very small consumption of 3HHx-CoA, whereas F314H exhibited remarkable activity (Figure 2-4B). The immunoblot analysis indicated that the expression levels of these enzymes were comparable (Figure 2-3). On the basis of this result, I determined that F314H possesses shifted substrate specificity toward 3HHx-CoA (Figure 2-4C) consistent with the *in vivo* polymer production result.

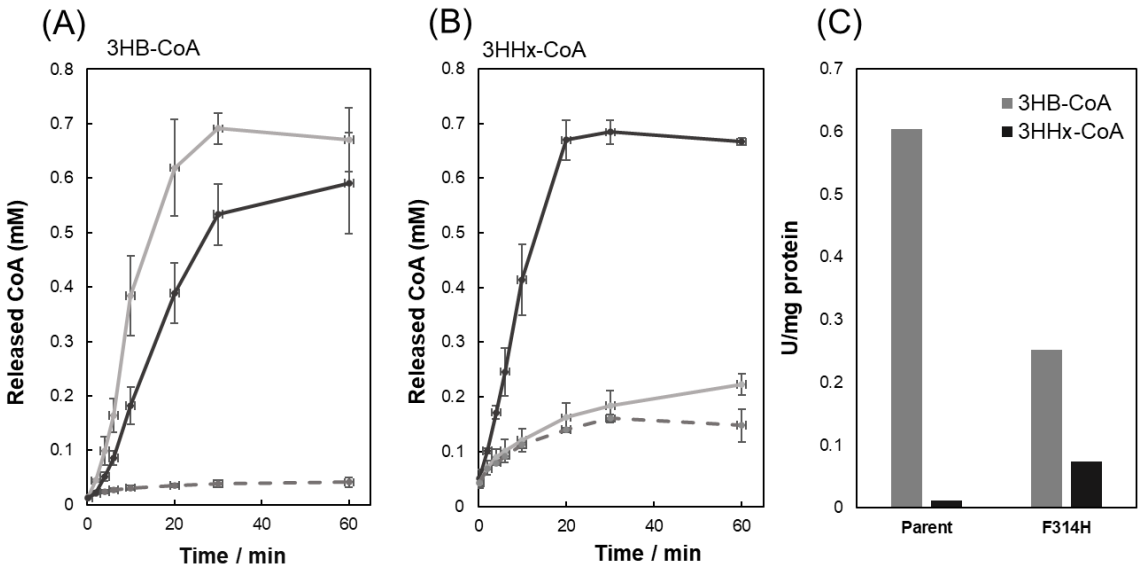

Figure 2-4. *In vitro* enzymatic activity analysis of the parent and F314H mutant of PhaC$_{AR}$. The CoA release from 3HB-CoA (A); the CoA release from 3HHx-CoA (B); and the enzymatic activity toward 3HB-CoA (grey bar) and 3HHx-CoA (black bar) (C). Enzyme activity was calculated using initial velocities. Grey lines, parent; black lines, F314H; and dashed lines, negative control (empty pUC18).

2.3.6. Monomer sequence analysis of copolymers synthesized by PhaC$_{AR}$F314H

The directed evolution of PhaC$_{AR}$ successfully created beneficial mutants with reinforced activity toward 3HHx-CoA. Among them, PhaC$_{AR}$F314H was used for the monomer sequence analysis of the polymers.

The monomer sequence of P(3HB-*co*-3HHx) synthesized by PhaC$_{AR}$F314H was determined by ^{13}C NMR analysis (Figure 2-5). The signals corresponding to the carbonyl group of 3HB and 3HHx were observed at δ 169–170. These signals were ascribed to the dyad sequences of 3HB*-3HB, 3HB*-3HHx or 3HHx*-3HB, and 3HHx*-3HHx[25] An abundance of 3HB-3HHx/3HHx-3HB dyads indicates that the P(3HB-*co*-3HHx) synthesized by PhaC$_{AR}$ F314H has a random sequence. In addition, I calculated D value, which is an index of monomer sequence.[26] The D value of the produced P(3HB-*co*-3HHx) was 0.74 (Appendix-II), also suggesting a random sequence and supporting the result of NMR.

Previously, it was reported that the presence of 2HB monomer is a key for block copolymer synthesis using the sequence-regulating PHA synthase, PhaC$_{AR}$. The capacity of PhaC$_{AR}$F314H to synthesize P(3HHx) homopolymer prompted me to synthesize the copolymers of 3HHx and 2HB (Table 2-3). P(2HB) synthesis was also attempted as a control. In this experiment, the monomer precursors were added at 2 h after inoculation, which facilitates the cell growth.

The F314H mutant was capable of synthesizing P(2HB), P(3HHx), and the binary polymer (Table 2-3). Notably, this is the first report of P(2HB) and P(3HHx) syntheses by class I PHA synthase. It has been known that synthesis by class I PHA synthase creates higher molecular weight polymer than that by class II PHA synthase. In fact, the molecular weight of the obtained homopolymers (Table 2-3) was one order of magnitude

higher than that of P(2HB) (M_w = 2.7 × 10^4)[17] and P(3HHx) (M_w = 2.7 × 10^5)[27] obtained by class II PHA synthase. In addition, ^{1}H NMR of the obtained binary polymer indicated that the resonance of methine proton of 2HB units, which is a fingerprint region to judge triad sequences, was observed at single chemical shift corresponding to a 2HB-2HB*-2HB triad (Figure 2-5B). No detection of 3HB-2HB sequence indicates that there is long region(s) containing successive 2HB units. These results indicate the presence of the P(2HB) homopolymer structure in the polymer. The obtained binary polymer is therefore either a block copolymer or a blend of the two homopolymers P(3HHx) and P(2HB). In contrast, the parent PhaC$_{AR}$ did not synthesize polymers under these conditions.

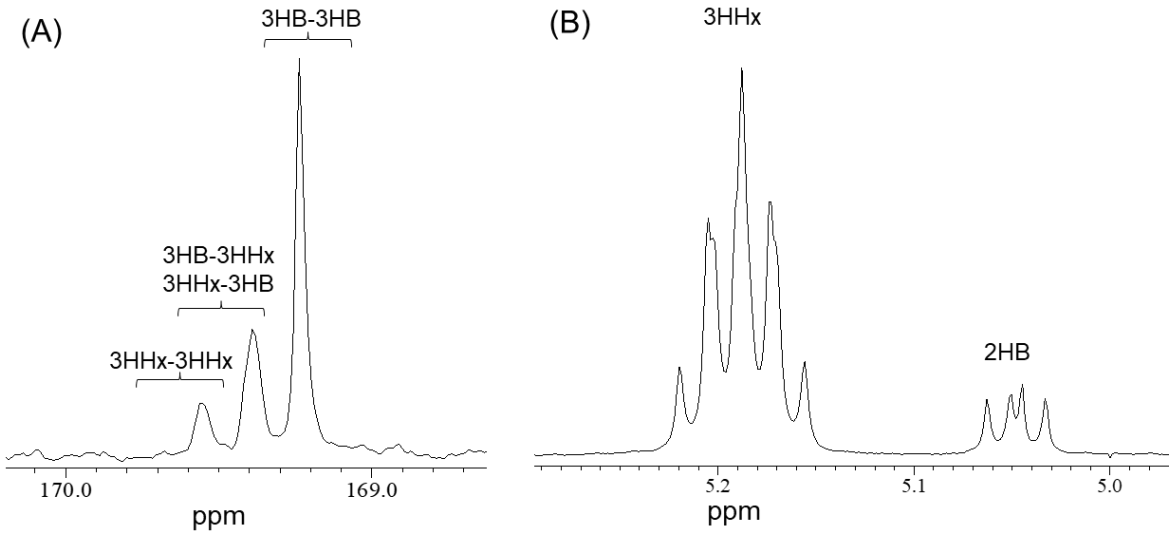

Figure 2-5. ^{13}C NMR of carbonyl carbons in P(3HB-*co*-3HHx) (A) and ^{1}H NMR of methine protons in binary polymer containing 3HHx and 2HB (B). The polymers in panels (A) and (B) were obtained using PhaC$_{AR}$F314H. Full spectra are shown in Figure S2-3 and Figure S2-4 in Appendix-III, respectively.

Table 2-3. P(2HB), P(3HHx), and binary polymer synthesis by $PhaC_{AR}$F314H mutant

$PhaC_{AR}$	Monomer precursor concentration (g/L)		Cell dry weight (g/L)	Polymer production (mg/L)	Monomer composition (mol%)		Molecular weight		
	3HHx	2HB			3HHx	2HB	M_n ($\times 10^5$)	M_w ($\times 10^5$)	M_w/M_n
Parent	1.0	0	1.8 ± 0.0	nd	nd	-			
Parent	0	2.5	2.7 ± 0.0	nd	-	nd			
Parent	1.0	2.5	0.5 ± 0.0	trace	nd	nd			
F314H	1.0	0	2.5 ± 0.1	115 ± 13	100	0	3.4	11.6	3.4
F314H	0	2.5	2.9 ± 0.1	59 ± 8	0	100	1.5	4.2	2.9
F314H	1.0	2.5	2.8 ± 0.1	122 ± 8	93	7	4.0	11.1	2.8

Note: Cells harboring $pBSP_{Re}phaC_{AR}$(opt)pctalkK (parent) and $pBSP_{Re}phaC_{AR}$(opt)F314HpctalkK (F314H) were used for polymer production. Cells were cultivated for 50 h. Precursors were added at 2 h after inoculation. Data are presented as mean ± standard deviation of the biological triplicate. nd, not detected.

2.3.7. Solvent fractionation

Solvent fractionation was performed to determine the presence or absence of a covalent linkage between P(3HHx) and P(2HB) segments in the binary polymer. The solubility test found that cyclohexane moderately dissolves P(3HHx) but not P(2HB). This distinct solubility in cyclohexane was utilized for the solvent fractionation. The blend of P(3HHx) and P(2HB) was dissolved in THF and precipitated by adding

cyclohexane. As expected, the cyclohexane-soluble fraction did not contain P(2HB) (Table 2-4). Detection of P(3HHx) in the cyclohexane-insoluble fraction may be due to co-precipitation with P(2HB). Next, the binary polymer synthesized by the F314H mutant was subjected to the same procedure. As a result, P(2HB) was detected not only in the cyclohexane-insoluble fraction but also in the cyclohexane-soluble fraction (Figure S2-5, Appendix-III). This result strongly indicates the presence of covalent linkage between P(3HHx) and P(2HB) segments. Based on these results, I concluded that the obtained polymer was a block copolymer P(3HHx)-*b*-P(2HB).

Table 2-4. Solvent fractionation of P(3HHx-*co*-2HB) synthesized by PhaC$_{AR}$F314H

Polymers[a]	Monomer composition (mol%)		Recovery (mol%)
	3HHx	2HB	
P(3HHx)	100	0	100
Soluble fraction	100	0	86
Insoluble fraction	-	-	trace
P(2HB)	0	100	100
Soluble fraction	-	-	trace
Insoluble fraction	0	100	90
Blend of P(3HHx) and P(2HB) (94:6 mixture)	94	6	100
Soluble fraction	100	0	29
Insoluble fraction	94	6	67
Original Copolymer	93	7	100
Soluble fraction	96	4	50
Insoluble fraction	91	9	48

Note: [a] The homopolymers and copolymers were synthesized using the conditions described in Table 3. The recovery ratio was calculated on the basis of the molar ratio of 3HHx and 2HB in each soluble and insoluble fraction compared with the original copolymer (before fractionation). The molar ratio of 3HHx and 2HB in copolymer was measured using ^{1}H NMR.

2.4. Discussions

This study describes the biosynthesis of the first MCL-SCL block copolymer, which was achieved by evolving the sequence-regulating PHA synthase. Conventional strategies for regulating physical properties of PHAs are based on reducing crystallinity by random copolymerization, which contributes to soft and pliable properties. Block copolymers can exert characteristic properties due to their microphase separation structure. For that, the combination of segments with distinct properties is preferable. The new component MCL homopolymer facilitates the molecular design of PHA block copolymers that combines soft and hard segments. MCL-SCL block copolymerization, therefore, provides an effective strategy for regulating PHA physical properties. The thermal and mechanical properties of P(3HHx)-*b*-P(2HB) will be reported in the future work.

Acquiring the P(3HHx)-synthesizing capacity was key to enabling MCL-SCL block copolymer synthesis, because the parental $PhaC_{AR}$ synthesizes no P(3HHx). The inability of homopolymer synthesis is also observed in other PHA synthases. For example, $PhaC1_{Ps}$ from *Pseudomonas* sp. 61-3 synthesized a tiny amount of P(3HB) (< 0.1 wt%) in *E. coli*,[28] whereas the enzyme synthesized P(92 mol% 3HB-*co*-MCL 3HA) with a polymer content of 45 wt% in *Pseudomonas* sp. 61-3.[29] Such incapability (or very low efficiency) of homopolymer synthesis is presumably due to the potential barrier to initiate the polymerization, which is observed as a slow reaction at the initial stage of the reaction. This stage is referred to as the lag phase. Some unpreferred monomer substrates may not overcome the barrier; thus, their homopolymers are not synthesized efficiently. The results of the present study demonstrate that the homopolymer-synthesizing capacity can be acquired by evolving PHA synthase. Similarly, $PhaC1_{Ps}$STQK, which is a derivative of $PhaC1_{Ps}$, synthesizes P(3HB) with content comparable with that of $PhaC_{Re}$.[21]

For the directed evolution of $PhaC_{AR}$, mutations were introduced into the entire sequence of the enzyme. The beneficial mutation sites were found in N- and C-terminal regions, suggesting that mutagenesis and screening were performed in an unbiased manner. In particular, the mutations at position 314 in $PhaC_{AR}$ effectively increased activity toward 3HHx-CoA. Position 314, which is adjacent to the catalytic center cysteine residue C315, likely contributes to interaction with substrates. The mutation at the corresponding position in $PhaC_{Ac}$, which was selected by a rational design based on enzyme structure, was recently reported to slightly increase the 3HHx fraction.[30] The distinct mutation effect in $PhaC_{AR}$ and $PhaC_{Ac}$ suggests that the slight structural difference of the substrate binding pocket could drastically influence the mutation effect. These results demonstrate the effectiveness of the function-based screening employed here. In addition, it should be noted that the parent enzyme (F314) exhibited the lowest 3HHx fraction in P(3HB-*co*-3HHx) among the F314X saturation mutants (Figure 2-2). Contrarily, the parent enzyme accumulated the highest amount of P(3HB) among them. These results clearly indicate that F314 is favored in the natural selection for producing P(3HB) rather than a 3HHx-containing copolymer. This interpretation correlates with the specific and high activity of $PhaC_{Re}$ toward 3HB-CoA.[31]

The N149D mutation is located near the junction site of $PhaC_{Ac}$ and $PhaC_{Re}$ regions. N149 in $PhaC_{AR}$ corresponds to D153 in $PhaC_{Re}$ based on the amino acid alignment. D153 in $PhaC_{Re}$ is highly conserved in other $PhaC_{Re}$ homologs, suggesting that the residue has an important role. In addition, the position of N149D mutation is the same as the beneficial mutation N149S found in $PhaC_{Ac}$, which was chosen on the basis of P(3HB) production as a selection criterion.[28] The selection of the same position from $PhaC_{AR}$ and $PhaC_{Ac}$ suggests that the N-terminal region including this position is responsible for independent function of the enzyme. These facts caused my interest in the

function and structure of the N-terminal region. Currently, interpreting the effect of mutation in the N-terminal region based on the 3-D structure is difficult because the full-length structure of PHA synthase has not been analysed. To overcome this limitation, the protein structure prediction of $PhaC_{AR}$ was performed using AlphaFold2, which can calculate highly confident structures without using homolog structures.[32] The major part of the enzyme structure was predicted with a high confidence score (Figure 2-6). The high confidence score of the C-terminal $PhaC_{Re}$ region (> 90% confidence score in most residues) is due to the availability of the crystal structure of the catalytic domain (Figure 6A).[33] The structure of the approximately 50 N-terminal residues is not reliable because of a low confidence score.

The predicted full-length structure showed that $PhaC_{AR}$ is composed of mainly two domains (referred as N- and C-terminal domains) (Figure 6A). It should be noted that the boundary of the domains does not correspond to the junction site between $PhaC_{Ac}$ and $PhaC_{Re}$ regions. The N-terminal domain mostly corresponds to the N-terminal region in the primary structure of the enzyme, and vice versa. An exception is the region of 383-408th residues [designated as the cross-domain (CD) region] containing two α-helices, which are parts of the C-terminal $PhaC_{Re}$ region but included in the N-terminal domain. The CD region is included in the previously proposed LID region, which was hypothesized to be opened so that the enzyme could accept the substrate.[34, 35] In fact, the predicted structure indicates the opened conformation of the region. N149 in $PhaC_{AR}$ is located close to the CD region (presumably interacting with N396). Interestingly, a similar structure is found in the predicted structure of class II $PhaC1_{Ps}$ (Figure 2-6B), which also possesses a CD region (359-385th residues). The E130 residue is located close to the CD region (presumably interacting with N372). The amino acid sequences of the CD regions in $PhaC_{AR}$ and $PhaC1_{Ps}$ have 24/26 identity, indicating an important and

common role of this region. Indeed, the E130D mutation in PhaC1$_{Ps}$ is known to increase activity toward 3HB-CoA.[36] The predictions suggest, therefore, that there is a common mechanism for the mutation effect between N149D in PhaC$_{AR}$ (as well as N149S in PhaC$_{Ac}$) and E130D in PhaC1$_{Ps}$.

The predicted structure of PhaC$_{AR}$ enables to estimate its surface hydrophobicity (Figure S2-6 in Appendix-III). The hydrophobicity map indicates the presence of a highly hydrophobic surface in the N-terminal domain, which could contribute to dimerization of the protein, association with PHA inclusions, or both. In fact, the N-terminal region was proposed to be important for dimerization.[34, 37] Substitutions of the N-terminal hydrophobic residues with hydrophilic residues abolished PHA synthesis,[38] indicating that the hydrophobic region is essential for PhaC activity. In addition, there are two tunnels in the predicted structure (Figure S2-6 in Appendix-III). The catalytic cysteine Cys315 is located at the end of the tunnels, and one of the two tunnels is connected to the N-terminal hydrophobic surface, suggesting that the tunnels could be an entrance of monomers and an exit of synthesized PHA chains. The interpretation is consistent with the previous proposal that N-terminal domain binds to the nascent PHA chains.[33]

The synthesis of a block copolymer by using F314H mutant indicates that sequence-regulating capacity of PhaC$_{AR}$ was maintained despite broadening its substrate specificity. Currently, the mechanism for the generation of block sequence is not fully understood. In the case of P(2HB)-*b*-P(3HB), contrasting activity of PhaC$_{AR}$ toward 2HB-CoA and 3HB-CoA partly accounts for the block copolymerization.[4] Detailed in vitro analysis using 3HHx-CoA is needed to clarify the problem.

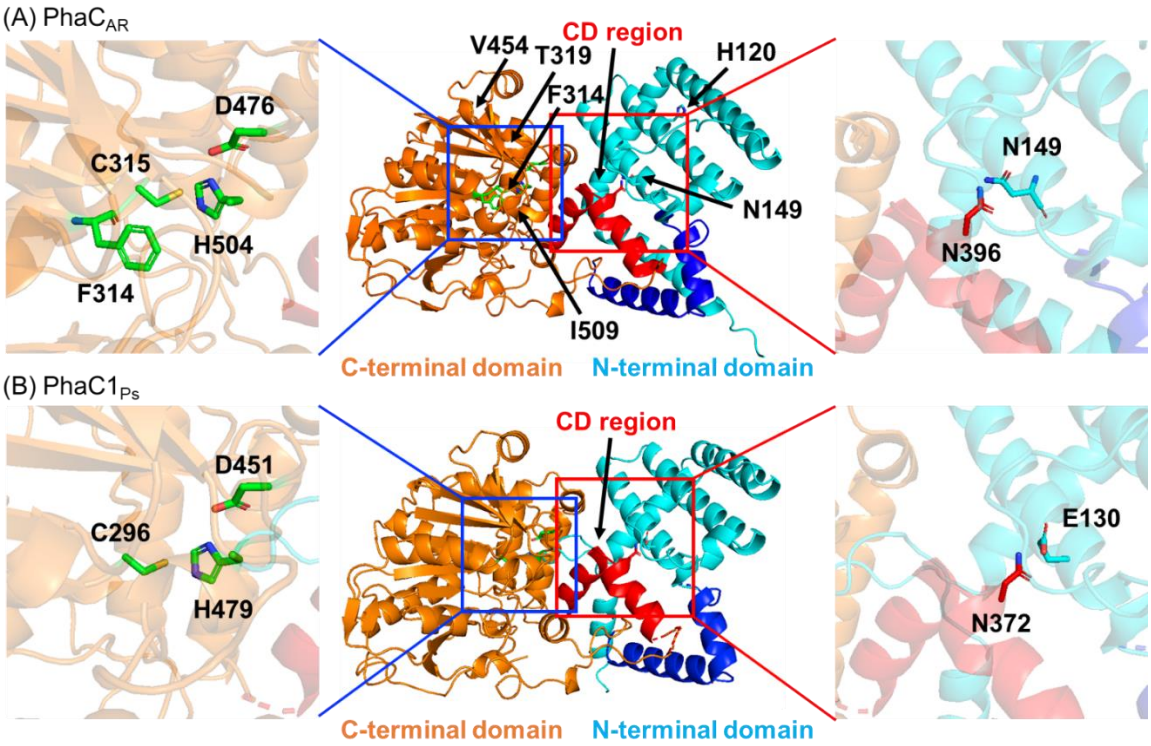

Figure 2-6. Predicted tertiary structures of PhaC$_{AR}$ and PhaC1Ps. Overall structures of PhaC$_{AR}$ (A). Cyan, PhaC$_{Ac}$ region (N-terminal domain); dark blue, part of PhaC$_{Re}$ region (N-terminal domain); orange, part of PhaC$_{Re}$ region (C-terminal domain); and red, cross-domain (CD) region (N-terminal domain). Overall structure of PhaC1Ps (B). Cyan, N-terminal domain; orange, C-terminal domain; and red, CD region. (Left) Magnified images of catalytic residues (Cys315, Asp476, and His504) and beneficial site (Phe314) in PhaC$_{AR}$ and catalytic residues (Cys296, Asp451, and His 479) in PhaC1Ps. (Right) Magnified images of CD regions and Asn149 of PhaC$_{AR}$ and Glu130 of PhaC1Ps. N396 and N372, which presumably interact with the beneficial positions 149 and 130, respectively, are highlighted.

2.5. Conclusions

Directed evolution of the sequence-regulating PHA synthase $PhaC_{AR}$ successfully increased activity toward the MCL substrate 3HHx-CoA. The F314H mutant is particularly useful because of high 3HHx incorporation and its capability to synthesize P(3HHx) homopolymer. The MCL PHA synthesized using class I PHA synthase had an advantage over that of class II enzymes in the polymer molecular weight, which was one order of magnitude higher (M_w ~10^6) than that obtained using a class II enzyme. In addition, these findings enabled me to synthesize a novel MCL-SCL PHA block copolymer P(3HHx)-*b*-P(2HB). The covalent linkage between the P(3HHx) and P(2HB) segments was verified by solvent fractionation. The predicted structure of $PhaC_{AR}$ by Alphafold2 suggests that there is a common mechanism among beneficial mutations in class I and II enzymes.

2.6. References

(1) Tripathi, L.; Wu, L.-P.; Chen, J.; Chen, G.-Q. Synthesis of diblock copolymer poly-3-hydroxybutyrate-*block*-poly-3-hydroxyhexanoate [PHB-*b*-PHHx] by a β-oxidation weakened *Pseudomonas putida* KT2442. *Microbial Cell Factories* **2012**, *11* (1), 44. DOI: 10.1186/1475-2859-11-44.

(2) Pederson, E. N.; McChalicher, C. W. J.; Srienc, F. Bacterial Synthesis of PHA Block Copolymers. *Biomacromolecules* **2006**, *7* (6), 1904-1911. DOI: 10.1021/bm0510101.

(3) Buckley, R. M.; Stubbe, J. Chemistry with an Artificial Primer of Polyhydroxybutyrate Synthase Suggests a Mechanism for Chain Termination. *Biochemistry* **2015**, *54* (12), 2117-2125. DOI: 10.1021/bi501405b.

(4) Matsumoto, K.; Hori, C.; Fujii, R.; Takaya, M.; Ooba, T.; Ooi, T.; Isono, T.; Satoh, T.; Taguchi, S. Dynamic changes of intracellular monomer levels regulate block sequence of polyhydroxyalkanoates in engineered *Escherichia coli*. *Biomacromolecules* **2018**, *19* (2), 662-671. DOI: 10.1021/acs.biomac.7b01768.

(5) Matsumoto, K. i.; Terai, S.; Ishiyama, A.; Sun, J.; Kabe, T.; Song, Y.; Nduko, J. M.; Iwata, T.; Taguchi, S. One-pot microbial production, mechanical properties, and enzymatic degradation of isotactic P[(*R*)-2-hydroxybutyrate] and its copolymer with (*R*)-lactate. *Biomacromolecules* **2013**, *14* (6), 1913-1918. DOI: 10.1021/bm400278j PubMed.

(6) Kageyama, Y.; Tomita, H.; Isono, T.; Satoh, T.; Matsumoto, K. Artificial polyhydroxyalkanoate poly[2-hydroxybutyrate-*block*-3-hydroxybutyrate] elastomer-like material. *Scientific Reports* **2021**, *11* (1), 22446. DOI: 10.1038/s41598-021-01828-9.

(7) Feng, H.; Lu, X.; Wang, W.; Kang, N. G.; Mays, J. W. Block Copolymers: Synthesis, Self-Assembly, and Applications. *Polymers (Basel)* **2017**, *9* (10). DOI: 10.3390/polym9100494 From NLM.

(8) Nomura, C. T.; Taguchi, S. PHA synthase engineering toward superbiocatalysts for custom-made biopolymers. *Appl Microbiol Biotechnol* **2007**, *73* (5), 969-979. DOI: 10.1007/s00253-006-0566-4.

(9) Wang, Q.; Tappel, R. C.; Zhu, C.; Nomura, C. T. Development of a new strategy for production of medium-chain-length polyhydroxyalkanoates by recombinant *Escherichia coli* via inexpensive non-fatty acid feedstocks. *Appl Environ Microbiol* **2012**, *78* (2), 519-527. DOI: 10.1128/aem.07020-11 From NLM.

(10) Taguchi, S.; Maehara, A.; Takase, K.; Nakahara, M.; Nakamura, H.; Doi, Y. Analysis of mutational effects of a polyhydroxybutyrate (PHB) polymerase on bacterial PHB

accumulation using an in vivo assay system. *FEMS Microbiol Lett* **2001**, *198* (1), 65-71. DOI: 10.1111/j.1574-6968.2001.tb10620.x From NLM.

(11) Spiekermann, P.; Rehm, B. H.; Kalscheuer, R.; Baumeister, D.; Steinbuchel, A. A sensitive, viable-colony staining method using Nile red for direct screening of bacteria that accumulate polyhydroxyalkanoic acids and other lipid storage compounds. *Arch Microbiol* **1999**, *171* (2), 73-80. DOI: 10.1007/s002030050681.

(12) Tomita, H.; Satoh, K.; Nomura, C. T.; Matsumoto, K. Biosynthesis of poly(glycolate-*co*-3-hydroxybutyrate-*co*-3-hydroxyhexanoate) in *Escherichia coli* expressing sequence-regulating polyhydroxyalkanoate synthase and medium-chain-length 3-hydroxyalkanoic acid coenzyme A ligase. *Bioscience, Biotechnology, and Biochemistry* **2021**, *86* (2), 217-223. DOI: 10.1093/bbb/zbab198.

(13) Hori, C.; Oishi, K.; Matsumoto, K. i.; Taguchi, S.; Ooi, T. Site-directed saturation mutagenesis of polyhydroxylalkanoate synthase for efficient microbial production of poly[(*R*)-2-hydroxybutyrate]. *Journal of Bioscience and Bioengineering* **2018**, *125* (6), 632-636. DOI: 10.1016/j.jbiosc.2017.11.013.

(14) Matsumoto, K.; Takase, K.; Aoki, E.; Doi, Y.; Taguchi, S. Synergistic effects of Glu130Asp substitution in the type II polyhydroxyalkanoate (PHA) synthase: Enhancement of PHA production and alteration of polymer molecular weight. *Biomacromolecules* **2005**, *6* (1), 99-104. DOI: 10.1021/bm049650b.

(15) Kato, M.; Bao, H. J.; Kang, C. K.; Fukui, T.; Doi, Y. Production of a novel copolyester of 3-hydroxybutyric acid and medium-chain-length 3-hydroxyalkanoic acids by *Pseudomonas* sp. 61-3 from sugars. *Applied Microbiology and Biotechnology* **1996**, *45* (3), 363-370. DOI: 10.1007/s002530050697.

(16) Yamada, M.; Matsumoto, K.; Nakai, T.; Taguchi, S. Microbial production of lactate-enriched poly[(*R*)-lactate-*co*-(*R*)-3-hydroxybutyrate] with novel thermal properties. *Biomacromolecules* **2009**, *10* (4), 677-681. DOI: 10.1021/bm8013846.

(17) Matsumoto, K.; Shozui, F.; Satoh, Y.; Tajima, K.; Munekata, M.; Taguchi, S. Kinetic analysis of engineered polyhydroxyalkanoate synthases with broad substrate specificity. *Polymer journal* **2009**, *41* (3), 237-240.

(18) Bradford, M. M. A rapid and sensitive method for the quantitation of microgram quantities of protein utilizing the principle of protein-dye binding. *Analytical Biochemistry* **1976**, *72* (1), 248-254. DOI: 10.1016/0003-2697(76)90527-3.

(19) Taguchi, S.; Nakamura, H.; Hiraishi, T.; Yamato, I.; Doi, Y. *In vitro* Evolution of a Polyhydroxybutyrate Synthase by Intragenic Suppression-Type Mutagenesis1. *The*

Journal of Biochemistry **2002**, *131* (6), 801-806. DOI: 10.1093/oxfordjournals.jbchem.a003168 (acccessed 7/19/2023).

(20) Peter, D. M.; Vogeli, B.; Cortina, N. S.; Erb, T. J. A Chemo-Enzymatic Road Map to the Synthesis of CoA Esters. *Molecules* **2016**, *21* (4), 517. DOI: 10.3390/molecules21040517.

(21) Takase, K.; Matsumoto, K. i.; Taguchi, S.; Doi, Y. Alteration of Substrate Chain-Length Specificity of Type II Synthase for Polyhydroxyalkanoate Biosynthesis by *in vitro* Evolution: *in vivo* and *in vitro* Enzyme Assays. *Biomacromolecules* **2004**, *5* (2), 480-485. DOI: 10.1021/bm034323+.

(22) Curley, J. M.; Hazer, B.; Lenz, R. W.; Fuller, R. C. Production of Poly(3-hydroxyalkanoates) Containing Aromatic Substituents by *Pseudomonas oleovorans*. *Macromolecules* **1996**, *29* (5), 1762-1766. DOI: 10.1021/ma951185a.

(23) Wu, B.; Lenz, R. W.; Hazer, B. Polymerization of Methyl Methacrylate and Its Copolymerization with ε-Caprolactone Catalyzed by Isobutylalumoxane Catalyst. *Macromolecules* **1999**, *32* (20), 6856-6859. DOI: 10.1021/ma990166o.

(24) Eisenberg, D.; Schwarz, E.; Komaromy, M.; Wall, R. Analysis of membrane and surface protein sequences with the hydrophobic moment plot. *Journal of Molecular Biology* **1984**, *179* (1), 125-142. DOI: 10.1016/0022-2836(84)90309-7.

(25) Wong, Y. M.; Brigham, C. J.; Rha, C.; Sinskey, A. J.; Sudesh, K. Biosynthesis and characterization of polyhydroxyalkanoate containing high 3-hydroxyhexanoate monomer fraction from crude palm kernel oil by recombinant *Cupriavidus necator*. *Bioresour Technol* **2012**, *121*, 320-327. DOI: 10.1016/j.biortech.2012.07.015.

(26) Kamiya, N.; Yamamoto, Y.; Inoue, Y.; Chujo, R.; Doi, Y. Microstructure of bacterially synthesized poly(3-hydroxybutyrate-*co*-3-hydroxyvalerate). *Macromolecules* **1989**, *22* (4), 1676-1682. DOI: 10.1021/ma00194a030.

(27) Wang, H. H.; Zhou, X. R.; Liu, Q.; Chen, G. Q. Biosynthesis of polyhydroxyalkanoate homopolymers by *Pseudomonas putida*. *Appl Microbiol Biotechnol* **2011**, *89* (5), 1497-1507. DOI: 10.1007/s00253-010-2964-x.

(28) Kichise, T.; Taguchi, S.; Doi, Y. Enhanced accumulation and changed monomer composition in polyhydroxyalkanoate (PHA) copolyester by *in vitro* evolution of *Aeromonas caviae* PHA synthase. *Appl Environ Microbiol* **2002**, *68* (5), 2411-2419. DOI: 10.1128/AEM.68.5.2411-2419.2002.

(29) Matsusaki, H.; Abe, H.; Doi, Y. Biosynthesis and Properties of Poly(3-hydroxybutyrate-*co*-3-hydroxyalkanoates) by Recombinant Strains of *Pseudomonas* sp. 61-3. *Biomacromolecules* **2000**, *1* (1), 17-22. DOI: 10.1021/bm9900040.

(30) Harada, K.; Kobayashi, S.; Oshima, K.; Yoshida, S.; Tsuge, T.; Sato, S. Engineering of *Aeromonas caviae* Polyhydroxyalkanoate Synthase Through Site-Directed Mutagenesis for Enhanced Polymerization of the 3-Hydroxyhexanoate Unit. *Front Bioeng Biotechnol* **2021**, *9*, 627082. DOI: 10.3389/fbioe.2021.627082.

(31) Yuan, W.; Jia, Y.; Tian, J.; Snell, K. D.; Müh, U.; Sinskey, A. J.; Lambalot, R. H.; Walsh, C. T.; Stubbe, J. Class I and III Polyhydroxyalkanoate Synthases from *Ralstonia eutropha* and *Allochromatium vinosum*: Characterization and Substrate Specificity Studies. *Archives of Biochemistry and Biophysics* **2001**, *394* (1), 87-98. DOI: 10.1006/abbi.2001.2522.

(32) Cramer, P. AlphaFold2 and the future of structural biology. *Nat Struct Mol Biol* **2021**, *28* (9), 704-705. DOI: 10.1038/s41594-021-00650-1.

(33) Wittenborn, E. C.; Jost, M.; Wei, Y.; Stubbe, J.; Drennan, C. L. Structure of the Catalytic Domain of the Class I Polyhydroxybutyrate Synthase from *Cupriavidus necator*. *J Biol Chem* **2016**, *291* (48), 25264-25277. DOI: 10.1074/jbc.M116.756833.

(34) Chek, M. F.; Kim, S. Y.; Mori, T.; Arsad, H.; Samian, M. R.; Sudesh, K.; Hakoshima, T. Structure of polyhydroxyalkanoate (PHA) synthase PhaC from *Chromobacterium* sp. USM2, producing biodegradable plastics. *Sci Rep* **2017**, *7* (1), 5312. DOI: 10.1038/s41598-017-05509-4 From NLM.

(35) Chek, M. F.; Kim, S. Y.; Mori, T.; Tan, H. T.; Sudesh, K.; Hakoshima, T. Asymmetric Open-Closed Dimer Mechanism of Polyhydroxyalkanoate Synthase PhaC. *iScience* **2020**, *23* (5), 101084. DOI: 10.1016/j.isci.2020.101084.

(36) Matsumoto, K. i.; Takase, K.; Aoki, E.; Doi, Y.; Taguchi, S. Synergistic Effects of Glu130Asp Substitution in the Type II Polyhydroxyalkanoate (PHA) Synthase: Enhancement of PHA Production and Alteration of Polymer Molecular Weight. *Biomacromolecules* **2005**, *6* (1), 99-104. DOI: 10.1021/bm049650b.

(37) Lim, H.; Chuah, J.-A.; Chek, M. F.; Tan, H. T.; Hakoshima, T.; Sudesh, K. Identification of regions affecting enzyme activity, substrate binding, dimer stabilization and polyhydroxyalkanoate (PHA) granule morphology in the PHA synthase of *Aquitalea* sp. USM4. *International Journal of Biological Macromolecules* **2021**, *186*, 414-423. DOI: 10.1016/j.ijbiomac.2021.07.041.

(38) Kim, Y. J.; Choi, S. Y.; Kim, J.; Jin, K. S.; Lee, S. Y.; Kim, K. J. Structure and function of the N-terminal domain of Ralstonia eutropha polyhydroxyalkanoate synthase, and the proposed structure and mechanisms of the whole enzyme. *Biotechnol J* **2017**, *12* (1). DOI: 10.1002/biot.201600649 From NLM.

Masayoshi Tomoi, (2019) By evolutionary engineering methods sequence-controllable polyhydroxyalkanoic acid modification of substrate specificity of polymerization enzyme $PhaC_{AR}$ [Master thesis, Hokkaido University, Faculty of Engineering, Department of Applied Science and Engineering, Applied Chemistry Course, Laboratory of Biomolecular Engineering]

Guex Maureen, (2019) Engineering of polyhydroxyalkanoate synthase for the production of sequence-regulated polymers [Master thesis, HES-SO Valais-Wallis, University of Applied Sciences and Arts, Western Switzerland]

Appendixes

Appendix-I. Amino acid sequence of *phaC*$_{AR}$ with the codon-optimized *phaC*$_{Re}$ region

msqpsygplfealahyndkllamakaqtertaqallqtnlddlgqvleqgsqqpwqliqaqmnwwqdqlklmqhtl lksagqpsepvitpersdrrfkaeawseqpiydylkqsylltarhllasvdalegvpqksrerlrfftrqyvnamapsNFL ATNPEAQRLLIESGGESLRAGVRNMMEDLTRGKISQTDESAFEVGRNVAVTEG AVVFENEYFQLLQYKPLTDKVHARPLLMVPPCINKYYILDLQPESSLVRHVVEQ GHTVFLVSWRNPDASMAGSTWDDYIEHAAIRAIEVARDISGQDKINVLGFCVG GTIVSTALAVLAARGEHPAASVTLLTTLLDFADTGILDVFVDEGHVQLREATLG GGAGAPCALLRGLELANTFSFLRPNDLVWNYVVDNYLKGNTPVPFDLLFWNG DATNLPGPWYCWYLRHTYLQNELKVPGKLTVCGVPVDLASIDVPTYIYGSRED HIVPWTAAYASTALLANKLRFVLGASGHIAGVINPPAKNKRSHWTNDALPESP QQWLAGAIEHHGSWWPDWTAWLAGQAGAKRAAPANYGNARYRAIEPAPGR YVKAKA

Lowercase and uppercase letters indicate the PhaC$_{Ac}$ and PhaC$_{Re}$ regions, respectively. The codons of the underlined amino acid residues were optimized for *E. coli*.

Appendix-II: Calculation of D value of P(3HB-co-3HHx) produced by PhaCARF314H. Based on 13C NMR of P(3HB-co-3HHx) produced by PhaCARF314H (Fig. S3), D value was calculated as follows. From the signals of carbonyl carbon at δ ~ 169-170, the relative resonance intensities ascribed to each dyad sequence were determined.

F3HB-3HB = 0.50

F3HB-3HHx + F3HHx-3HB = 0.24

F3HHx-3HHx = 0.12

Here, FX-Y is a relative resonance intensity corresponding to X-Y dyad. From these values, D value was calculated as follows.

D = (F3HB-3HB × F3HHx-3HHx)/(F3HB-3HHx × F3HHx-3HB) = 4.2

This suggests that the copolymer has a random sequence.

D ~ 0: alternative copolymer

D ~ 1: random copolymer

D >> 1: block copolymer

Appendix-III: Full spectra of NMR analysis, Immunoblot analysis data, the predicted structure of $PhaC_{AR}$

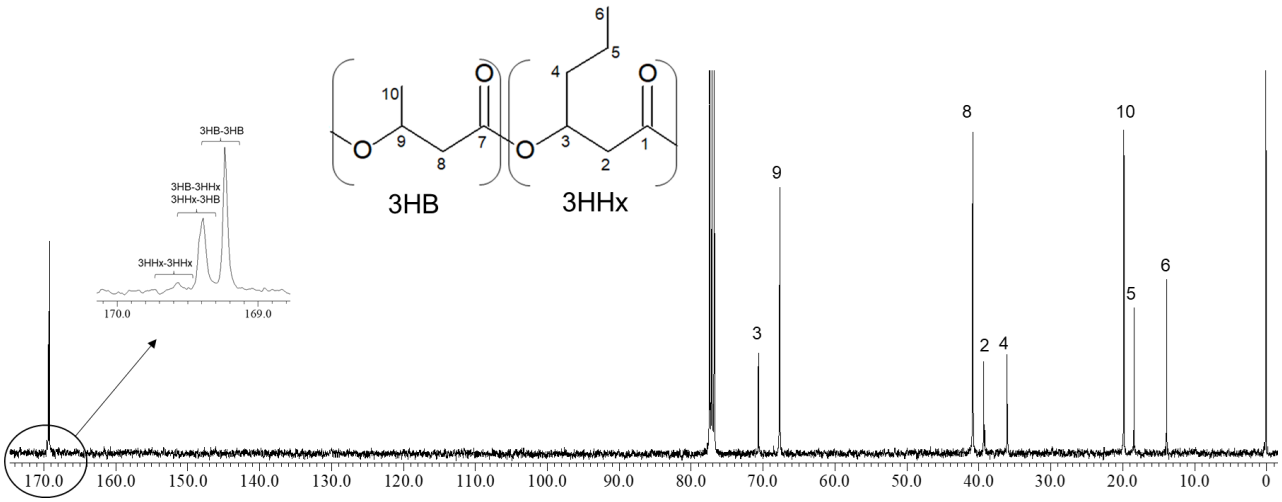

Figure S2-1. ^{13}C NMR spectrum of P(3HB-*co*-3HHx) produced by parent $PhaC_{AR}$.

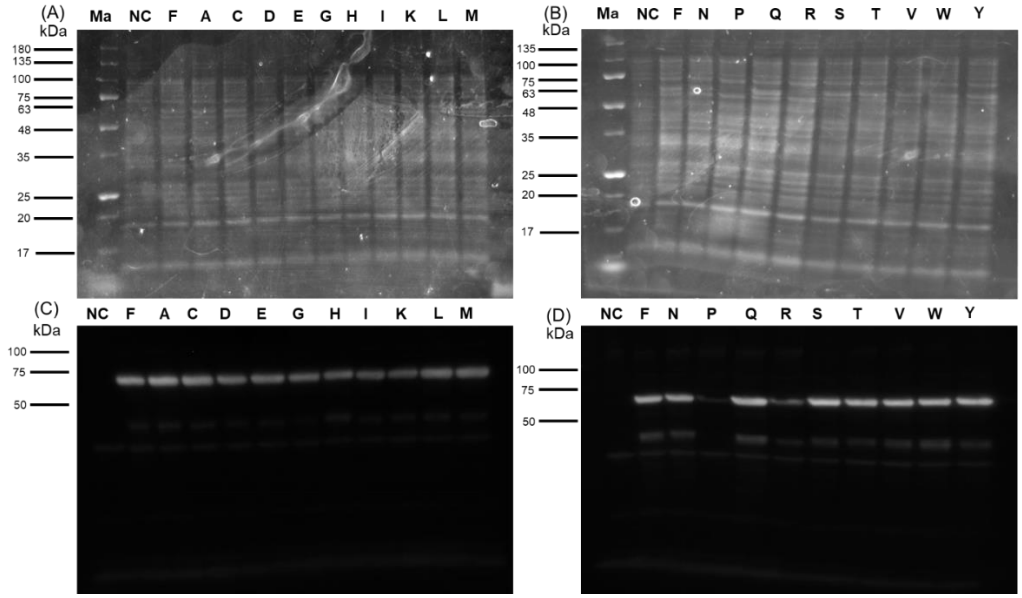

Figure S2-2. Immunoblot analysis of saturation mutations at position 314 in $PhaC_{AR}$ using crude cell extracts and the anti-$PhaC_{Re}$ antibody. Ma, size maker (invisible in chemiluminescence). NC, negative control (the crude extract of *E. coli* harboring the empty plasmid, pUC18); single letters indicate F314X substitutions.

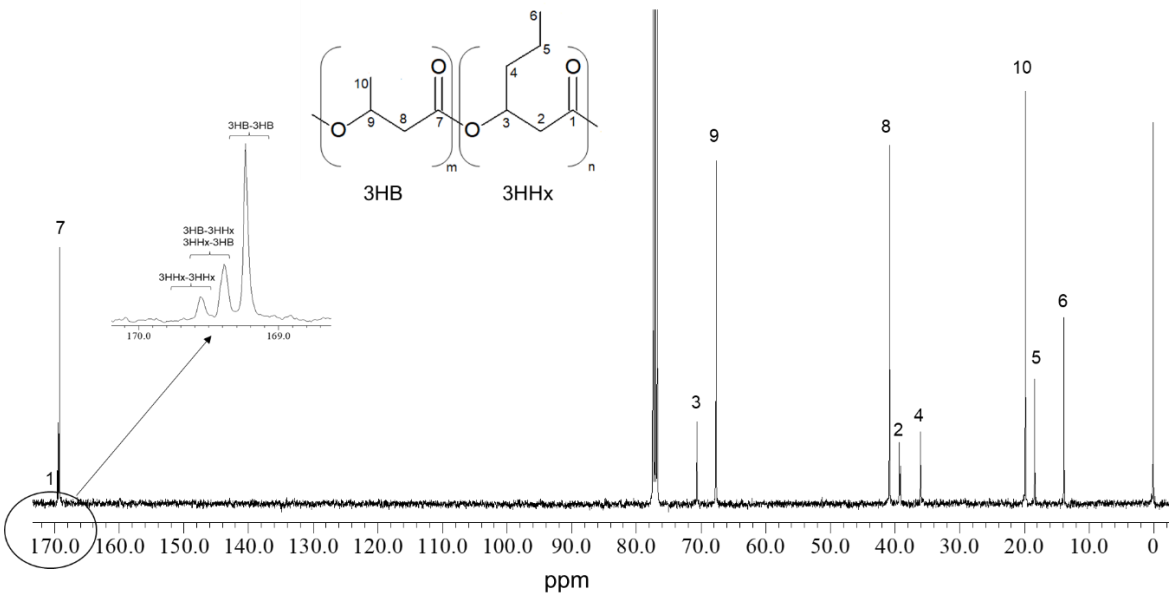

Figure S2-3. ^{13}C NMR spectrum of P(3HB-co-3HHx) produced by PhaCARF314H

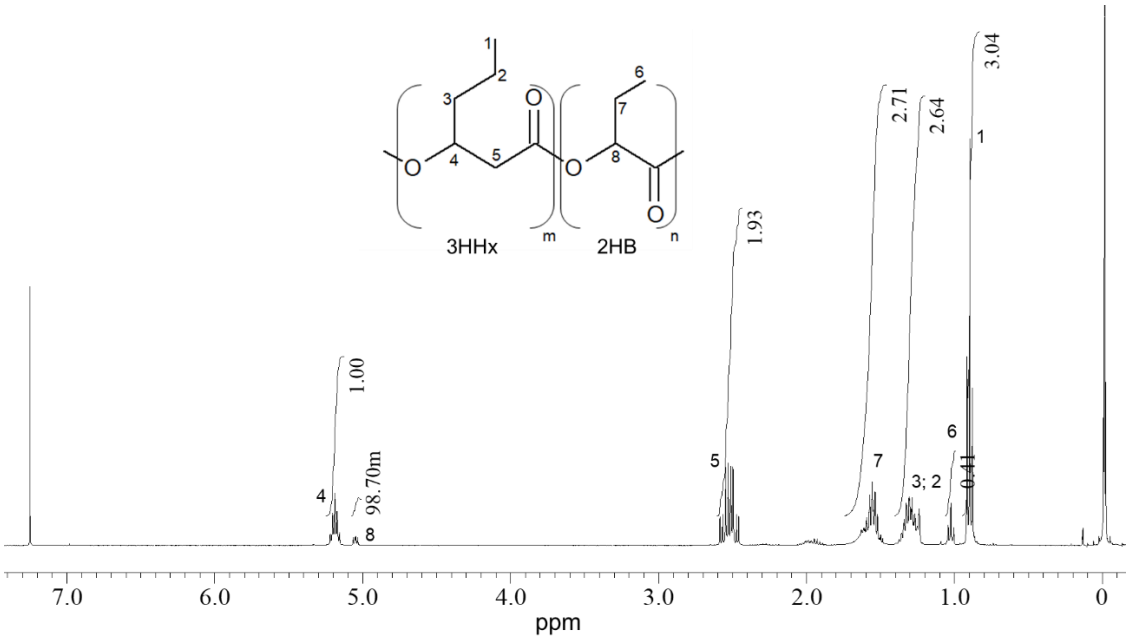

Figure S2-4. ^{1}H NMR spectrum of P(3HHx)-b-(2HB) produced by PhaCARF314H

(A) Original P(3HHx)-*b*-(2HB) before fractionation

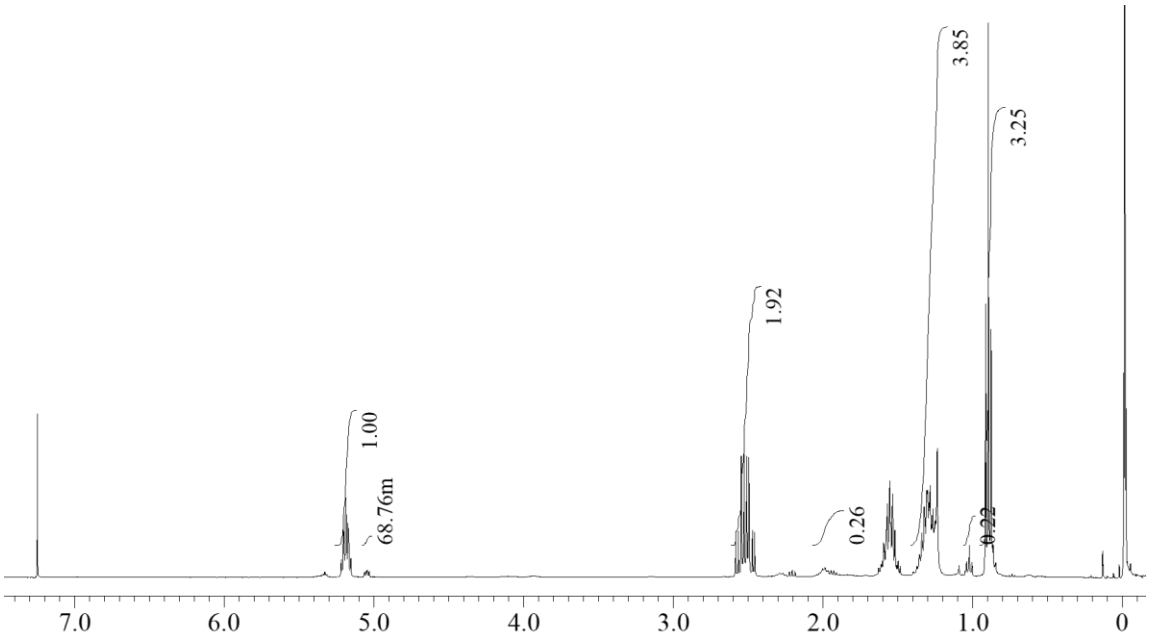

(B) P(3HHx)-*b*-(2HB) in the cyclohexane-soluble fraction

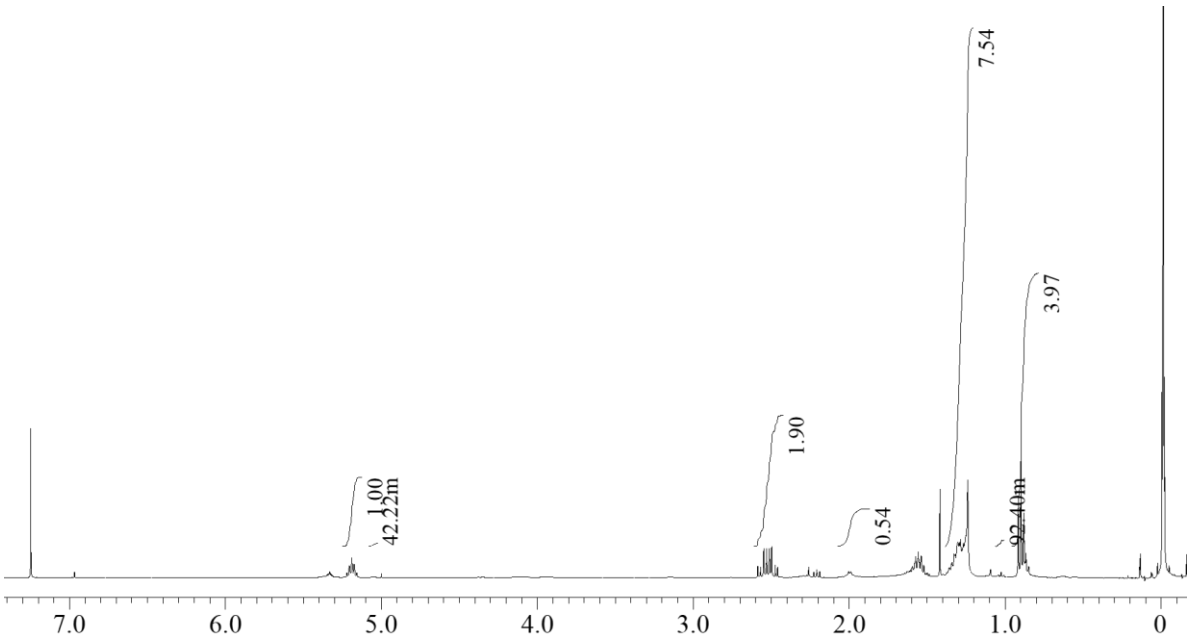

(C) P(3HHx)-*b*-(2HB) in the cyclohexane-insoluble fraction

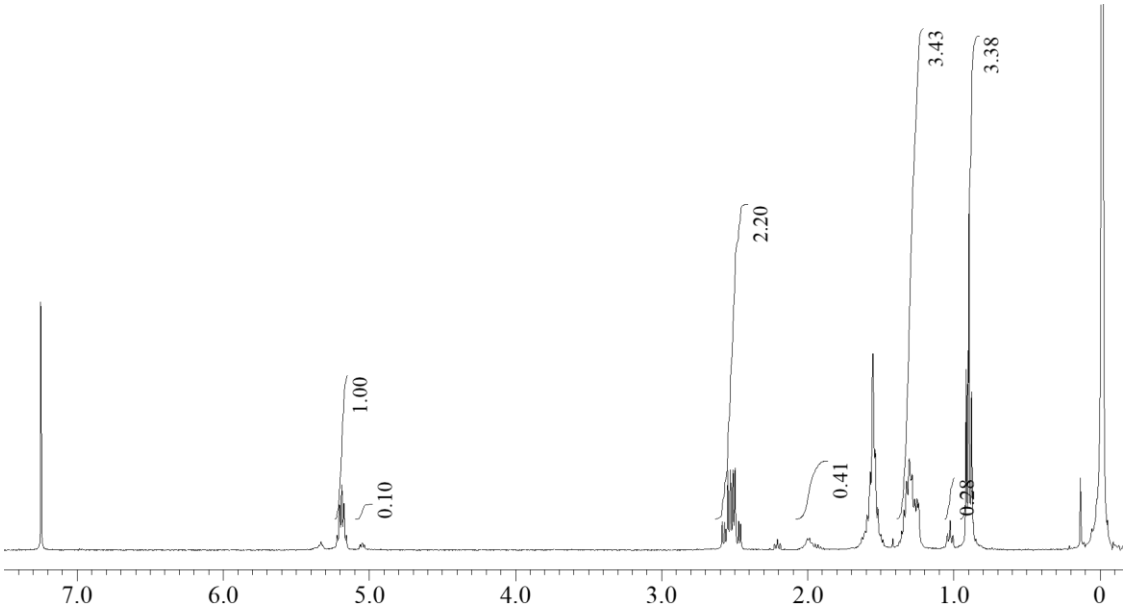

(D) Blend of P(3HHx) and P(2HB) before fractionation

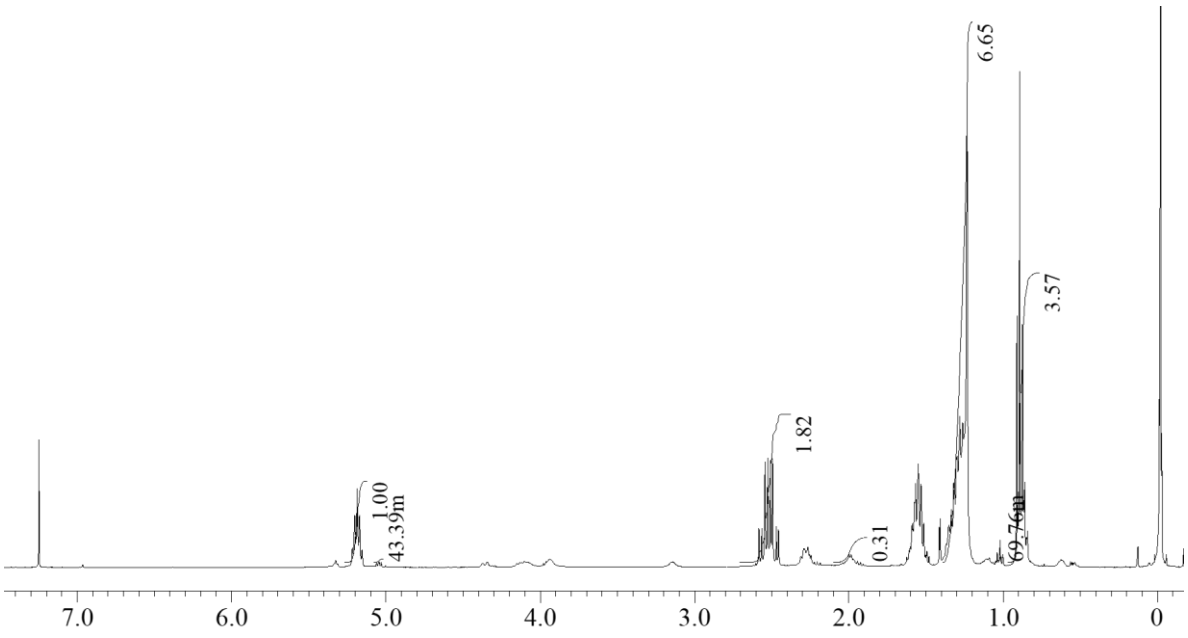

(E) Cyclohexane-soluble fraction of the blend

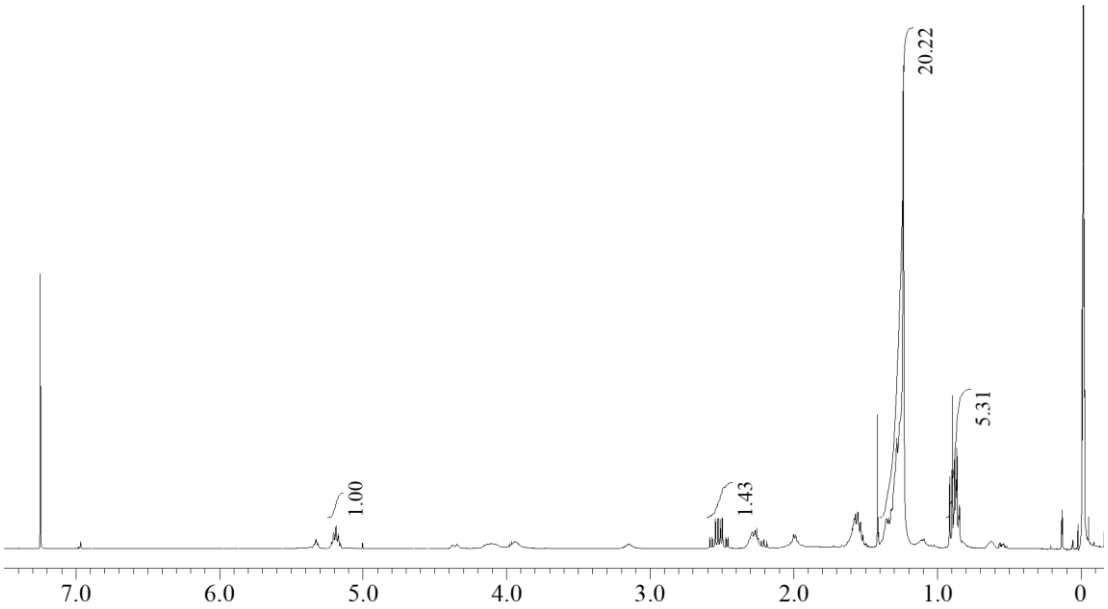

(F) Cyclohexane-insoluble fraction of the blend

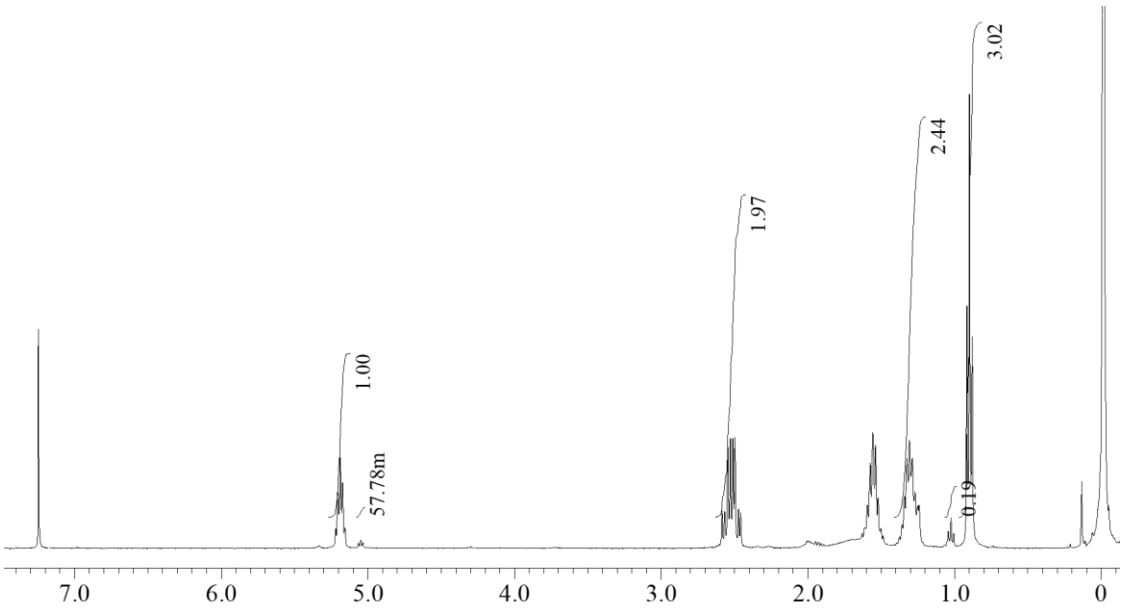

(G) P(3HHx) before fractionation

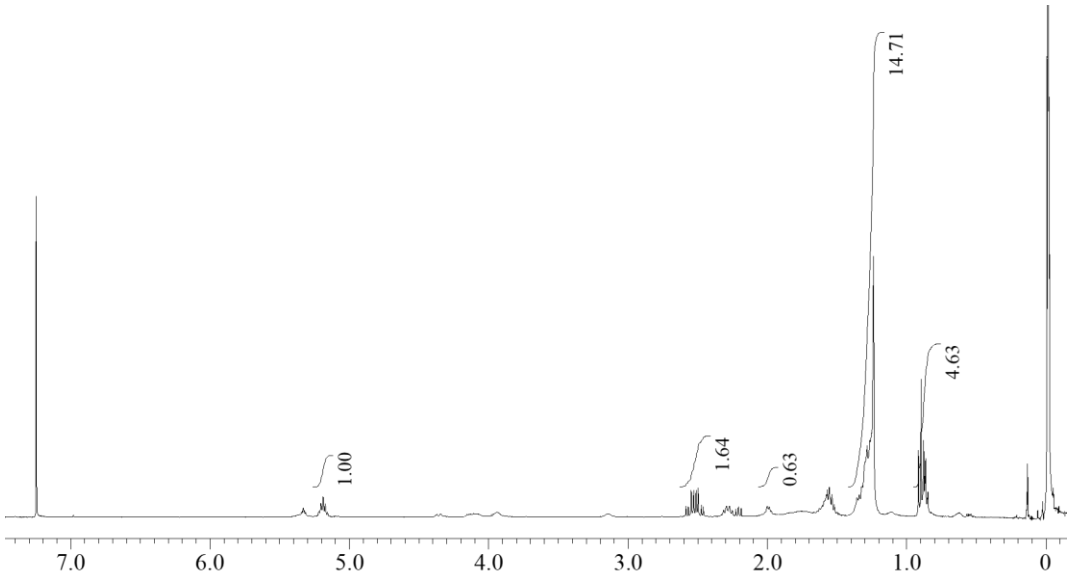

(H) P(3HHx) in the cyclohexane-soluble fraction

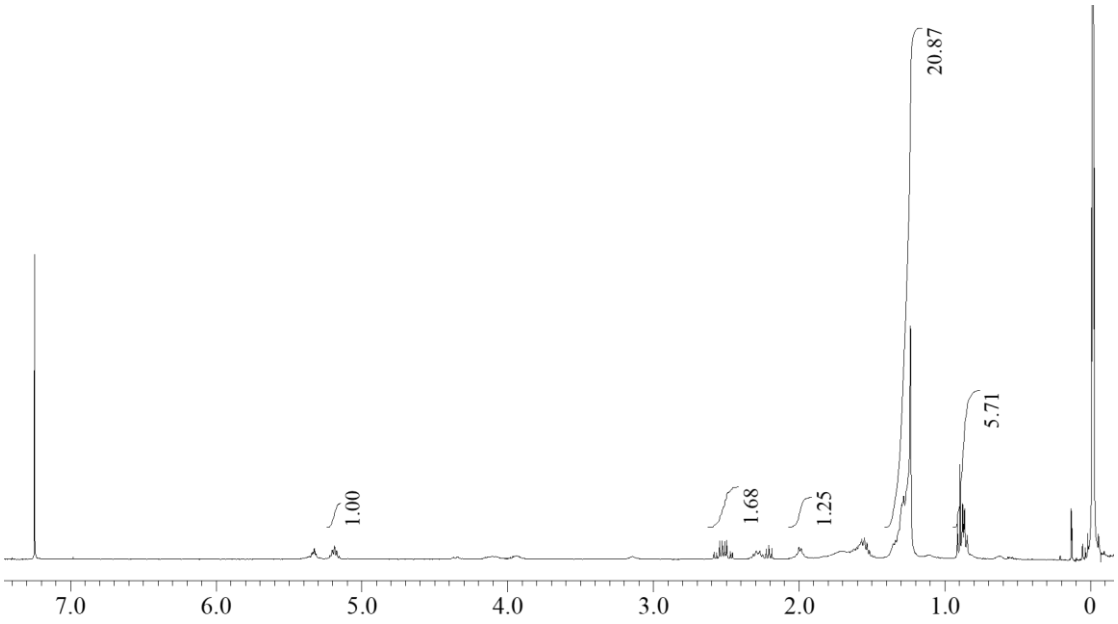

(I) P(3HHx) in the cyclohexane-insoluble fraction

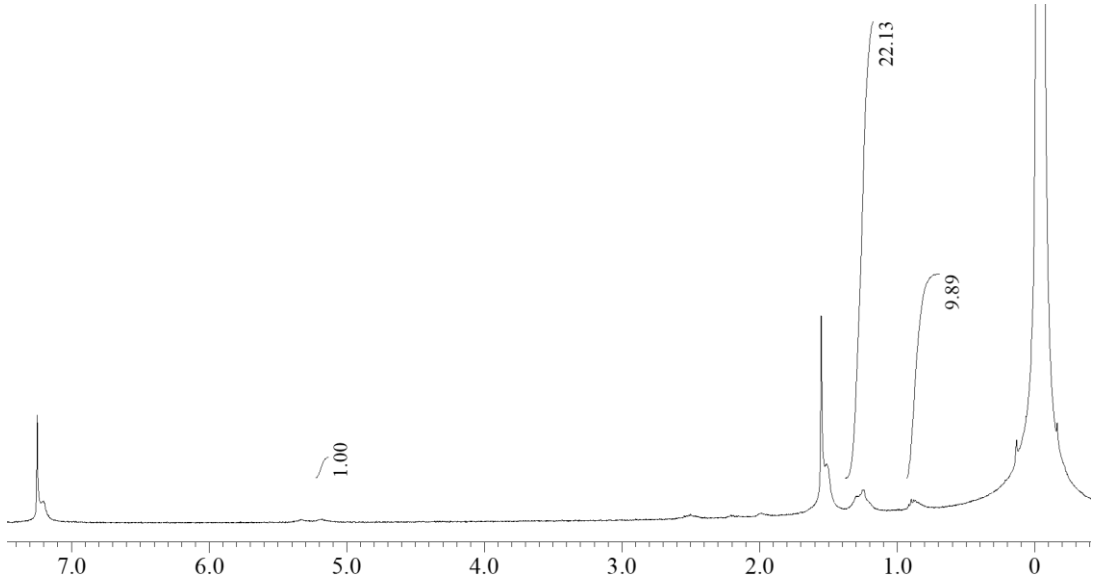

(J) P(2HB) before fractionation

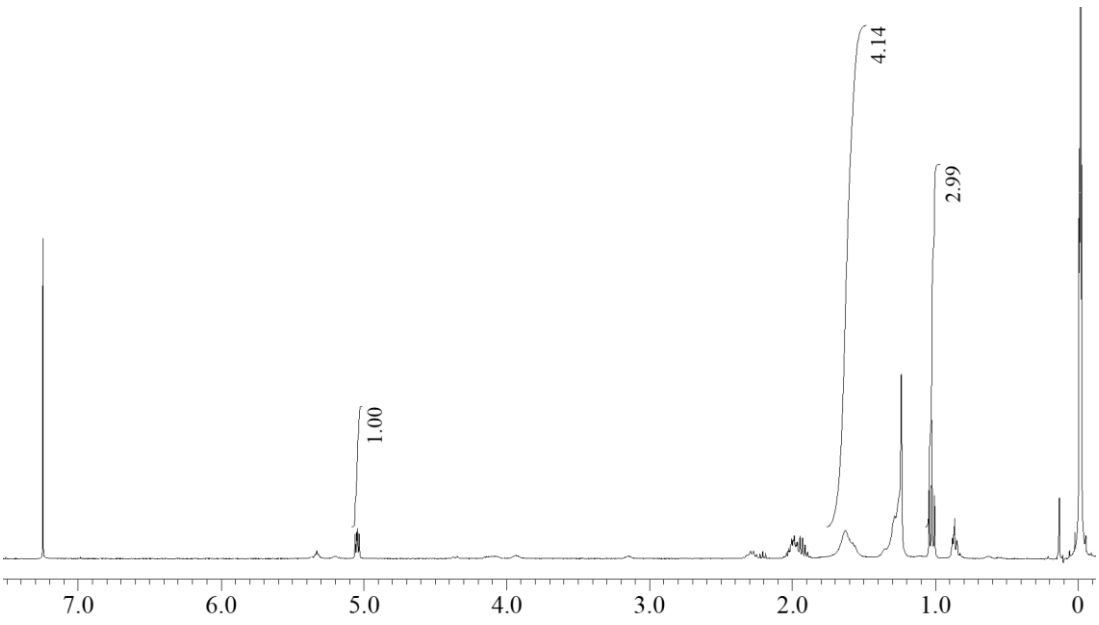

(K) P(2HB) in the cyclohexane-soluble fraction

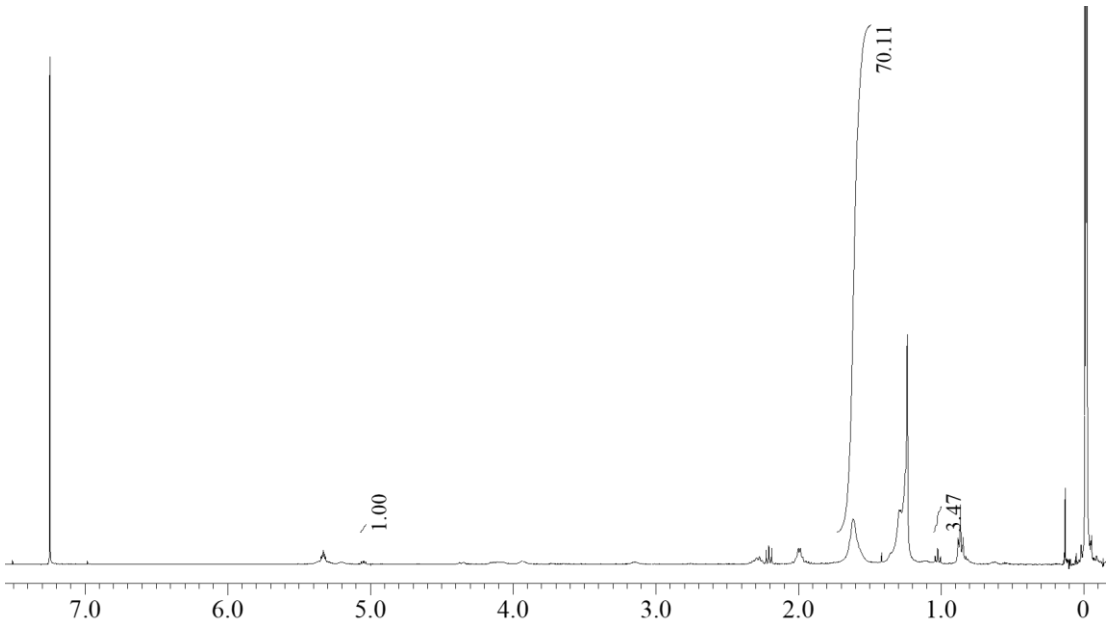

(L) P(2HB) in the cyclohexane-insoluble fraction

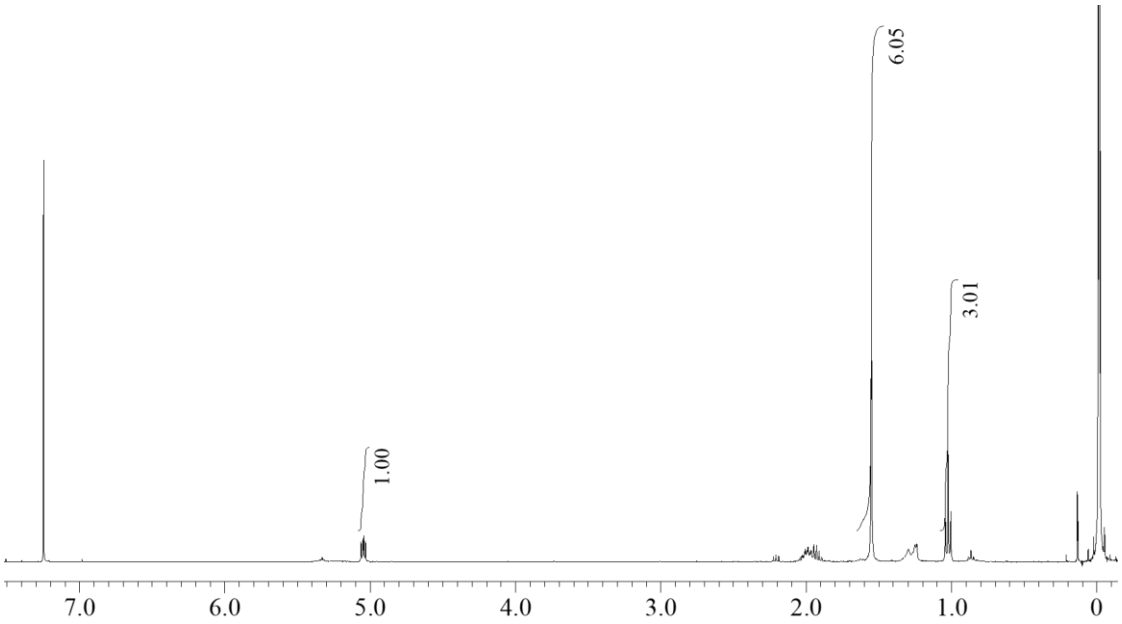

Figure S2-5. ^{1}H NMR analysis of the original block copolymer, blend polymer, and homopolymer of P(3HHx) and P(2HB) before and after fractionation (A, B, C, D, E, F, G, H, K, and L)

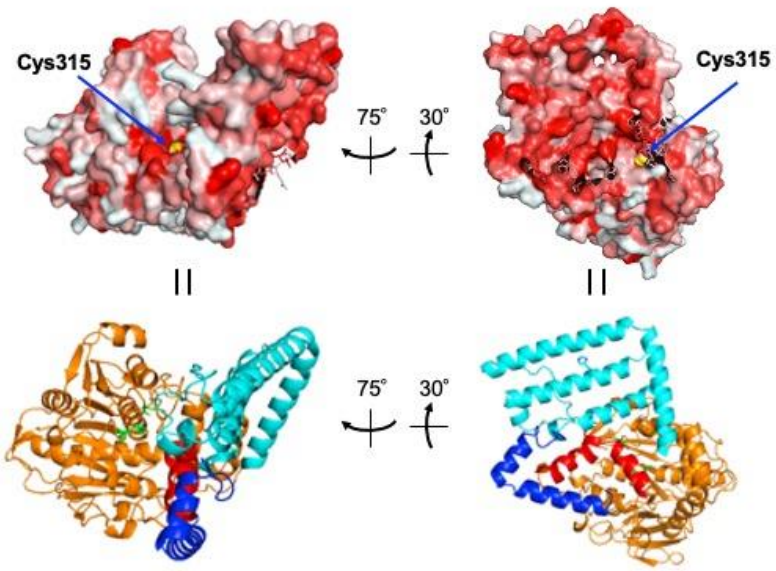

Figure S2-6. (Upper) Calculated surface hydrophobicity of the predicted structure of PhaC$_{AR}$. Red: hydrophobic, white: hydrophilic. N-terminal 30 residues are not shown because of their low fidelity of the prediction. The yellow residue is the catalytic center Cys315. (Lower) The corresponding cartoon images. The colors are same as Figure 2-6.

Chapter 3.

Effect of mutations on LA-incorporation ability in block copolymer production

3.1. Introduction

In the Chapter 2, I had successfully on designing soft segment, P(3HHx) and enabled to synthesize a new type of PHA block copolymer, P(3HHx)-*b*-7mol%P(2HB). Based on the results, it is crucial to take hard segments into consideration when broadening the substrate range of $PhaC_{AR}$ to include MCL-SCL block copolymers.

In this chapter, I aimed to utilize polylactate [PLA or poly(2-hydroxypropionate)] as a such hard segment of PHA block copolymers. PLAs are utilized as biobased, biocompatible, non-toxic, and processible polymer materials in various applications. They are also a potent segment of block copolymers because of their properties, such as toughness and transparency. In addition, PLA, and PHAs are immiscible.[1] Immiscibility is necessary for forming microphase separation, which plays an important role in the physical properties of block copolymers.[2]

A breakthrough discovery was made in 2008, which was an engineered bacterial PHA synthase, $PhaC1_{Ps}$STQK, capable of synthesizing LA-based polyesters.[3] The enzyme incorporates LA units into the polymer chain using the CoA thioester of LA, lactyl (LA)-CoA, as a substrate. $PhaC1_{Ps}$STQK is a class II PHA synthase derived from *Pseudomonas* sp. 61-3 containing Ser325Thr/Gln481Lys mutations. In contrast to the engineered enzyme, natural PHA synthases strictly recognize (*R*)-3-hydroxyacyl (3HA)-CoAs as the substrates [3-5] and have no activity toward LA-CoA. Notably, $PhaC1_{Ps}$STQK enantiospecifically polymerizes D-LA-CoA. Thus, enantiopure D-LA-based polymers can be synthesized from inexpensive feedstock using a D-LA-producing microbial platform, such as *Escherichia coli,* expressing $PhaC1_{Ps}$STQK.

A drawback of $PhaC1_{Ps}$STQK was, however, the limited regulation of LA fraction in the copolymer. There was an inverse relationship between LA fraction and polymer production [3, 6] when $PhaC1_{Ps}$STQK polymerized random copolymers of LA and 3HAs.

In particular, biosynthesis of PDLA homopolymer (and PDLA-like copolymer) is severely limited to low yield and low molecular weight. The phenomenon is presumably due to the high glass transition temperature (T_g) of PLA (60 °C) than that of a typical PHA poly(3-hydroxybutyrate) (4 °C). To overcome the limitation, several attempts have been done to increase the activity of PhaC1$_{Ps}$STQK by means of *in vitro* evolution and to explore other LA-CoA-polymerizing PhaCs. Class I PhaC was also tested. A class I PhaC from *Ralstonia eutropha* (*Cupriavidus necator*) with A510 mutation, which corresponds to position 481 in PhaC1$_{Ps}$STQK, slightly exhibited LA-incorporating capacity.[7] Despite these efforts, high-molecular-weight PDLA biosynthesis remained unachieved.

The 2HA units play an essential role in block copolymerization of PHA. PhaC$_{AR}$ is the first class I enzyme that efficiently incorporates 2HA units, 2-hydroxybutyrate (2HB), and glycolate. For examples, P(3HP)-*b*-P(2HB)[8], P(3HB)-*b*-P(GL-*co*-3HB)[9] and P(3HB-*co*-3HHx)-*b*-P(GL-*co*-3HB)[10] were synthesized from the corresponding precursors. However, in the previous polymer productions using PhaC$_{AR}$, LA units were not detected despite the intrinsic LA production of *E. coli*. Previously, we performed the directed evolution of PhaC$_{AR}$ to reinforce the activity toward 3HHx-CoA and successfully identified three beneficial point mutations N149D (ND), F314H (FH), and T319I (TI) that increased the 3HHx-incorporating capacity of the enzyme.[11] In order to find a beneficial mutant that can incorporate significantly LA units, there two new mutants were created including NDFH (A pairwise mutant PhaC$_{AR}$ ND/FH) and NDFHTI (contain triple mutations ND, FH, and TI). Therefore, I conceived the idea of using these mutants to synthesize LA-containing polymers. Notably, these mutations were effective in incorporating LA. Using the evolved PhaC$_{AR}$, a novel PHA block copolymer containing PLA as a segment was synthesized.

3.2. Materials and Methods

3.2.1. Plasmid construction

Two beneficial mutations in $PhaC_{AR}$, namely, N149D (ND) and F314H (FH), were identified previously.[11] $pBSP_{Re}phaC_{AR}$N149DpctalkK and $pBSP_{Re}phaC_{AR}$F314HpctalkK were digested by *Nde*I and *Bgl*II, and the resulting 0.5 and 8.3 kb fragments, respectively, were ligated to yield $pBSP_{Re}phaC_{AR}$N149DF314HpctalkK (NDFH), which harbors a pairwise mutation in $PhaC_{AR}$.

3.2.2. Culture conditions, polymer extraction, and analysis

Recombinant *E. coli* JM109 harboring $pBSP_{Re}phaC_{AR}$pctalkK and its derivatives were used for polymer production. The cells were grown on 1.5 mL of LB medium containing 100 μg/mL of ampicillin at 30 °C for 12 h for preculture. The seed culture was used to inoculate 100 mL of LB medium containing 1.0 g/L of sodium (*R*,*S*)-3HHx, 2.5 g/L of sodium (*R*,*S*)-3HB, and/or 10.0 g/L of sodium D-LA [(*R*)-LA] in 500-mL shake flasks, which were cultivated with reciprocal shaking at 120 rpm and 30 °C for 48 h. LA-Na was prepared by neutralizing 99% D-lactic acid with sodium hydroxide (Musashino Chemical Laboratory, Ltd.). 3HHx-Na was prepared by hydrolyzing ethyl 3-hydrohexanoate as previously described.[12] All chemicals were purchased from Tokyo Chemical Industry (Japan), Junsei Chemical (Japan), or FUJIFILM Wako Pure Chemicals Corporation unless otherwise stated. The polymers were extracted from lyophilized cells with chloroform for 48 h at 60 °C and purified by reprecipitation by adding an excess amount of methanol as previously described.[11] The purified polymers were subjected to ^{1}H NMR, ^{13}C NMR, and DOSY-NMR analyses. The molecular weight of the polymers was determined using size-exclusion chromatography (JASCO Corporation, Japan) equipped with two tandem Shodex K-806L columns (with the range of M_w 3×10^2–2×10^8

(particle size 10 µm, Shodex, Japan), particle size 10 µm. Polystyrene standards were used for calibration.[13]

3.2.3. Chiral gas chromatography (GC)

P(49 mol% 3HHx-*co*-LA) was dissolved in 500 µL of chloroform to a LA concentration of 5 mg/mL and combined with 500 µL of 15 vol% sulfuric acid in ethanol. The mixture was heated at 100 °C for 2 h for ethanolysis. PDLA and PLLA were treated with the same procedure. The obtained ethyl esters were applied to GC equipped with a chiral capillary column Rt-bDEXsa (Fisher Scientific).

3.2.4. Solvent fractionation

Approximately 20 mg of the purified polymer was dissolved in 1 mL of tetrahydrofuran in a glass tube with a screw cap by heating at 100°C for 10 min. The solution was subsequently combined with 8 mL of cyclohexane and incubated at 4°C for 1 h. Cyclohexane-soluble and -insoluble fractions were separated by passing through a PTFE membrane filter with a pore size of 0.2 µm. Each fraction was applied to ^{1}H NMR. A blend of P(3HHx) and PLLA was tested using the same conditions as the control.

3.2.5. Differential scanning calorimetry (DSC) analysis

The thermal properties of the solvent-cast films (approximately 2 – 3 mg) were examined using a DSC3+STARe system (Mettler Toledo). The DSC measurements were conducted by performing two heating cycles as described previously.[14]

3.3. Results

3.3.1. Effect of different mutants on polymer production

Firstly, all the single-mutants (ND, FH and TI) and multiple-mutants (NDFH and NDFHTI) has been examined on its polymer production from mixture of substrate or single substrate. The result showed in Figure 3-1 (A), (B).

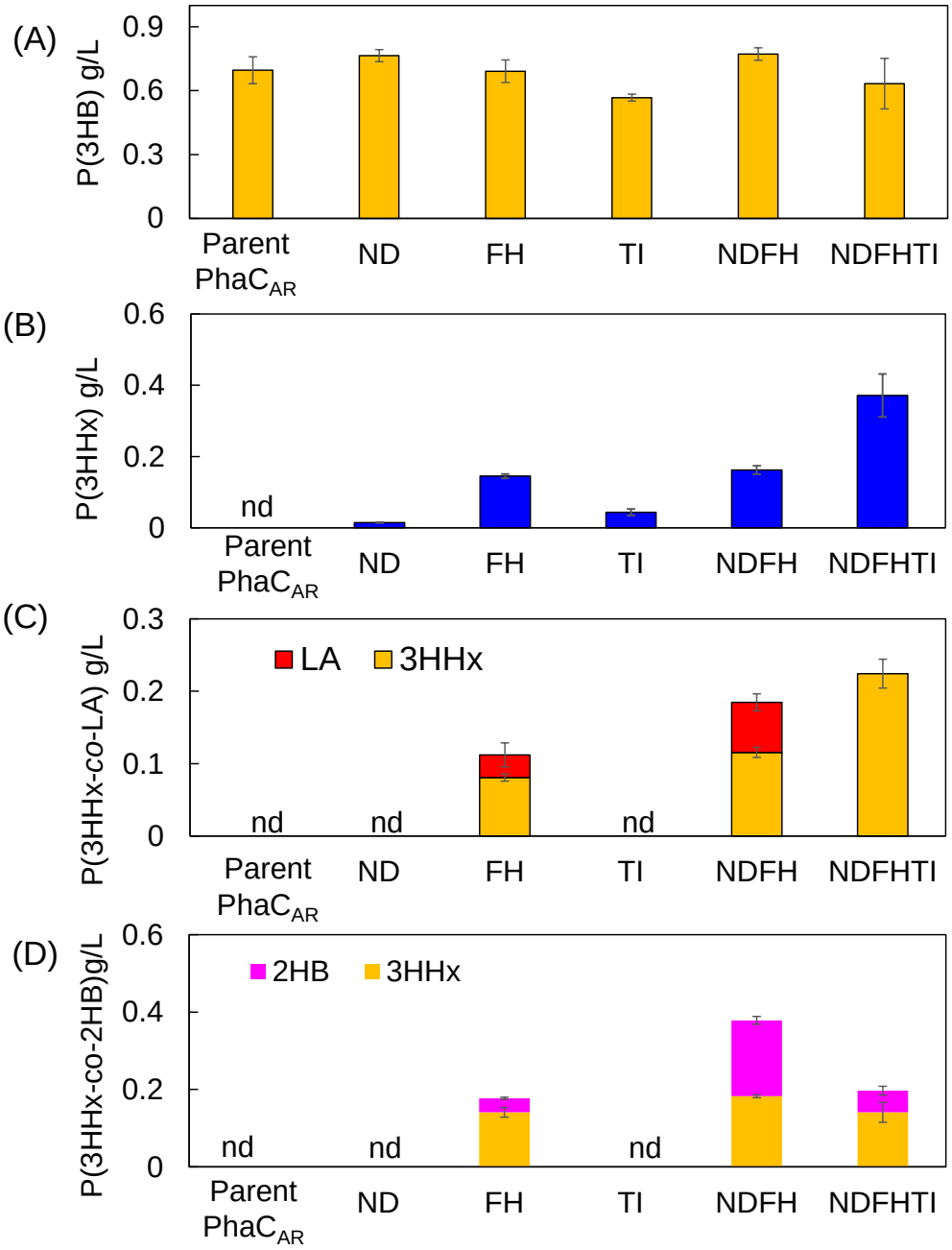

Figure 3-1. Production of homopolymers P(3HB) and P(3HHx) (A), (B) and copolymers P(3HHx-*co*-2HB), P(3HHx-*co*-LA) (C), (D). Data are the average ± standard deviation of three trials. nd, not detected

Figure 3-1 (A) and (B) show that all mutants are capable of generating P(3HB), and that while the original $PhaC_{AR}$ was unable to generate P(3HHx), its variants, particularly triple mutants NDFHTI, showed a significant capacity to do so, generating 0.37 g/l of this homopolymer. Al Only single FH and double mutant NDFH were initially able to synthesize 2HA-based copolymers in P(3HHx-LA) synthesis; parent $PhaC_{AR}$ and ND were unable to do so, as explained in Chapter 3. Even though the largest 3HHx proportion was found in the copolymer created by the triple mutant NDFHTI, there is not LA inclusion. Another illustration is the apparent drop in polymer production caused by the TI triple mutant in P(3HHx-2HB) production. It is possible that the substrate specificity has shifted from single to triple mutant, as NDFHTI prefers the activity of 3HHx-CoA but not 2HA-CoA. These findings led to the choice of NDFH for the biosynthesis of the LA-based copolymer.

3.3.2. Incorporation of LA units into the polymers synthesized using $PhaC_{AR}$ and its derivatives.

Recombinant *E. coli* JM109 cells expressing each of the parent $PhaC_{AR}$, ND, FH, and NDFH mutants were cultured on LB medium with supplementation of 3HB, LA, or combination. The metabolic pathways for polymer production are shown in Figure 3-2. Consequently, the parent $PhaC_{AR}$, and its mutants produced comparable amounts of P(3HB) (Table 3-1, entries 1–4). No PLA homopolymer production was observed under all conditions tested (entries 5–8). By contrast, when 3HB, and LA were co-supplied, the polymers containing 3HB and LA were produced (entries 9–12). In particular, NDFH could highly incorporate LA units (21 mol%). Therefore, the combination of ND, and FH mutations showed a synergistic effect on LA incorporation, although these mutations

were originally identified on the basis of the selection criterion of the elevation of 3HHx incorporation.[11]

Thus, in this study, the synthesis of a copolymer comprising 3HHx and LA was examined (Table 3-2). Under the copolymer synthesis conditions, FH and NDFH produced polymers containing 3HHx and LA (entries 19 and 20). The LA fractions (46 mol% and 51 mol%) were higher than those in the case of 3HB/LA (2 mol%–21 mol% LA). These results indicate that NDFH can highly incorporate 3HHx and LA units. For P(3HHx) production, FH and NDFH produced the same amount of polymer (entries 15 and 16).

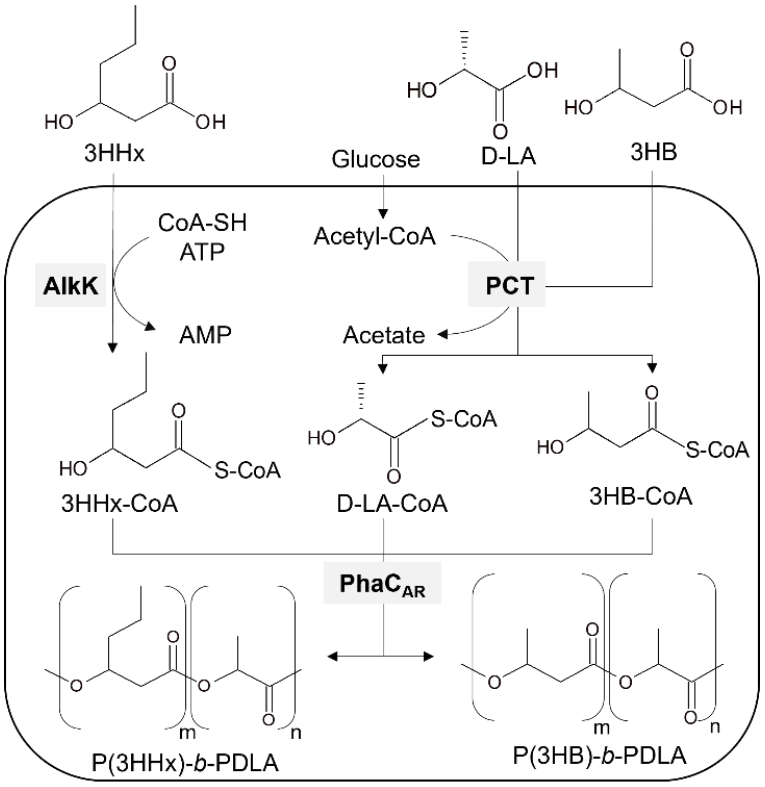

Figure 3-2. Metabolic pathways for the synthesis of P(3HB)-*b*-PDLA and P(3HHx)-*b*-PDLA in *E. coli*. PCT and propionyl-CoA transferase. AlkK, CoA ligase.

Table 3-1. Polymer production containing 3HB and LA in *E. coli* expressing PhaC$_{AR}$ and its mutants

Entry	$PhaC_{AR}$ mutants	Precursor (g/L)		Cell dry weight (g/L)	Polymer production (g/L)	Monomer composition (mol%)	
		3HB	LA			3HB	LA
1	Parent	2.5	-	3.9 ± 0.4	0.6 ± 0.02	100	0
2	ND	2.5	-	3.9 ± 0.1	0.5 ± 0.01	100	0
3	FH	2.5	-	4.2 ± 0.1	0.6 ± 0.02	100	0
4	NDFH	2.5	-	4.3 ± 0.2	0.6 ± 0.03	100	0
5	Parent	-	10	2.0 ± 0.1	nd	-	-
6	ND	-	10	2.0 ± 0.1	nd	-	-
7	FH	-	10	2.1 ± 0.1	nd	-	-
8	NDFH	-	10	2.5 ± 0.2	nd	-	-
9	Parent	2.5	10	3.8 ± 0.8	0.6 ± 0.1	98	2
10	ND	2.5	10	3.9 ± 0.5	0.6 ± 0.1	96	4
11	FH	2.5	10	4.3 ± 0.3	0.7 ± 0.1	91	9
12	NDFH	2.5	10	3.7 ± 0.1	0.8 ± 0.1	78	21

nd: not detected. The full NMR spectra are shown in Figure S3-1in Appendix.

Table 3-2. Polymer production containing 3HHx and LA in *E. coli* expressing $PhaC_{AR}$ and its mutants

Entry	$PhaC_{AR}$ mutants	Precursor (g/L)		Cell dry weight (g/L)	Polymer production (g/L)	Monomer composition (mol%)	
		3HHx	LA			3HHx	LA
13	Parent	1.0	-	1.9 ± 0.1	nd	-	-
14	ND	1.0	-	2.0 ± 0.0	trace	100	0
15	FH	1.0	-	2.6 ± 0.1	0.22 ± 0.01	100	0
16	NDFH	1.0	-	2.6 ± 0.1	0.22 ± 0.01	100	0
17	Parent	1.0	10	2.2 ± 0.0	nd	-	-
18	ND	1.0	10	2.2 ± 0.0	nd	-	-
19	FH	1.0	10	2.5 ± 0.0	0.29 ± 0.02	54	46
20	NDFH	1.0	10	2.6 ± 0.0	0.33 ± 0.02	49	51

nd: not detected. The full NMR spectra are shown in Appendix, Figure S3-2.

3.3.2. Monomer sequence analysis of P(3HHx-co-LA)

The polymer containing 3HHx and LA synthesized using FH was applied to ^{1}H and ^{13}C NMR analyses (Figures 3-3A and B). The resonance of the methine protons of the 3HHx and LA units is the fingerprint region to determine dyad and triad sequences. In addition, the resonance of the sample at 5.1–5.3 ppm was identical to that of P(3HHx) and PLA at 5.15–5.26 ppm and 5.12–5.20 ppm, respectively (Figure 3-3A [ii] and [iii]),[11, 13] indicating that the polymer contained P(3HHx) and PLA homopolymers as major components. The weak resonance at 5.06 ppm was ascribed to the LA*-3HHx linkage as previous report,[15] indicating that the polymer contained a small portion of the randomly polymerized structure. The 3HHx(3) resonance in LA-3HHx* homo dyad based on the analogy with P(LA-*co*-3HB),[16] and thus, the signal was overlapped with the signal of the homo dyad.

^{13}C NMR resonances of the sample were identical to those of P(3HHx) and PLA.[13] In addition, the peaks around 169.42–169.72 ppm were split into two distinguished peaks, which were ascribed to dyad sequences of 3HHx*-3HHx and LA*-LA.[15] Collectively, the obtained polymer was either a block copolymer of P(3HHx) and PLA or their blend.

A.

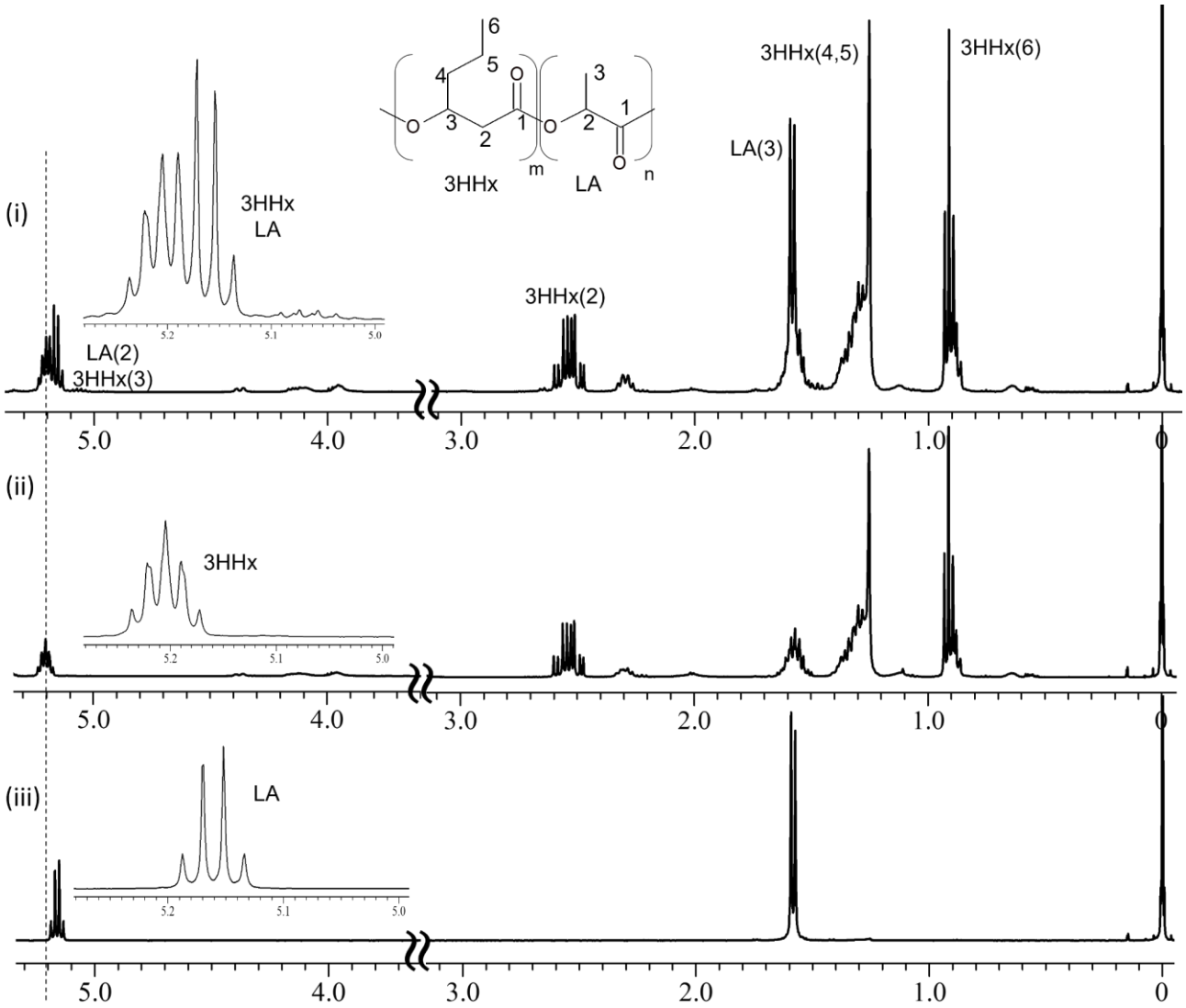

B.

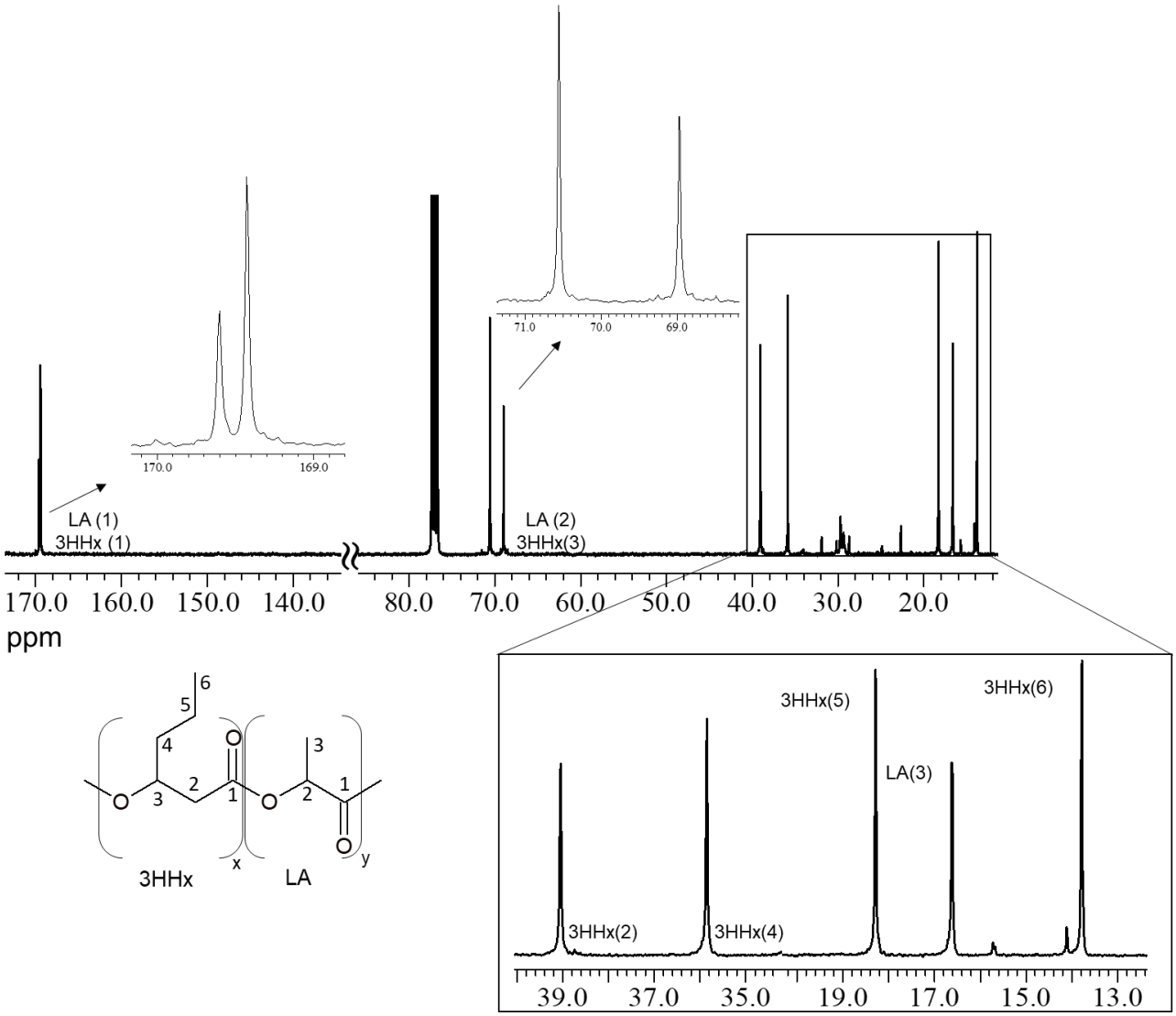
LA (1)
3HHx (1)
LA (2)
3HHx(3)
170.0 160.0 150.0 140.0 80.0 70.0 60.0 50.0 40.0 30.0 20.0
ppm
3HHx
LA
3HHx(5)
3HHx(6)
LA(3)
3HHx(2)
3HHx(4)
39.0 37.0 35.0 19.0 17.0 15.0 13.0

C.

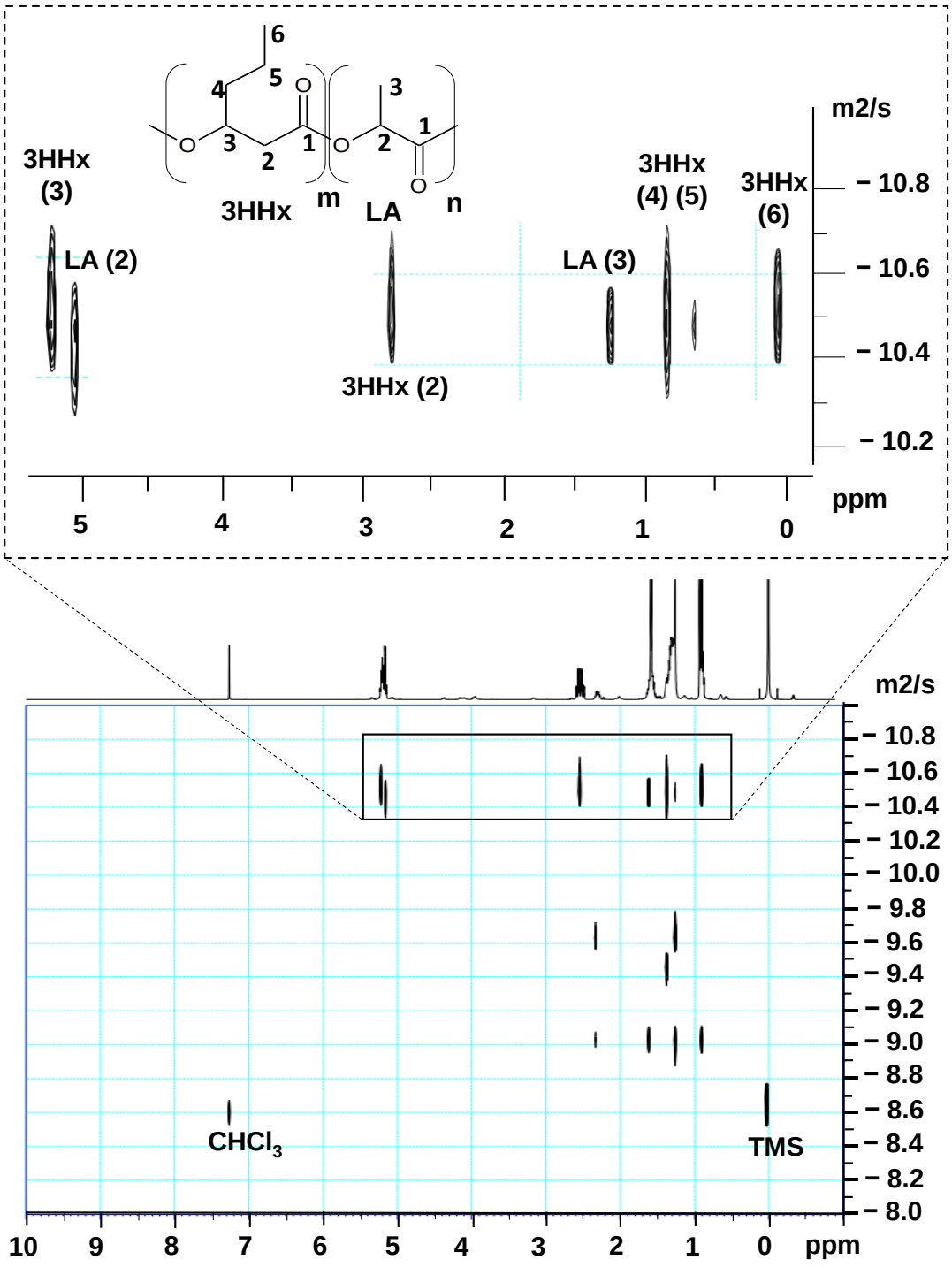

Figure 3-3. ^{1}H NMR (A), ^{13}C NMR (B), and DOSY-NMR (C) spectra of polymers synthesized by recombinant *E. coli* JM109 expressing FH. A(i): Binary polymer containing 3HHx and LA, A(ii): P(3HHx), A(iii): PLLA. The full spectra are shown in Appendix, Figure S3-3, S3-4, S3-6

3.3.3. Enantiomer analysis of LA units

The enantiomer of LA units in the polymer synthesized by NDFH (entry 20) was determined using chiral GC. The ethanolysis product of the polymer sample exhibited a peak corresponding to the D-LA standard (Figure 3-4), indicating that the polymer was composed of D-LA. Given that PCT recognizes D, L-LA as substrates,[17] the result was due to strict enantiospecificity of NDFH.

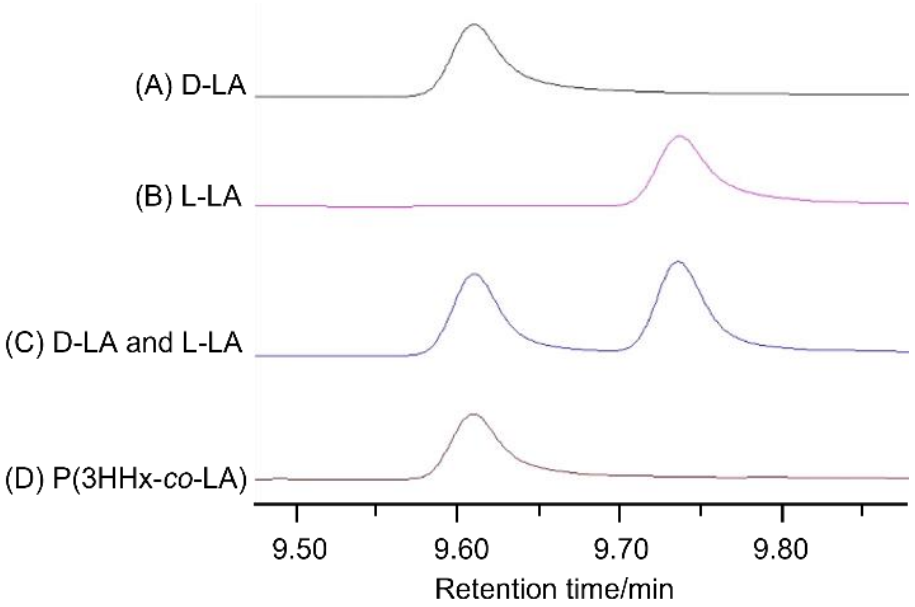

Figure 3-4. Enantiomeric analysis of the LA units in P(3HHx-*co*-LA) synthesized using NDFH by chiral GC (D). (A), (B), and (C): L-LA and D-LA standards.

3.3.4. Solvent fractionation

Solvent fractionation was performed to identify whether the obtained polymer was a polymer blend or block copolymer of P(3HHx) and PLA. P(3HHx) is soluble in cyclohexane, whereas PLAs are insoluble. Given their distinct solubility, the polymer samples were separated into cyclohexane-soluble and -insoluble fractions (Table 3-3). When a polymer blend of P(3HHx) and PLA was applied to fractionation, the

cyclohexane-soluble fraction did not contain PLA. By contrast, when the copolymers produced by FH and NDFH were tested, PLA was detected in the cyclohexane-soluble fraction, indicating the presence of a covalent linkage between P(3HHx) and PLA segments. Therefore, the copolymers produced by FH and NDFH mutants were a block copolymer P(3HHx)-*b*-PDLA.

Table 3-3. Solvent fractionation of polymers comprising 3HHx and LA

Polymers	Fractions	Monomer composition (mol%)		Recovery (mol%)
		3HHx	LA	
Polymer blend of P(3HHx) and PLLA	Original blend	50	50	100
	Soluble fraction	100	0	47
	Insoluble fraction	31	69	51
Copolymer synthesized by FH	Original copolymer	52	48	100
	Soluble fraction	81	19	31
	Insoluble fraction	32	68	56
Copolymer synthesized by NDFH	Original copolymer	48	52	100
	Soluble fraction	78	22	36
	Insoluble fraction	42	58	51

Full NMR spectra are shown in Figure S3-3 in Appendix.

3.3.5. Molecular weight analysis

The weight-average molecular weight of P(3HHx) synthesized using FH and NDFH was 2.3×10^6 and 1.3×10^6 (M_w), respectively (Table 3-4), indicating that FH achieved a higher molecular weight than NDFH. The polymer containing 3HHx and LA had lower molecular weights (3.5×10^5 and 8.6×10^5 (M_w), respectively) than P(3HHx). The polymer was eluted as a unimodal peak by SEC (Figure S3-7 in Appendix), supporting that the sample was a block copolymer rather than blend. In fact, the DOSY NMR of the polymer, which indicated the similar diffusion coefficients of LA and 3HHx units, agreed with the interpretation (Figures 3-3C and Figure S3-6 in Appendix).

On the other hand, polymers that comprise both 3HB and LA segments had their molecular weight lowered along with an increase in the LA fraction in copolymers (Table 3-4, entries 21–24).[18] This result is consistent with other research and suggests that the rate-limiting step in polymer elongation would likely be the insertion of LA units into the polymer chain. Additionally, as the fraction of LA increased, notably in polymers with 21mol% LA, the melting temperatures of these polymers decreased. This result demonstrated that, as reported in previous studies,[18, 19] the rising LA fraction decreased the crystallinity of P(LA-*co*-3HB)s.

Table 3-4. Molecular weight and thermal properties of polymers

Entry	Sample	Molecular weight			Thermal property	
		M_w ($\times 10^5$)	M_n ($\times 10^5$)	$ĐM$	T_m (°C)	T_g (°C)
15	P(3HHx)	23	5.1	4.6	44	-17
16	P(3HHx)	13	3.8	3.5	nt	nt
19	P(54mol% 3HHx-*co*-LA)	3.5	1.9	1.7	nt	nt
20	P(49mol% 3HHx-*co*-LA)	8.6	3.7	2.3	144	-15; 41
21	P(3HB-*co*-2mol%LA)	0.6	0.3	2.0	164.3	2.3
22	P(3HB-*co*-4mol%LA)	0.7	0.2	3.5	164.4	2.7
23	P(3HB-*co*-9mol%LA)	0.4	0.2	2.0	160.8	3.1
24	P(3HB-*co*-21mol%LA)	0.3	0.1	3.0	159.3	4.1

M_w, weight-average molecular weight; M_n, number-average molecular weight; ĐM = M_w/M_n polydispersity index; T_g: glass-transition temperature; T_m: melting temperature. nt, not tested

3.4. Discussion

The first LA-incorporating PHA synthase was reported in 2008, which was an engineered bacterial PHA synthase, PhaC1$_{Ps}$STQK.[3] The enzyme is a class II PHA

synthase derived from *Pseudomonas* sp. 61-3 containing Ser325Thr/Gln481Lys mutations and randomly copolymerized lactyl-CoA (LA-CoA) and 3HB-CoA. However, PhaC1$_{Ps}$STQK had a limited range of LA fraction in the copolymer. An inverse relationship was observed between the LA fraction and polymer production of random copolymers of LA and 3HAs.[3, 20] In particular, the production and molecular weight of biosynthesized PDLA homopolymer (and PDLA-like copolymer) was severely limited to low values (molecular weight was 10^3 order of magnitude). Previously, *in vitro* analysis of PhaC1$_{Ps}$STQK using LA-CoA demonstrated that the synthesis of a PDLA homopolymer stopped at the initial stage of the reaction, at which the molecular weight is approximately 2,000.[21] The anomalous behavior might be due to the high glass transition temperature of PLA (60°C).

In this study, high-molecular-weight PDLA-containing PHAs were successfully biosynthesized for the first time. NDFH exhibited a greater capacity of incorporating LA than the parent PhaC$_{AR}$. NDFH has enhanced 3HHx-incorporating capacity and synthesized a novel block copolymer P(3HHx)-*b*-PDLA. The molecular weight (M_w) of P(3HHx)-*b*-PDLA was 10^5 order of magnitude. Given the molar fraction of LA (nearly 50 mol%), the molecular weight of the PDLA segment was estimated to be also 10^5 order of magnitude, which was considerably greater than the abovementioned upper limit. The generation of the high-molecular-weight PDLA segment was also supported by DOSY NMR analysis (Figure 3-2B). On the contrary, the PDLA homopolymer was not obtained using NDFH (Table 3-1, entry 8), indicating that the synthesis of P(3HB) and P(3HHx) segments is an enabling factor of the synthesis of a PDLA chain. These results indicate that block copolymerization could breakthrough the limitation of PDLA synthesis and enable the utilization of high-molecular-weight PDLA as a component of PHA. At present, the mechanism of PDLA synthesis remains unknown. The P(3HHx) segment seemed to

have a greater promoting effect on the PDLA segment synthesis than the P(3HB) segment. *In vitro* analysis of the block copolymer synthesis is necessary to elucidate the role of P(3HHx) segment in the synthesis of the PDLA segment.

For the biosynthesis of PHA block copolymers using $PhaC_{AR}$, 3HA, and 2HA units it is required to combine 3-hydroxyalkanoate (3HA), and 2HA units.[8] P(2HB) and P(glycolate-*ran*-3HB) have been reported as 2HA-based segments.[8, 10] In this study, PDLA was considered as an option in the molecular design of PHA block copolymers. Given the broad substrate scope of NDFH, the finding expanded the structural variety of PHA block copolymers. The PDLA region in the copolymer can serve as a hard segment. This finding is contrary to the previously reported block copolymer P(3HB)-*b*-P(2HB), in which P(2HB) serves as a soft segment. The physical properties of P(3HHx)-*b*-PDLA will be addressed in future work.

The PHA production in the present system utilizes extracellularly supplemented 3HHx as a precursor. The use of precursors facilitates the construction of a metabolic pathway and its regulation. On the other hand, 3HHx-CoA can be supplied via β-oxidation, de novo fatty acid biosynthesis, and unidentified pathways.[22] In addition, an artificial pathway partly using reverse β-oxidation reportedly supplied 3HHx-CoA.[23] The combination of NDFH and such pathways can be used to synthesize block copolymers from non-related carbon sources. The strategy is effective in improving the productivity of the polymers.

3.5. Conclusions

In this work, the high-molecular-weight PDLA-containing block copolymers, P(3HB)-*b*-PDLA and P(3HHx)-*b*-PDLA were successfully synthesized using evolved ($PhaC_{AR}$)s. NDFH has a particularly high capacity incorporating LA units. The molecular weight of the PDLA segments was estimated to be 10^5 order of magnitude. The covalent linkages of P(3HHx) and PDLA segments were verified by solvent fractionation. P(3HHx) segment may facilitate the enzymatic synthesis of PDLA.

3.6. References

(1) Gerard, T.; Budtova, T. Morphology and molten-state rheology of polylactide and polyhydroxyalkanoate blends. *European Polymer Journal* **2012**, *48* (6), 1110-1117. DOI: 10.1016/j.eurpolymj.2012.03.015.

(2) Steube, M.; Johann, T.; Barent, R. D.; Müller, A. H. E.; Frey, H. Rational design of tapered multiblock copolymers for thermoplastic elastomers. *Progress in Polymer Science* **2022**, *124*. DOI: 10.1016/j.progpolymsci.2021.101488.

(3) Taguchi, S.; Yamada, M.; Matsumoto, K. i.; Tajima, K.; Satoh, Y.; Munekata, M.; Ohno, K.; Kohda, K.; Shimamura, T.; Kambe, H.; et al. A microbial factory for lactate-based polyesters using a lactate-polymerizing enzyme. *Proceedings of the National Academy of Sciences* **2008**, *105* (45), 17323-17327. DOI: doi:10.1073/pnas.0805653105.

(4) Taguchi, S.; Doi, Y. Evolution of polyhydroxyalkanoate (PHA) production system by "enzyme evolution": successful case studies of directed evolution. *Macromol Biosci* **2004**, *4* (3), 146-156. DOI: 10.1002/mabi.200300111.

(5) Smolke, C. *The Metabolic Pathway Engineering Handbook*; CRC Press, 2009. DOI: 10.1201/9781439802977.

(6) Matsumoto, K. i.; Ishiyama, A.; Sakai, K.; Shiba, T.; Taguchi, S. Biosynthesis of glycolate-based polyesters containing medium-chain-length 3-hydroxyalkanoates in recombinant *Escherichia coli* expressing engineered polyhydroxyalkanoate synthase. *Journal of Biotechnology* **2011**, *156* (3), 214-217. DOI: 10.1016/j.jbiotec.2011.07.040.

(7) Ochi, A.; Matsumoto, K.; Ooba, T.; Sakai, K.; Tsuge, T.; Taguchi, S. Engineering of class I lactate-polymerizing polyhydroxyalkanoate synthases from *Ralstonia eutropha* that synthesize lactate-based polyester with a block nature. *Appl Microbiol Biotechnol* **2013**, *97* (8), 3441-3447. DOI: 10.1007/s00253-012-4231-9.

(8) Satoh, K.; Kawakami, T.; Isobe, N.; Pasquier, L.; Tomita, H.; Zinn, M.; Matsumoto, K. Versatile aliphatic polyester biosynthesis system for producing random and block copolymers composed of 2-, 3-, 4-, 5-, and 6-hydroxyalkanoates using the sequence-regulating polyhydroxyalkanoate synthase $PhaC_{AR}$. *Microbial Cell Factories* **2022**, *21* (1), 84. DOI: 10.1186/s12934-022-01811-7.

(9) Arai, S.; Sakakibara, S.; Mareschal, R.; Ooi, T.; Zinn, M.; Matsumoto, K. Biosynthesis of Random-Homo Block Copolymer Poly[Glycolate-*ran*-3-Hydroxybutyrate (3HB)]-*b*-Poly(3HB) Using Sequence-Regulating Chimeric Polyhydroxyalkanoate Synthase in

Escherichia coli. *Front Bioeng Biotechnol* **2020**, *8*, 612991. DOI: 10.3389/fbioe.2020.612991.

(10) Tomita, H.; Satoh, K.; Nomura, C. T.; Matsumoto, K. Biosynthesis of poly(glycolate-*co*-3-hydroxybutyrate-*co*-3-hydroxyhexanoate) in *Escherichia coli* expressing sequence-regulating polyhydroxyalkanoate synthase and medium-chain-length 3-hydroxyalkanoic acid coenzyme A ligase. *Bioscience, Biotechnology, and Biochemistry* **2021**, *86* (2), 217-223. DOI: 10.1093/bbb/zbab198.

(11) Phan, H. T.; Hosoe, Y.; Guex, M.; Tomoi, M.; Tomita, H.; Zinn, M.; Matsumoto, K. Directed evolution of sequence-regulating polyhydroxyalkanoate synthase to synthesize a medium-chain-length–short-chain-length (MCL–SCL) block copolymer. *Biomacromolecules* **2022**, *23* (3), 1221-1231. DOI: 10.1021/acs.biomac.1c01480.

(12) Matsumoto, K. i.; Takase, K.; Aoki, E.; Doi, Y.; Taguchi, S. Synergistic Effects of Glu130Asp Substitution in the Type II Polyhydroxyalkanoate (PHA) Synthase: Enhancement of PHA Production and Alteration of Polymer Molecular Weight. *Biomacromolecules* **2005**, *6* (1), 99-104. DOI: 10.1021/bm049650b.

(13) Goto, S.; Hokamura, A.; Shiratsuchi, H.; Taguchi, S.; Matsumoto, K.; Abe, H.; Tanaka, K.; Matsusaki, H. Biosynthesis of novel lactate-based polymers containing medium-chain-length 3-hydroxyalkanoates by recombinant *Escherichia coli* strains from glucose. *J Biosci Bioeng* **2019**, *128* (2), 191-197. DOI: 10.1016/j.jbiosc.2019.01.009.

(14) Kageyama, Y.; Tomita, H.; Isono, T.; Satoh, T.; Matsumoto, K. Artificial polyhydroxyalkanoate poly[2-hydroxybutyrate-*block*-3-hydroxybutyrate] elastomer-like material. *Scientific Reports* **2021**, *11* (1), 22446. DOI: 10.1038/s41598-021-01828-9.

(15) Matsumoto, K.; Taguchi, S. Biosynthetic polyesters consisting of 2-hydroxyalkanoic acids: current challenges and unresolved questions. *Appl Microbiol Biotechnol* **2013**, *97* (18), 8011-8021. DOI: 10.1007/s00253-013-5120-6.

(16) Yamada, M.; Matsumoto, K.; Nakai, T.; Taguchi, S. Microbial production of lactate-enriched poly[(*R*)-lactate-*co*-(*R*)-3-hydroxybutyrate] with novel thermal properties. *Biomacromolecules* **2009**, *10* (4), 677-681. DOI: 10.1021/bm8013846.

(17) Schweiger, G.; Buckel, W. On the dehydration of (*R*)-lactate in the fermentation of alanine to propionate by *Clostridium propionicum*. *FEBS Lett* **1984**, *171* (1), 79-84. DOI: 10.1016/0014-5793(84)80463-9.

(18) Yamada, M.; Matsumoto, K. i.; Shimizu, K.; Uramoto, S.; Nakai, T.; Shozui, F.; Taguchi, S. Adjustable Mutations in Lactate (LA)-Polymerizing Enzyme for the

Microbial Production of LA-Based Polyesters with Tailor-Made Monomer Composition. *Biomacromolecules* **2010**, *11* (3), 815-819. DOI: 10.1021/bm901437z.

(19) Abe, H.; Doi, Y.; Hori, Y.; Hagiwara, T. Physical properties and enzymatic degradability of copolymers of (*R*)-3-hydroxybutyric acid and (*S,S*)-lactide. *Polymer* **1998**, *39* (1), 59-67. DOI: 10.1016/S0032-3861(97)00240-1.

(20) Song, Y.; Matsumoto, K.; Yamada, M.; Gohda, A.; Brigham, C. J.; Sinskey, A. J.; Taguchi, S. Engineered *Corynebacterium glutamicum* as an endotoxin-free platform strain for lactate-based polyester production. *Appl Microbiol Biotechnol* **2012**, *93* (5), 1917-1925. DOI: 10.1007/s00253-011-3718-0.

(21) Matsumoto, K.; Iijima, M.; Hori, C.; Utsunomia, C.; Ooi, T.; Taguchi, S. *In vitro* analysis of D-Lactyl-CoA-polymerizing polyhydroxyalkanoate synthase in polylactate and poly(lactate-*co*-3-hydroxybutyrate) syntheses. *Biomacromolecules* **2018**, *19* (7), 2889-2895. DOI: 10.1021/acs.biomac.8b00454.

(22) Liu, S.; Narancic, T.; Tham, J. L.; O'Connor, K. E. *β*-oxidation-polyhydroxyalkanoates synthesis relationship in *Pseudomonas putida* KT2440 revisited. *Appl Microbiol Biotechnol* **2023**, *107* (5-6), 1863-1874. DOI: 10.1007/s00253-023-12413-7.

(23) Saito, S.; Imai, R.; Miyahara, Y.; Nakagawa, M.; Orita, I.; Tsuge, T.; Fukui, T. Biosynthesis of poly(3-hydroxybutyrate-*co*-3-hydroxyhexanoate) from glucose by *Escherichia coli* through butyryl-CoA formation driven by Ccr-Emd combination. *Front Bioeng Biotechnol* **2022**, *10*, 888973. DOI: 10.3389/fbioe.2022.888973.

Appendix

(A)

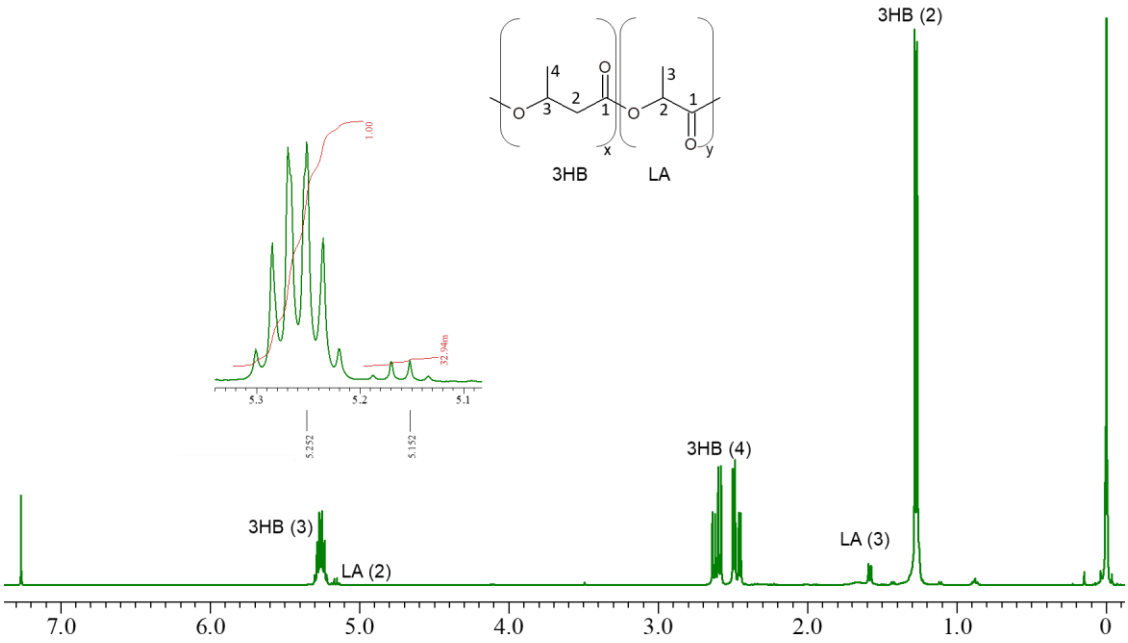

(B)

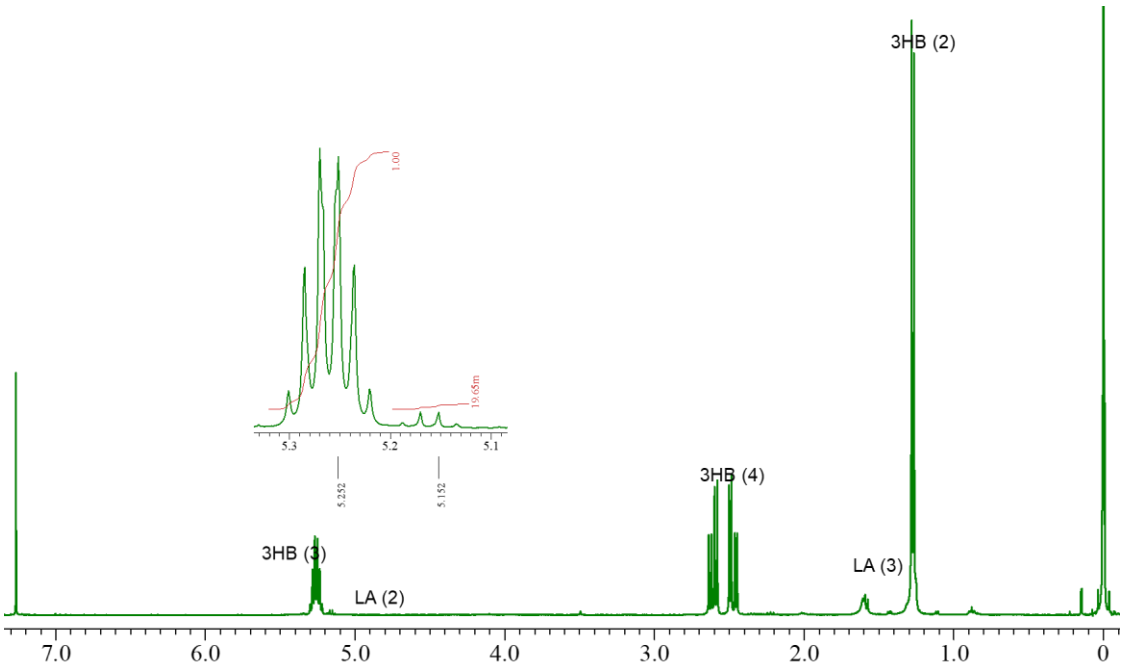

(C)

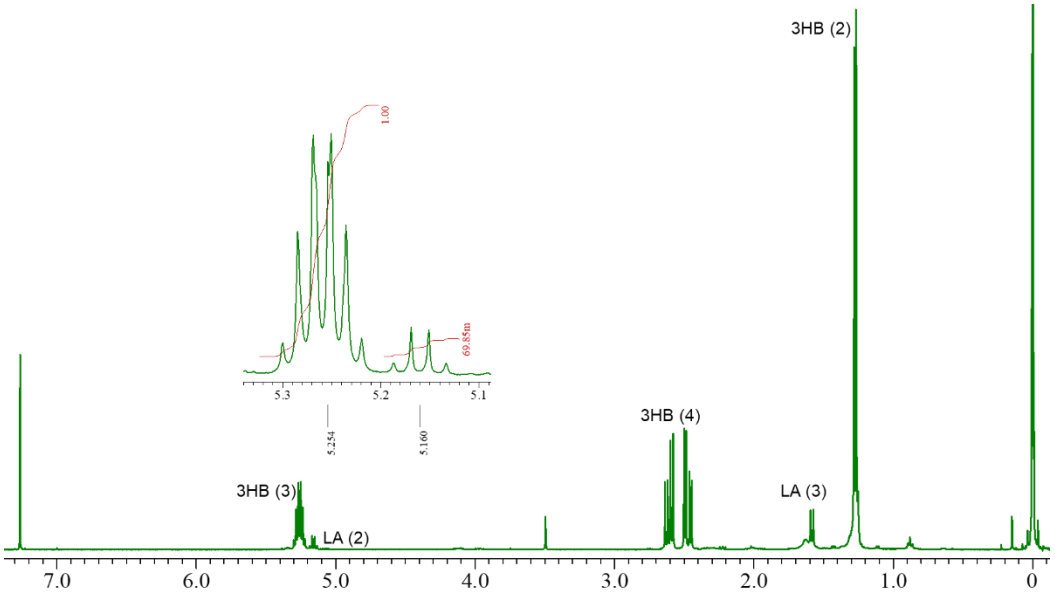

(D)

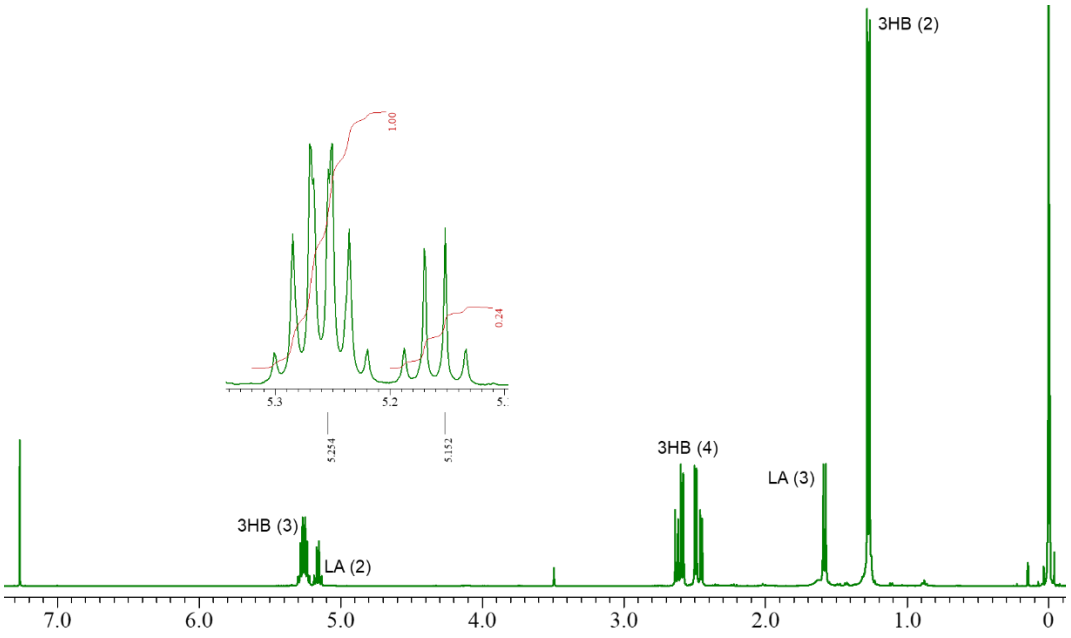

Figure S3-1. ^{1}H NMR spectra of P(3HB-*co*-LA) synthesized using parent $PhaC_{AR}$ (A), and its variants ND (B), FH (C), and NDFH (D)

(E)

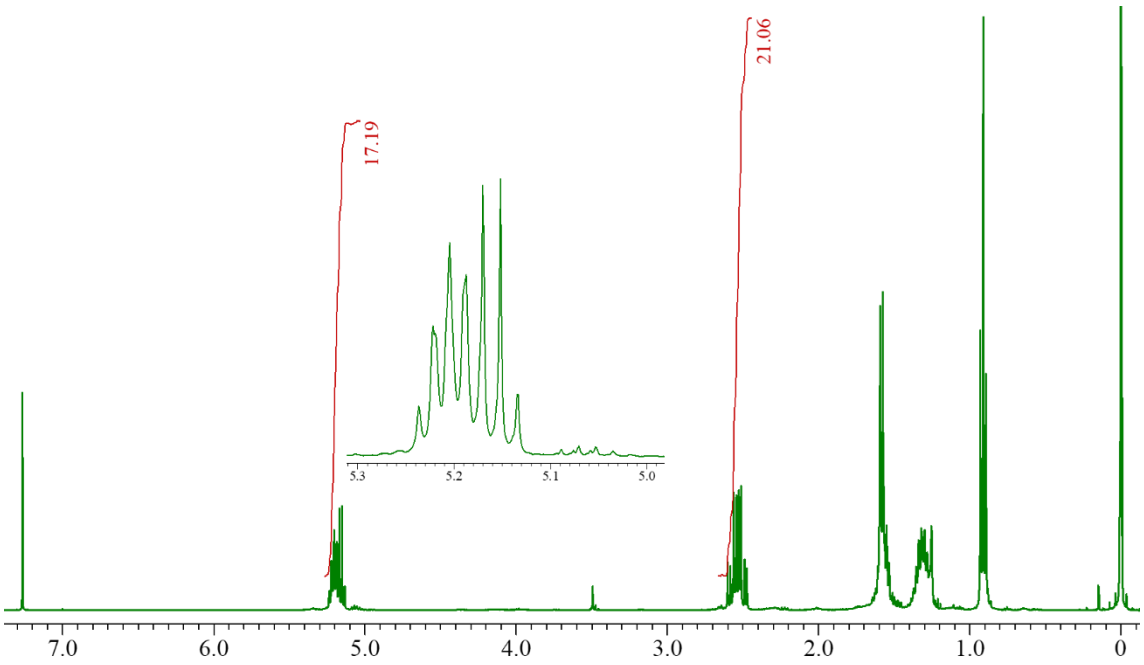

(F)

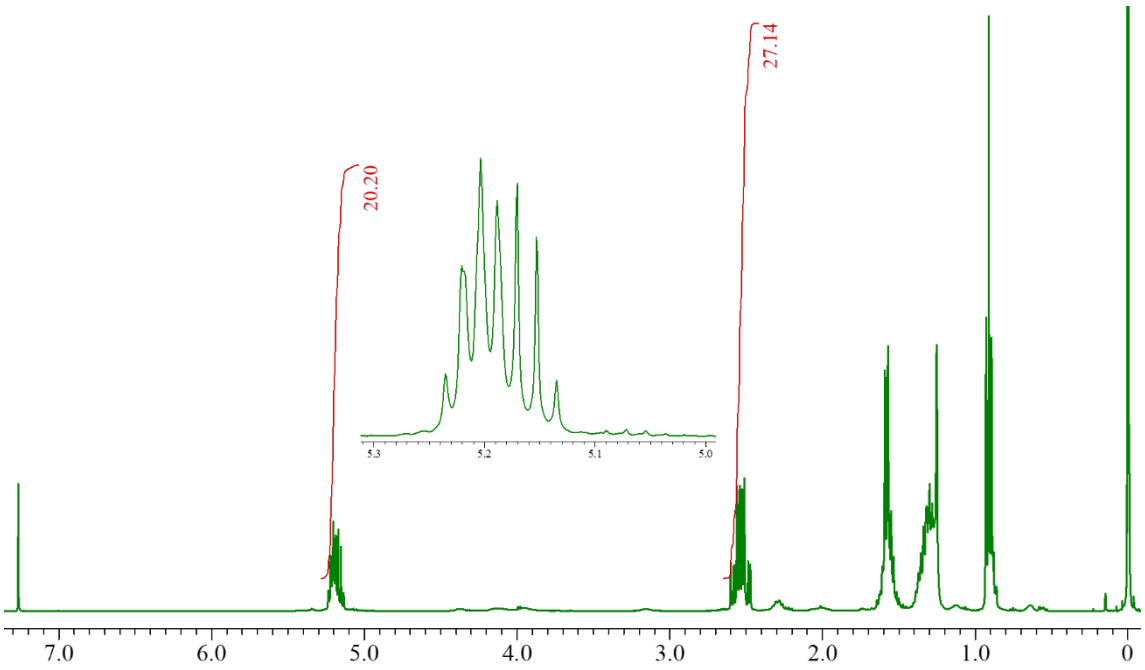

Figure S3-2. ^{1}H NMR spectra of P(3HHx-*co*-LA) synthesized using FH (E) and NDFH (F)

G) Original P(3HHx-*co*-LA) from FH

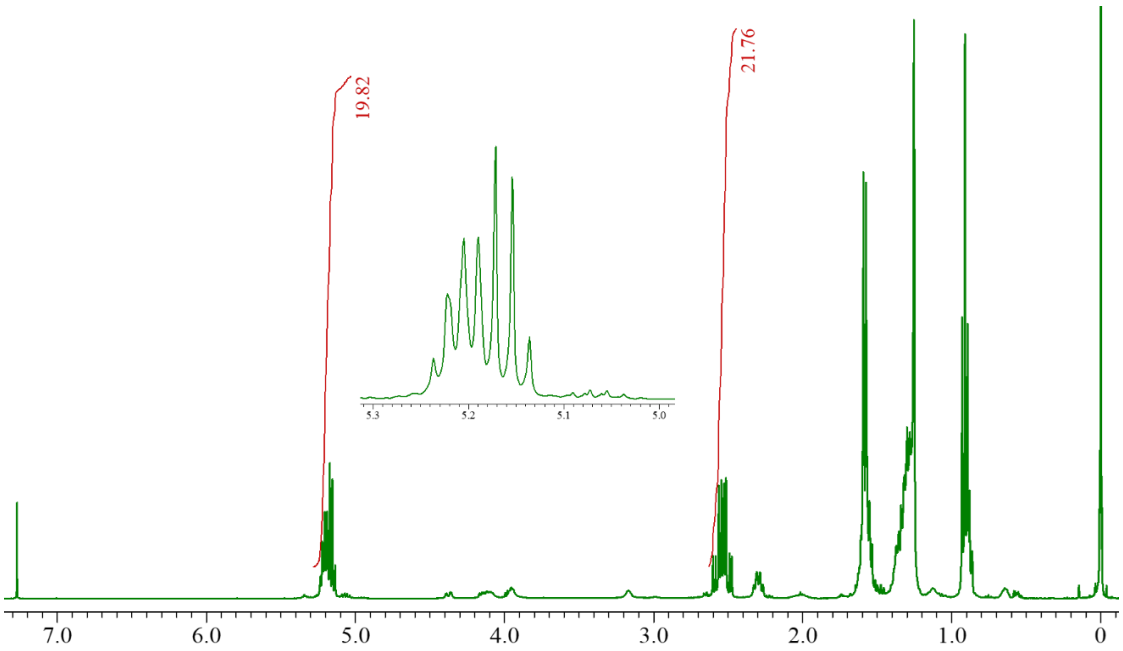

(H) Cyclohexane-soluble P(3HHx-*co*-LA) from FH

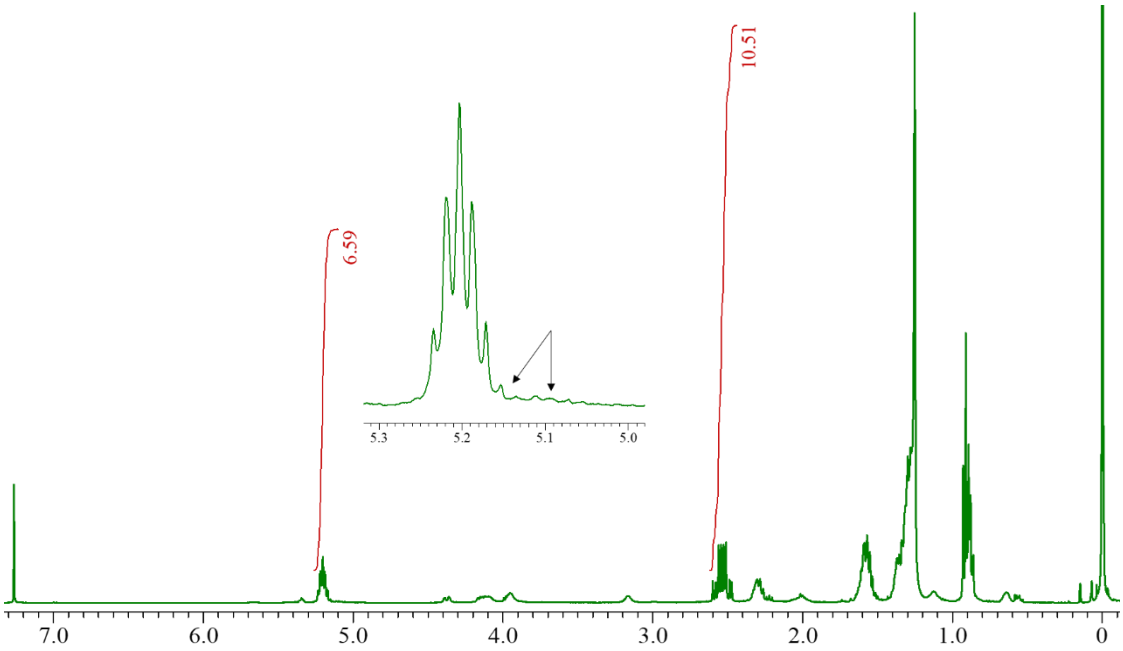

(I) Cyclohexane-insoluble P(3HHx-*co*-LA) from FH

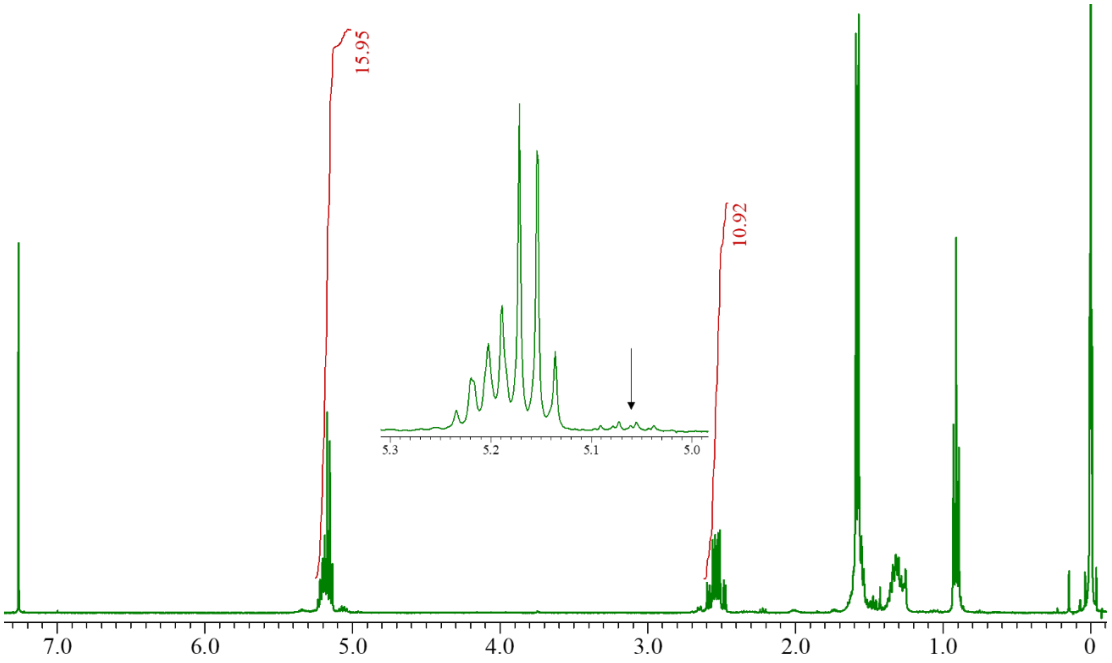

(J) Original P(3HHx-*co*-LA) from NDFH

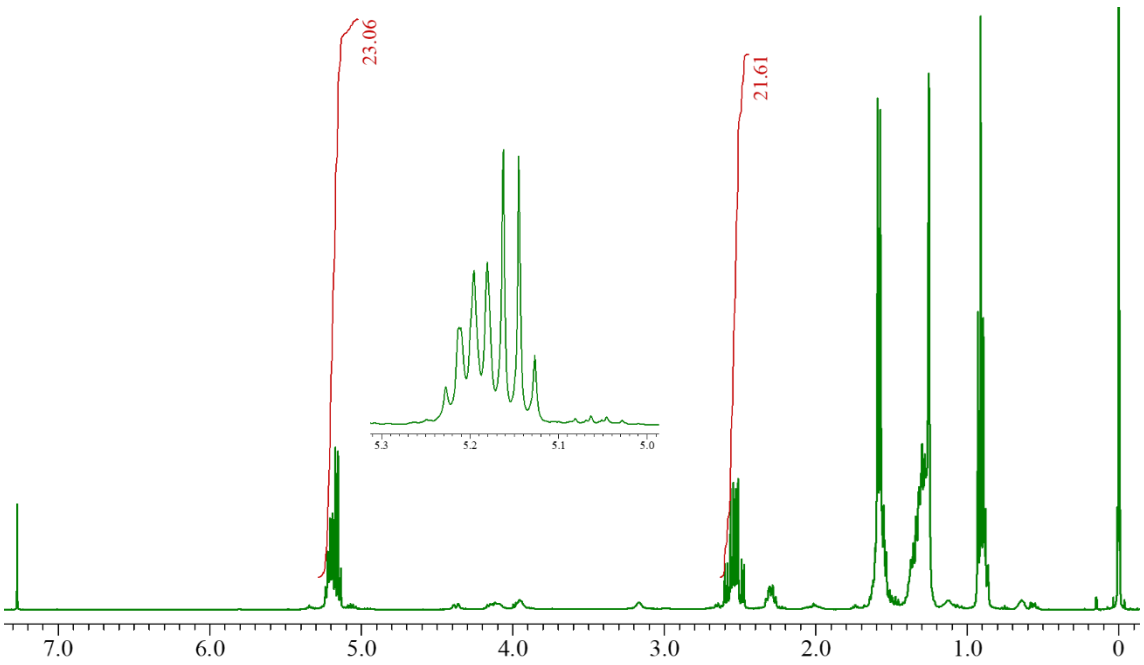

(K) Cyclohexane-soluble P(3HHx-*co*-LA) from NDFH

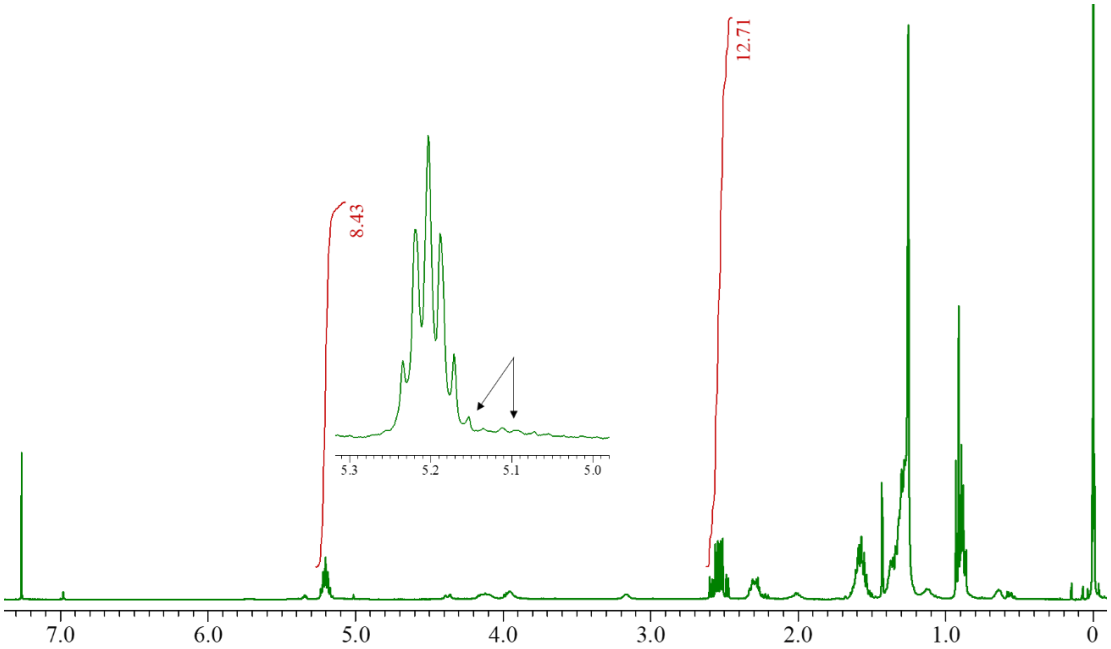

(L) Cyclohexane-insoluble P(3HHx-*co*-LA) from NDFH

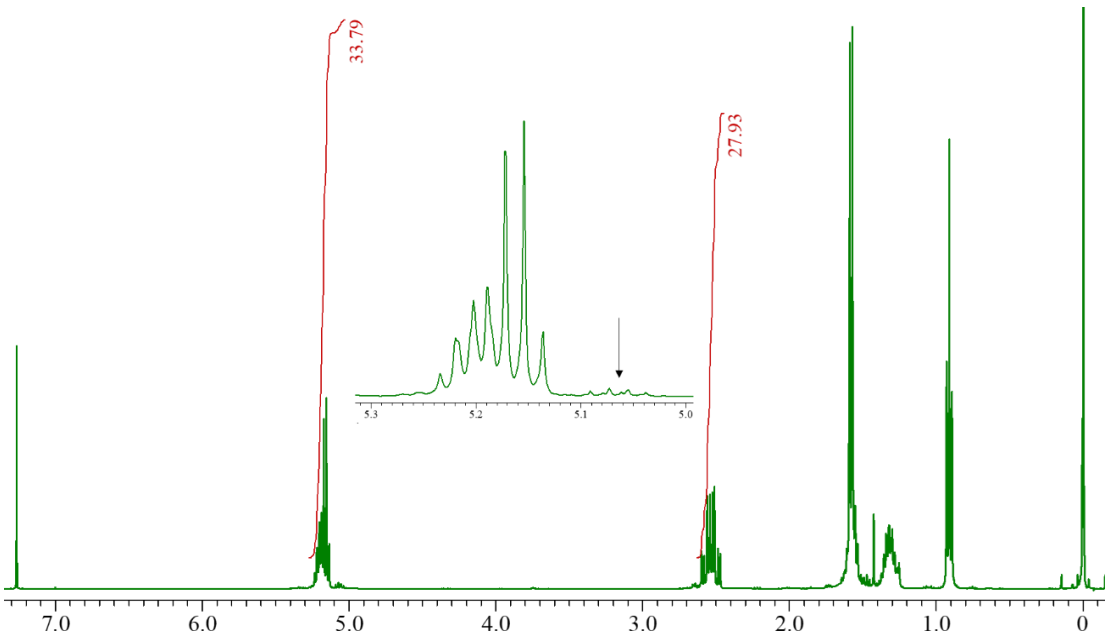

(M) Original polymer blend containing P(3HHx) and PLLA

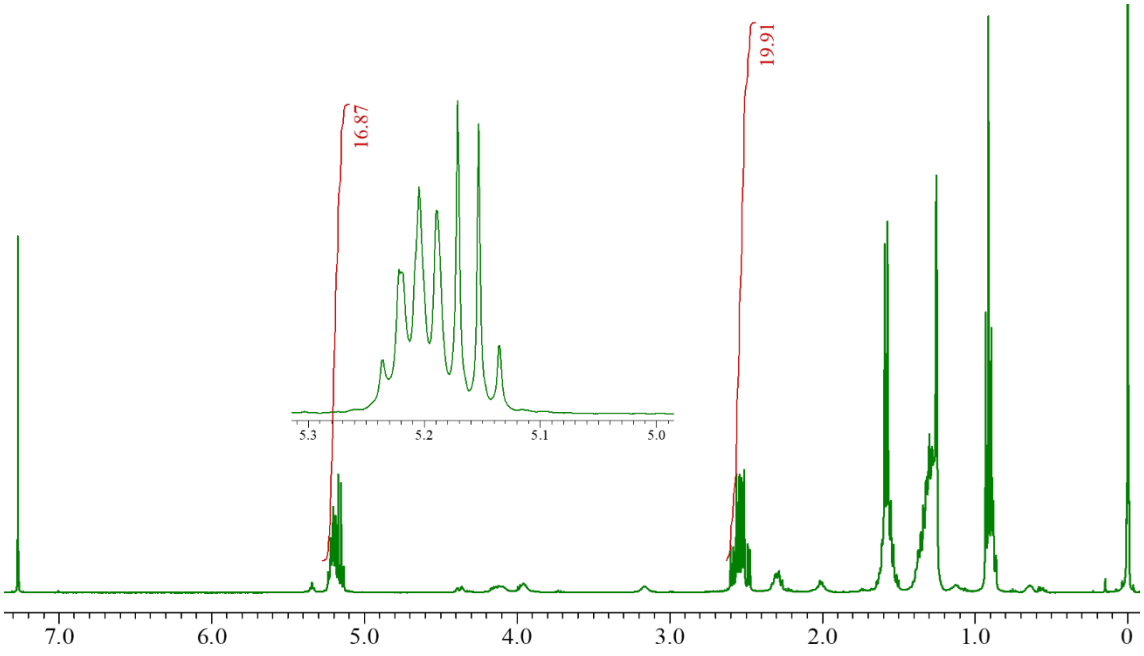

(N) Cyclohexane-soluble of polymer blend containing P(3HHx) and PLLA

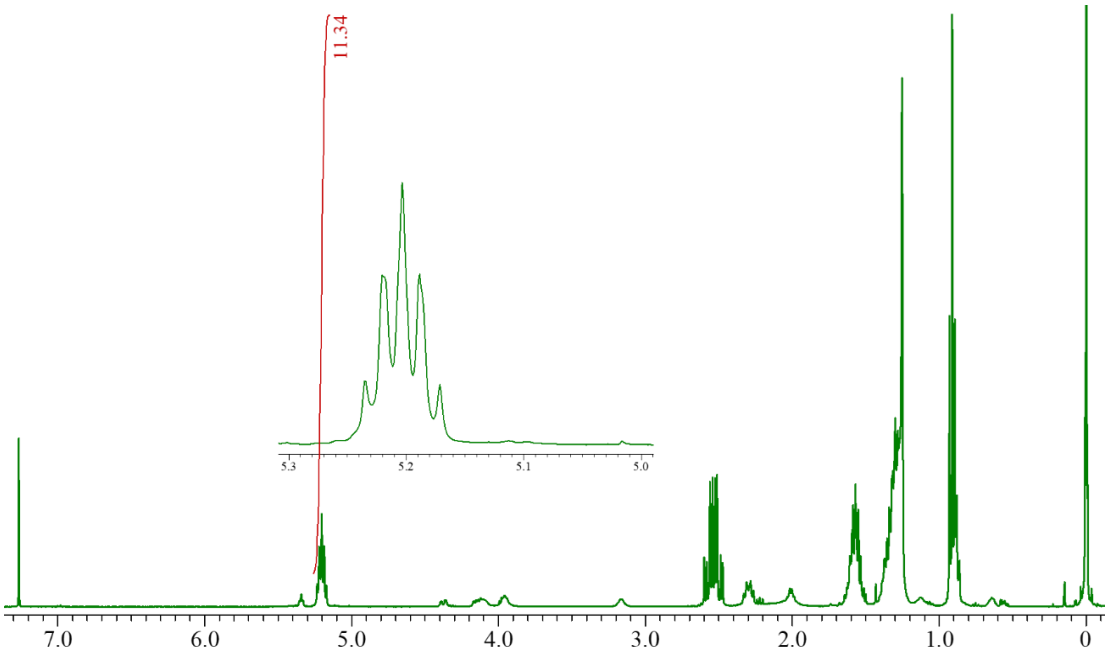

(O) Cyclohexane-insoluble of polymer blend containing P(3HHx) and PLLA

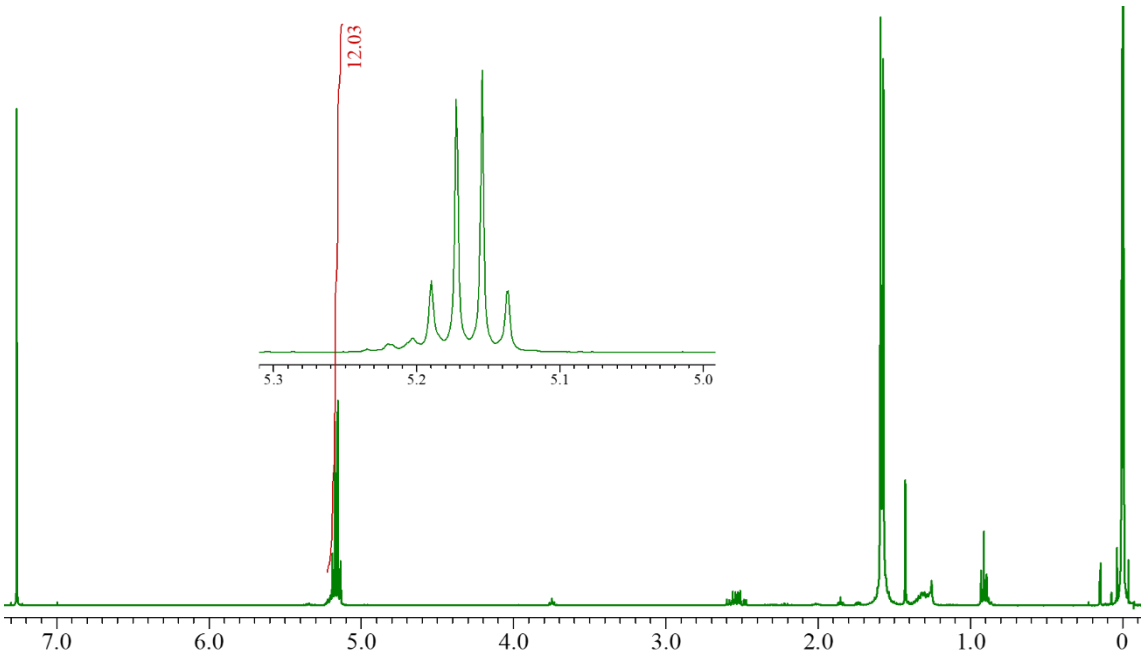

Figure S3-3. ^{1}H NMR spectra of solvent fractionation samples. Original P(3HHx-*co*-LA) before solvent fractionation synthesized using FH (G) and NDFH (J). Cyclohexane-soluble fractions of FH (H) and NDFH (K). Cyclohexane-insoluble fraction of ND (I) and NDFH (L). Blend polymers of P(3HHx) and PLLA before fractionation (M), its cyclohexane-soluble fraction (N), and its cyclohexane-insoluble fraction (O).

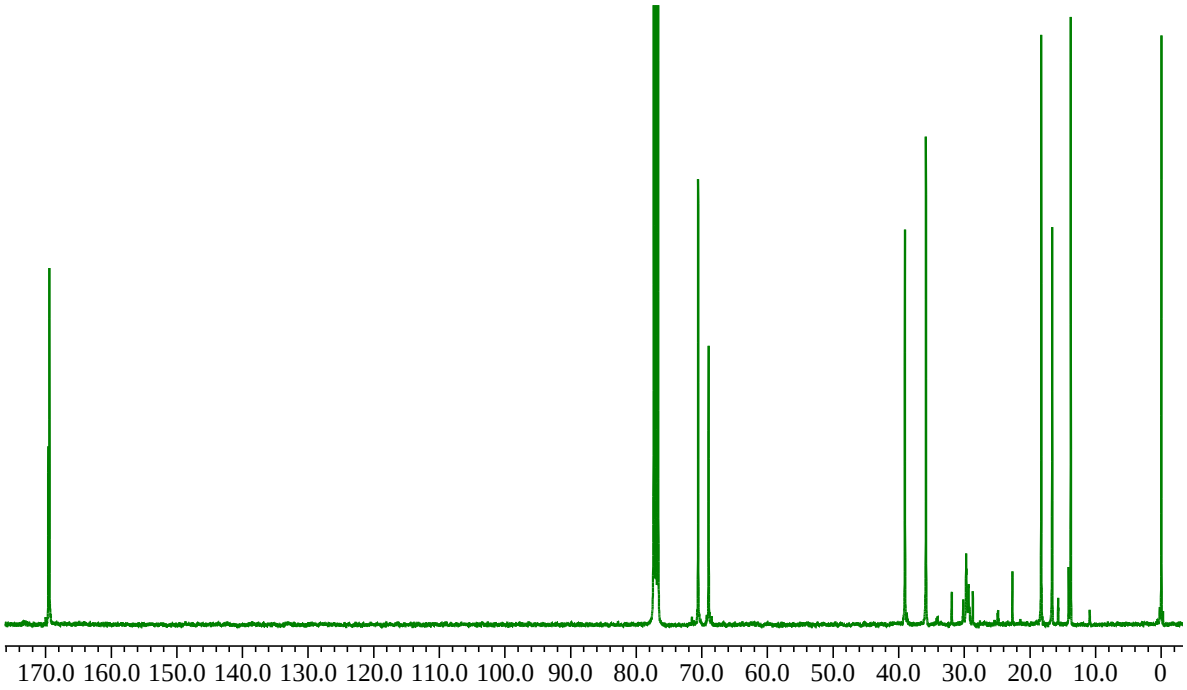

Figure S3-4. ^{13}C NMR spectra of P(3HHx-co-LA) synthesized using NDFH

(A)

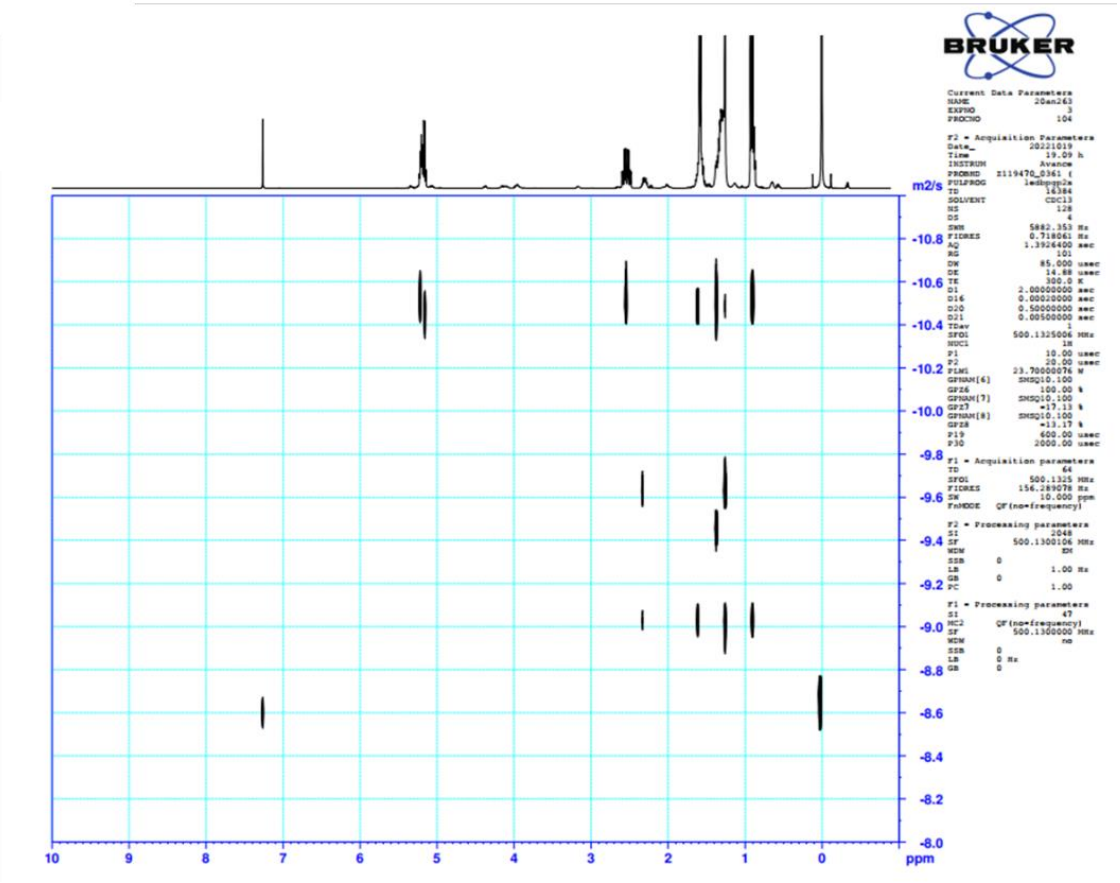

(B)

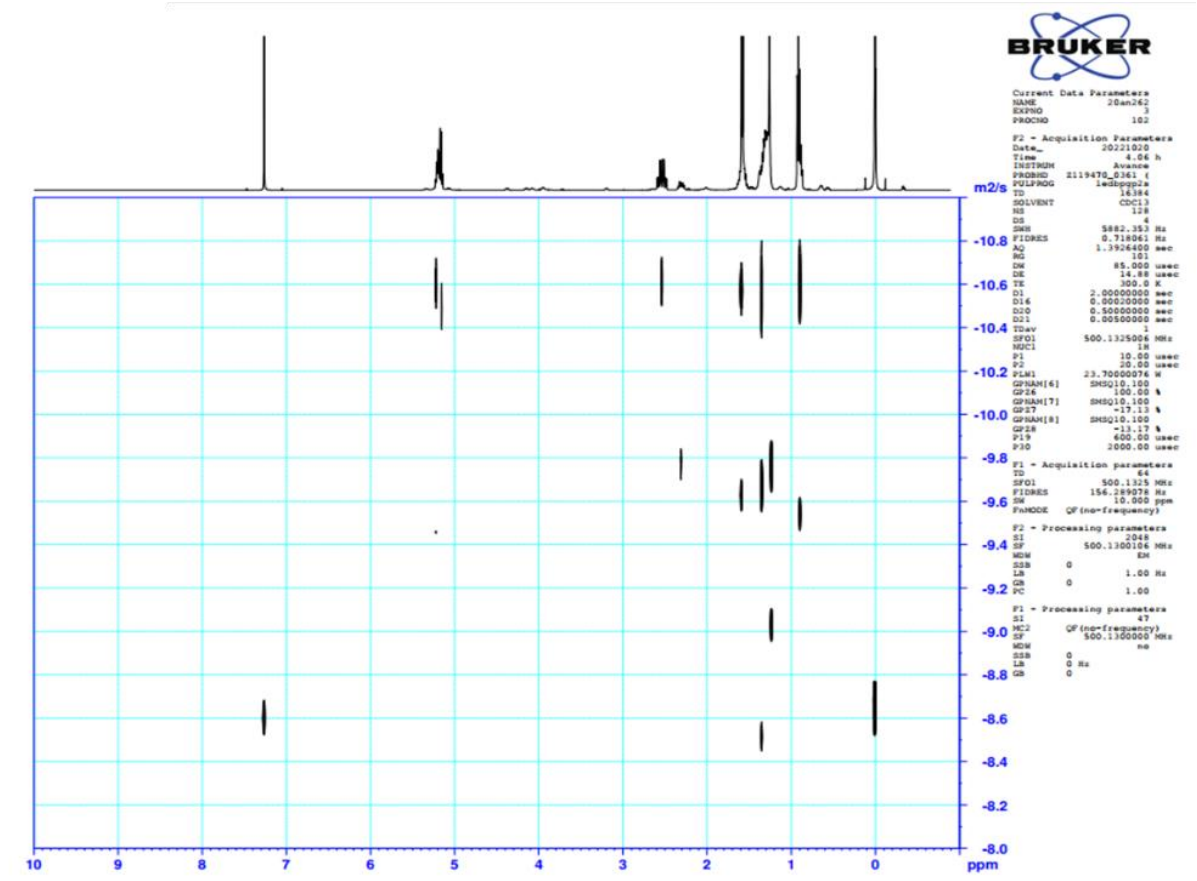

Figure S3-6. DOSY-NMR spectra of P(3HHx-*co*-LA) synthesized by FH (A) and NDFH (B)

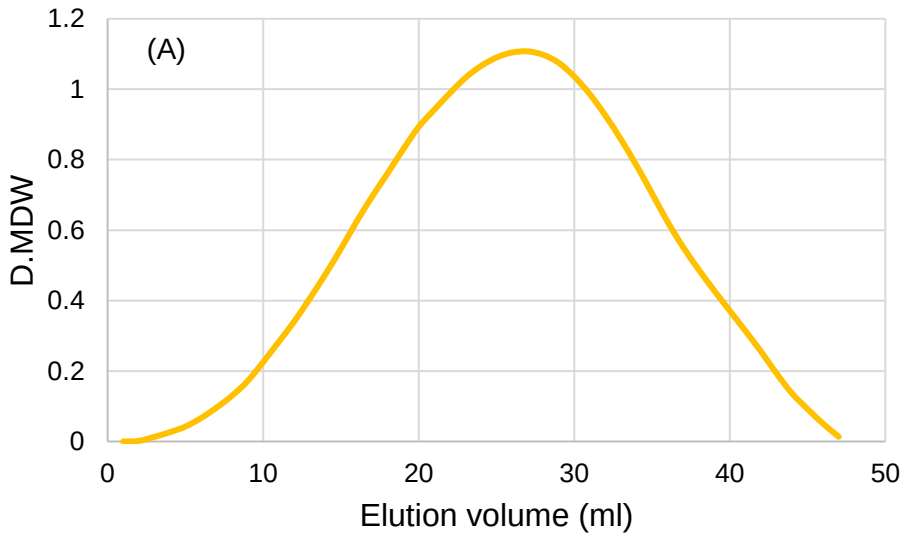

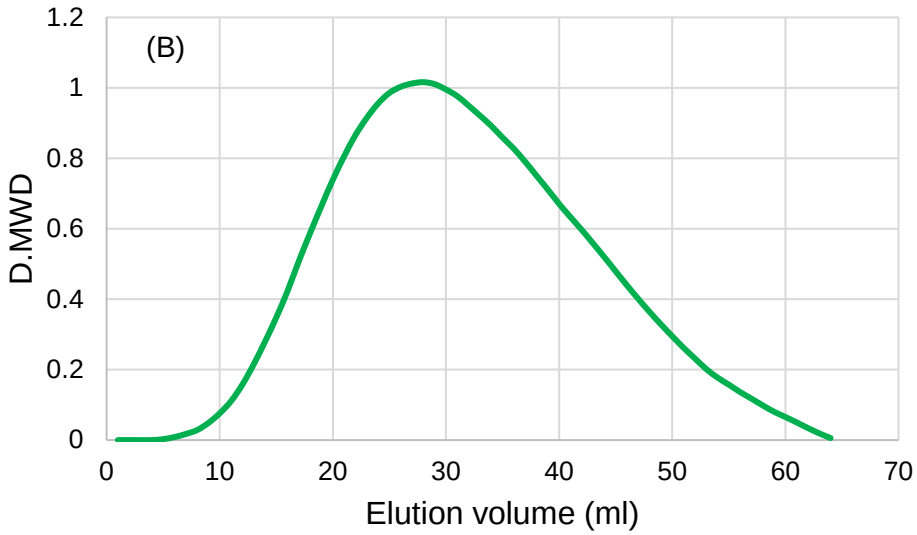

Figure S3-7. Size exclusion chromatography trace of P(3HHx)-*b*-PDLA synthesized using FH (A, Entry 19) and NDFH (B, Entry 20).

Chapter 4.

Directed evolution of $PhaC_{AR}$ by random mutagenesis for expanding enzyme activity toward 3-hydroxyoctanoyl-CoA

4.1. Introduction

From Chapter 3, LA-based copolymers produced using NDFH mutant possess high molecular weight and characteristic thermal properties. I found that the block copolymer P(3HHx)-*b*-PDLA has a higher molecular weight than P(3HB)-*b*-PDLA. The presence of high-molecular-weight PDLA segment was supported by the result that P(3HHx)-*b*-PDLA has a melting temperature corresponding to the PDLA crystals (144 °C). Although the effect of P(3HHx) segment on the polymer synthesis and thermal properties of the block copolymer has not been fully understood, P(3HHx) seems to promote the PDLA segment synthesis. From that, it is possible to assume that the appearance of a segment composed of longer-side-chain units, such as 3-hydroxyoctanoate (3HO), in LA-based copolymer might facilitate the PDLA-containing block copolymers and give useful thermal properties of the obtained copolymer.

Therefore, I attempted to expand the substrate scope of $PhaC_{AR}$ to improve the activity toward 3-hydroxyoctanoyl-CoA (3HO-CoA). There was a technical barrier to examine the 3HO-incorporating ability of $PhaC_{AR}$ and its variants as mentioned below. In addition, optimization of the monomer composition of the medium used for mutant screening was needed. The goal of this chapter therefore is to develop a new screening system and to improve the enzyme activity toward 3HO-CoA.

The mutant screening system was designed by modifying the previous method, in which random mutagenesis of $PhaC_{AR}$ and screening were conducted.[1] The $PhaC_{AR}$ mutant NDFH was selected as a parent enzyme of mutagenesis, because the mutant showed high enzyme activity toward 3HHx-CoA. This mutant efficiently synthesized LA-based copolymers P(3HB-*co*-LA) and P(3HHx-*co*-LA).

Since the polymer accumulation level and the fluorescence intensity of colonies are correlated, colonies with a greater PHA accumulation will be selected based on the

intensity of fluorescence. To meet this goal, adjustment of fluorescence intensity in the screening system is important. For screening using Nile red agar plate, it is necessary to detect a small difference in fluorescence intensity between colonies. Figure 4-1shows an example of the correlation between fluorescence intensity and PHA accumulation. Figure 4-1 (A) shows low fluorescence intensity of colonies with no PHA accumulation. In contrast, Figure 4-1 (C) shows colonies with high PHA accumulation that exhibited very high fluorescence intensity. Because the intensity is saturated, it is hard to detect the difference between colonies. However, under the conditions of a moderated fluorescence intensity [Figure 4-1 (B)] (Figure 4-1(B)), it is relatively easy to compare the fluorescent intensities among colonies and to select beneficial candidates. To optimize the sensitivity of the screening, proper substrate concentration, cultivation time, and colony density should be selected.

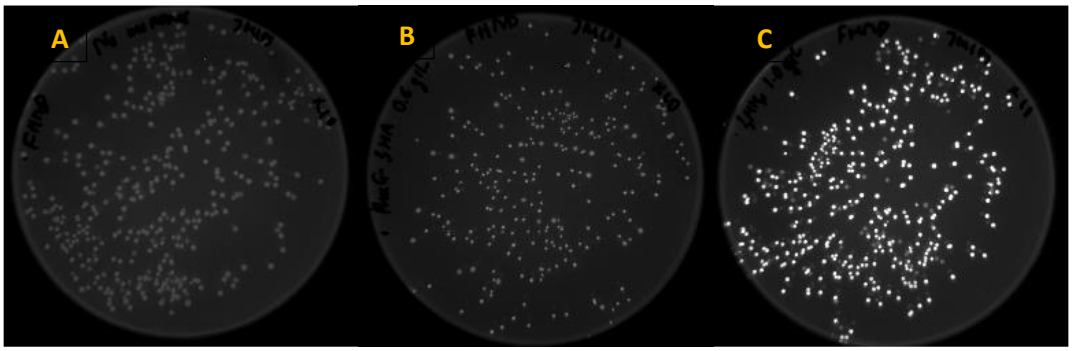

Figure 4-1. The fluorescence intensity correlated with the PHA accumulation

Besides, in this screening system, it is impossible to detect the monomer composition of polymer synthesized on the agar plates. Therefore, the monomer composition of the polymer synthesized using the selected candidates was determined using GC analysis of the cells obtained by the liquid culture.

Another problem of the screening was the supply of C8 monomer substrate. 3HO can be purchased from chemical companies but it is very expensive to use in the screening

experiments. Alternatively, I used an MCL 3-hydroxyalkaoic acid (3HA) mixture including 3HO (C8) prepared using PhaG (3-hydroxyacyl-ACP: CoA transferase)-expressing *E. coli*. Figure 4-2 shows the metabolic pathway of 3HA (C_6, C_8, C_{10}, and C_{12}) biosynthesis using PhaG.[2] The 3HAs synthesized by PhaG from *de novo* fatty acid biosynthesis pathway are secreted into the medium, and thus, can be recovered via extraction using organic solvent.

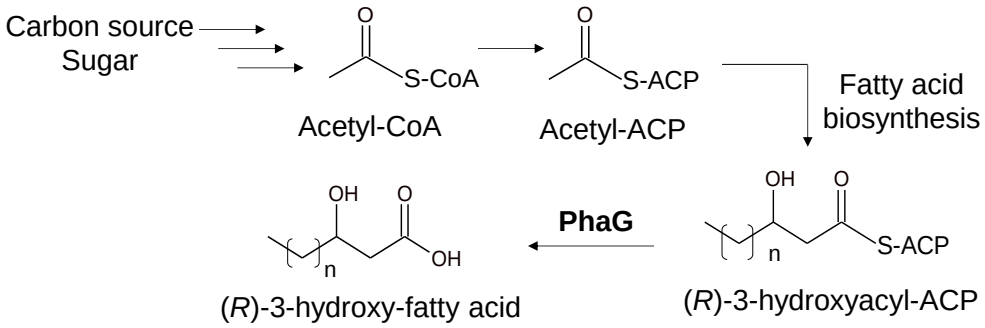

Figure 4-2. PhaG-mediated metabolic pathway of PHA MCL synthesis from acetyl-CoA 3HA-fatty acid

In this chapter, the screening system was built up. I determined the appropriate concentration of substrates and cultivation time effective to observe a difference in fluorescence. For selecting substrates, I prepared two trial assays, one in which only 3HA-CoA is supplied and the other in which 3HA-Na and 3HHx-Na are co-supplied into the medium All the trials were conducted on a liquid medium through enzyme expression of *E. coli* and the results were analyzed by GC.

4.2. Materials and Methods

4.2.1. Bacteria and plasmids

E. coli JM109 was selected as a host strain used. This strain has a high transformation efficiency and is able to stably maintain introduced plasmids. Thus, it is

commonly used in genetic recombination experiments. The plasmids are listed in Table 4-1.

Table 4-1. Plasmids used in Chapter 4.

Abbreviation	Gene	Description	Purpose
C_{AR}	Original PhaC_{AR}, pct, alkK	pBSPrePhaC_{AR}(opt)pctalkK	Negative control
NDFH	NDFH Mutant, pct, alkK	pBSPrePhaC_{AR}(opt)NDFHpctalkK	Starting plasmid for screening (parent)
STQK	PhaC1STQK, alkK	pBSSTQKalkK	Positive control

4.2.2. Preparation of 3HA-monomer substrate using from PhaG

pBSPhaG was used forthe biosynthesis of a mixture of 3HAs. *E. coli* JM109 was transformed with this plasmid, and a single colony was used for seed culture. The medium for the main culture was composed of 10 g/L Bactotryptone, 5 g/L Bacto yeast extract, and 10 g/L NaCl (LB medium), 100 μg/mL ampicillin, and 20 g/L fructose. 1 mM IPTG was added into the culture at 6 h after inoculation and the culture was further cultivated 48 h. Then the supernatant was collected by centrifugation (5000 rpm, 10 min, 4 °C) for 3HA extraction. HCl solution was added to the supernatant to acidify it to pH 5-6. 3HAs were recovered via dual-phase extraction using ethyl acetate. The organic phase containing 3HAs was then collected and dried by passing through a column filled with Na_2SO_4. The composition of 3HAs was analyzed by GC. Then, ethyl acetate was removed by evaporation. The obtained oil containing 3HAs was dissolved in Dimethyl sulfoxide (DMSO). The pH was adjusted to approximately 7 by adding NaOH solution. The pH was measured using a test paper. Sodium 3HHx and sodium 3HB are prepared as the similar manner as described in chapter 2 and chapter 3.

4.2.3. Random mutagenesis by error-prone PCR

As for the parent enzyme NDFH, this is derived from the original $PhaC_{AR}$ including two mutations N149D (ND) and F314H (FH) in the N- and C-terminal regions of $PhaC_{AR}$, respectively. Both mutants exhibited increased polymerization activity toward 3HHx-CoA, and the activity of FH mutant is higher than ND. $PhaC_{AR}$ NDFH mutant was selected as a parent (starting plasmid) for directed evolution by random mutagenesis followed by the Nile Red agar plate screening. The C-terminal region of NDFH mutant was randomly mutated. The C-terminal region contains a catalytic triad (cysteine, aspartic acid, histidine), which is known as an essential region in $PhaC_{AR}$.[3]

Two restriction sites were used to construct the mutant library. Two restriction enzymes, *Bgl* II and *Mun* I, cleaved the C-terminal region out as shown Figure 4-3. The length of this plasmid is 8879 bp. The total length of the gene region of $PhaC_{AR}$ is 1758 bp and the coded protein is composed of 586 amino acids. Error prone PCR amplifies a length of 1032 bp corresponding to the target mutagenesis region as shown in Figure 4-3. The primers designed for error-prone PCR are follows; Primer *Bgl* II-F: [5'-TGACACGCGGCAAGATCTCGCAG-3'] and Primer *Mun* I-R: [5'-TACCATGATGTTCAATTGCGCCT -3']. The PCR production was digested with *Bgl*II and *Mun*I and inserted into the corresponding position of $pBSPrePhaC_{AR}$NDFHpctalkK to yield the mutant library. Table 4-2 shows the error-prone PCR condition.

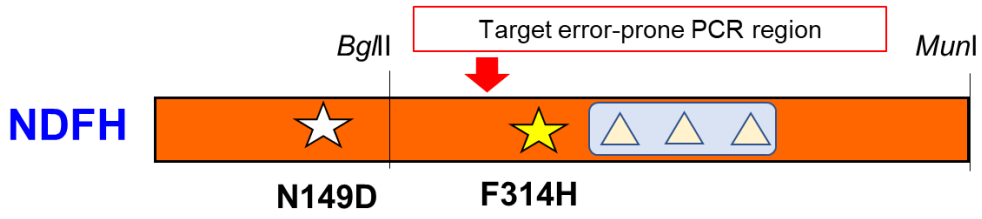

Figure 4-3. Random mutagenesis region in primary structure of NDFH

Table 4-2. Error-prone PCR condition

50 µL reaction	Concentration	Thermal cycle
DNA	50 ng/50 µL	
10 x PCR buffer	5 µL	
25mM $MgCl_2$	3 µL	94 °C: 2 mins
dNTPs	5 µL	(98 °C: 10 sec; 68 °C: 1 min) × 30 cycles
Primer *Bgl* II-F	1 µL	
Primer *Mun* I- R	1 µL	10 °C: ∞
Distilled water	up to 50 µL	
Freezed-dried in 2 hours		
rTaq	0.5 µL	
D_2O	up to 50 µL	

4.2.4. Selection of substrate

For selecting the screening condition

LB medium with 15 g/L agar, 20 g/L glucose, 100 µg/mL ampicillin, 0.5% Nile Red was used to make agar plate. The sodium 3HA was supplied into the medium with the concentrations range of 0.3 – 0.6 g/L. For main screening, the same condition supplemented with 0.6 g/L sodium 3HA was used.

4.2.5. Ligation condition

Inserts and vectors digested using restriction enzymes were combined in a 1:2 molar ratio to form 7.5 μL, then 7.5 μL of ligation high ver. 2 (TOYOBO) was added. The mixture was incubated at 16 °C for 30 min.

4.2.6. Polymer production

Plasmids extracted from the selected candidates were introduced into *E. coli* JM109, and single colonies were used for the pre-culture using a liquid medium (1.5 ml LB medium with ampicillin, 12 hours). The pre-cultured media were inoculated into the 1.5 mL LB media containing 20 g/L glucose, 0.6 g/L sodium PhaG-3HA, 0.3 g/L of sodium 3HHx, and 100 μg/ml ampicillin in test tubes. The test tubes were incubated at 30 °C for approximately 65 hours. After that, cells were harvested by centrifugation (13000 rpm, 5 min, 4 °C) and subjected to GC analysis.

For polymer production P(3HB-*co*-3HA), 1.5 mL LB media containing 20 g/L glucose, 100 μg/ml, 0.6 g/L 3HA-Na and 0.1 g/L 3HB-Na were cultivated at 30 °C for 48 hours. Cells were harvested and the monomer composition was determined by GC.

4.2.7. GC analysis

Polymer production was quantified by gas chromatography as well as the previous Chapters.

4.3. Results and discussions

4.3.1. PhaG-3HA composition

Based on GC analysis, the 3HA mixture collected from the culture medium in which *E. coli* expressing PhaG was cultured contained C6-C12 3HAs. This mixture was referred as PhaG-3HA in the Chapter 4. PhaG-3HA contained 30 wt% of C8 (3HO).

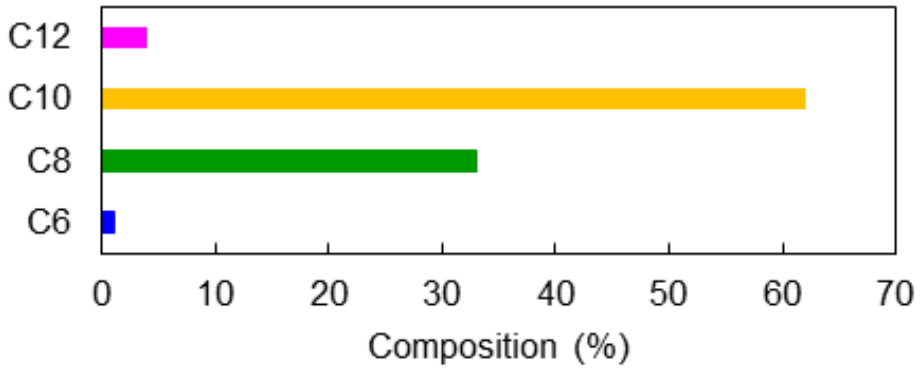

Figure 4-3. The composition of 3HA mixture prepared using PhaG-expressing *E. coli*

4.3.2. Selection of substrates in screening system

The first trial on production of 3HO-based polymers provided the basic for designing substrate concentration in screening assay. When using 3HO as precursorfor the screening system, it is necessary to consider toxicity effect of fatty acid mixture on bacterial growth. As a result, the medium with supplementation of 1.0 g/L 3HO-Na (for homopolymer production) and mixture of 3HO-Na 1.0 g/L and 3HHx-Na 1.0 g/L (for copolymer production) were selected. The results are shown in Table 4.3. $PhaC_{AR}$ mutantshave the potential ability to incorporate 3HO units in copolymer P(3HO-*co*-3HHx) but did not synthesize homopolymer P(3HO).

Table 4-3. Production of 3HO-based polymers

	PhaC$_{AR}$ mutants	**CDW (g/L)**	**Polymer content (mg/L)**	**Monomer composition (mol%)**	
				3HHx	3HO
3HO 1.0 g/L	Parent	2.9 ± 0.1	nd	nd	-
	F314H	2.9 ± 0.1	nd	nd	-
	F314L	2.9 ± 0.1	nd	nd	-
	F314Q	2.9 ± 0.3	nd	nd	-
	F314V	2.7 ± 0.1	nd	nd	-
3HO 1.0 g/L	Parent	1.8 ± 0.1	nd	nd	nd
3HHx 1.0 g/L	F314H	2.3 ± 0.1	151.8 ± 21.2	97.1 ± 0.4	2.9 ± 0.4
	F314L	1.9 ± 0.1	123.5 ± 7.1	93.5 ± 0.2	6.5 ± 0.2
	F314Q	2.3 ± 0.2	168.1 ± 58.5	93.7 ± 2.8	6.2 ± 2.8
	F314V	1.9 ± 0.1	72.6 ± 15.3	91.2 ± 0.5	8.8 ± 0.5

nd: not detectable

Referring to the results from Table 4-3, I prepared two conditions: one in which only 3HA-Na to select a reasonable concentration for cell growth, and another in which both 3HA-Na and 3HHx-Na are added to see the PHA accumulation.

Firstly, the concentration of single 3HA-Nashould be considered so that bacteria can grow on the solid medium because the toxicity of 3HAs to the cell growth is obvious. In the first trial, from the data of Table 4.3, when the culture medium contains1.0 g/L 3HO-Na, a cell can grow but no polymer was obtained in the cell. From this result, I

predicted that the conditions with a lower concentration of 3HO-Na can improve the PHA accumulation. The next trial therefore is conducted using a mixture of substrate PhaG-3HA. Since it is very difficult to purify 3HO from the 3HA mixture, PhaG-3HA, it is necessary to adjust the concentration of this mixture so that the cell can grow to a certain extent The examined range was 0.4 g/L, 0.5 g/L, and 0.6 g/L and the three plasmids shown in Table 4-1 were used.

The comparison of fluorescence intensity between colony density and cultivation time among plasmids would lead a reasonable concentration of 3HA-Na The results are shown below.

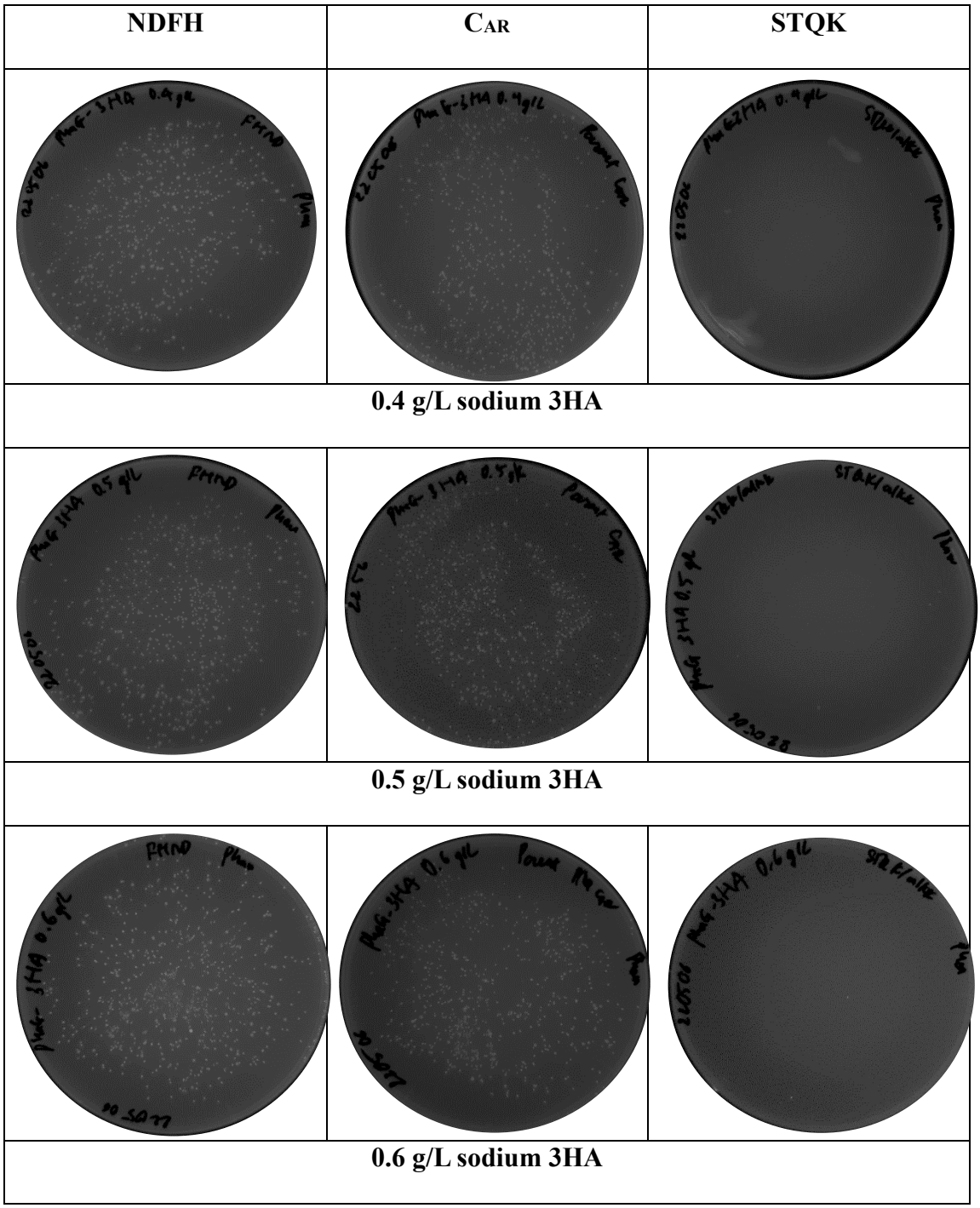

Figure 4-4. Nile Red agar plates containing 0.6 g/L sodium PhaG-3HA and 0.3 g/L sodium 3HHx at **28 h**

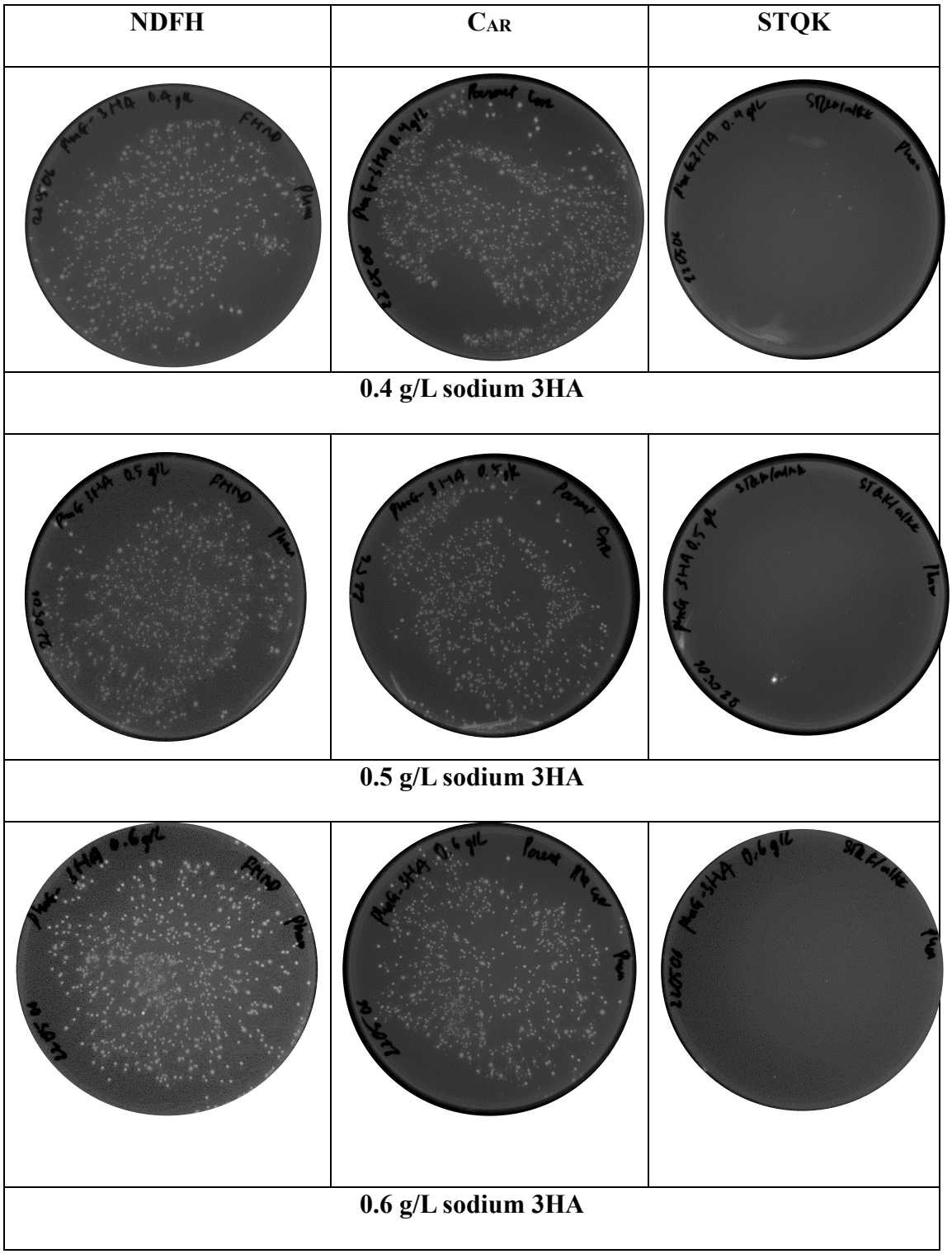

Figure 4-5. Nile Red agar plates containing 0.6 g/L sodium PhaG-3HA and 0.3 g/L sodium 3HHx at **65 h**

There is not too much difference in the sample at 28h. However, after 65 hours of cultivation, the fluorescence intensity at the plates shows a clear difference between

NDFH and parent $PhaC_{AR}$. I expected that the concentration of 3HA should be less than 1.0 g/L but not too low because the less 3HA sodium concentration becomes, the less 3HO (C8) concentration becomes.

From these results, 0.6 g/L 3HA-Na 0.6 has been selected for further experiments. Although the concentration of substrate has been determined, using a single substrate in the screening system is not the aim of this experiment. Based on the result of Table 4.3, it was found that 3HHx is essential for 3HO incorporation by $PhaC_{AR}$ mutant as a monomer component. For this reason, 3HHx-Na and PhaG-3HA-Na (0.6 g/L as a targeted concentration) should be co-supplemented into the screening medium.

I noticed that the parent NDFH preferred 3HHx-CoA as indicated in Chapter 3. However, the 3HHx-Na concentration should not be over 1.0 g/L, because if too much 3HHx is added into LB Nile Red medium agar, the cells did not grow. In addition, the 3HHx concentration should not be higher than that of 3HA-Na, because the abundance of 3HHx may direct the screening toward greater 3HHx-incorporating activity rather than that of 3HO. In addition, fluorescence intensity should be slightly higher than that the fluorescence intensity of the colony containing no mutation to avoid saturation of the staining. Given these factors, to determine a good composition, Nile Red- LB medium with various sodium 3HHx concentrations (0.1 g/L, 0.2 g/L, and 0.3 g/L) was prepared. *E. coli* expressing randomly mutagenized NDFH was cultivated in the medium and the difference in fluorescence intensity was examined.

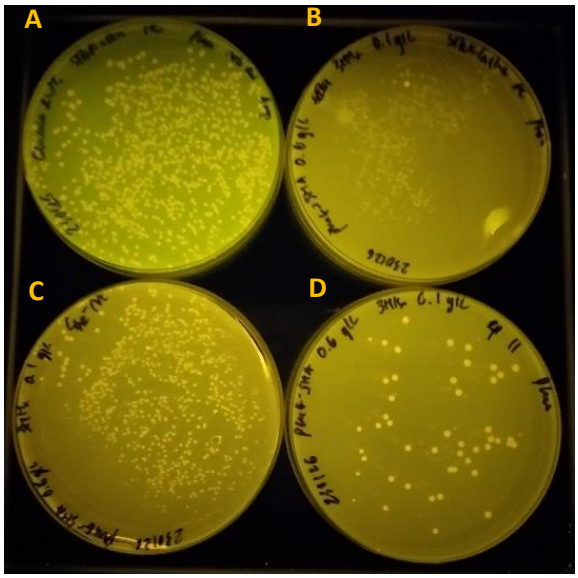 Colony density observed at plate **D**	**65 hours cultivation** **A**: Nile Red LB/amp agar plate contained only glucose 2wt% The rest of plates are Nile Red LB/amp agar plate contained PhaG-3HA-Na: 0.6 g/L, **3HHx-Na: 0.1 g/L** **B**: STQK/AlkK **C**: Original $PhaC_{AR}$ **D**: error prone mutant NDFH
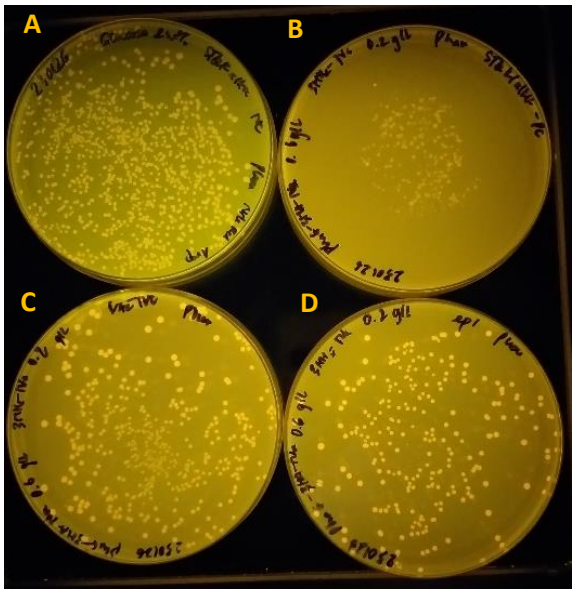 Sufficient colony density at plate **D**	**65 hours cultivation** **A**: Nile Red LB/amp agar plate contained only glucose 2wt% The rest of plates are Nile Red LB/amp agar plate contained PhaG-3HA-Na: 0.6 g/L, **3HHx-Na: 0.2 g/L** **B**: STQK/AlkK **C**: Original $PhaC_{AR}$ **D**: error prone mutant NDFH

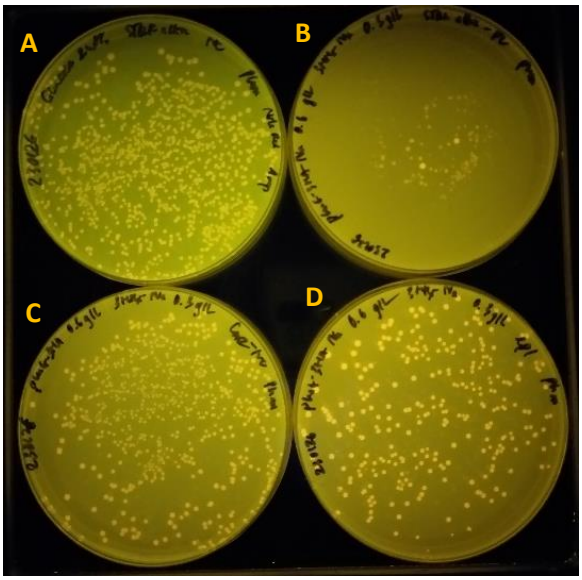 Sufficient colony density and high fluorescence intensity at plate **D**	**65 hours cultivation** **A**: Nile Red LB/amp agar plate contained only glucose 2wt% The rest of plates are Nile Red LB/amp agar plate contained PhaG-3HA-Na: 0.6 g/L, **3HHx-Na: 0.3 g/L** **B**: STQK/AlkK **C**: Original $PhaC_{AR}$ **D**: error prone mutant NDFH

Based on these results, monomer composition of Nile Red LB/amp medium have been selected in screening system are 0.3 g/L 3HHx-Na and 0.6 g/L 3HA-Na.

Figure 4-4. Plate culture of the cells transformed with plasmids containing the error-prone PCR fragments. The plate medium consists of Nile Red, LB, amp, 0.6 g/L 3HA-Na, and 0.3 g/L 3HHx.

4.3.3. Acquisition of beneficial mutants by screening

The introduction of mutations on $PhaC_{Re}$ region of $PhaC_{AR}$ were followed by the colony screening. The cells were cultivated on LB/agar plates with ampicillin, glucose as a substrate, 3HA-Na and 3HHx-Na as precursors, and Nile red staining to show polymer formation inside the cells. ImageJ software was used to select colonies with the high fluorescence. The pixel intensity was assessed for this purpose.

Total 11 plates were utilized for the cells transformed with a plasmid carrying error insert (an amplified insert by error prone PCR), and around 5000 colonies were screened., Figure 4-4 is an example. Five colonies with higher fluorescence were selected from these plates for plasmid extraction and polymer synthesis at 30 °C for 65 hours. The cells were harvested from the culture, lyophilized, and concentrated. The polymer content of the dry cells was determined using GC. Cells carrying the initial plasmid, as well as a plasmid with an error insert were cultured and analyzed.

(A)

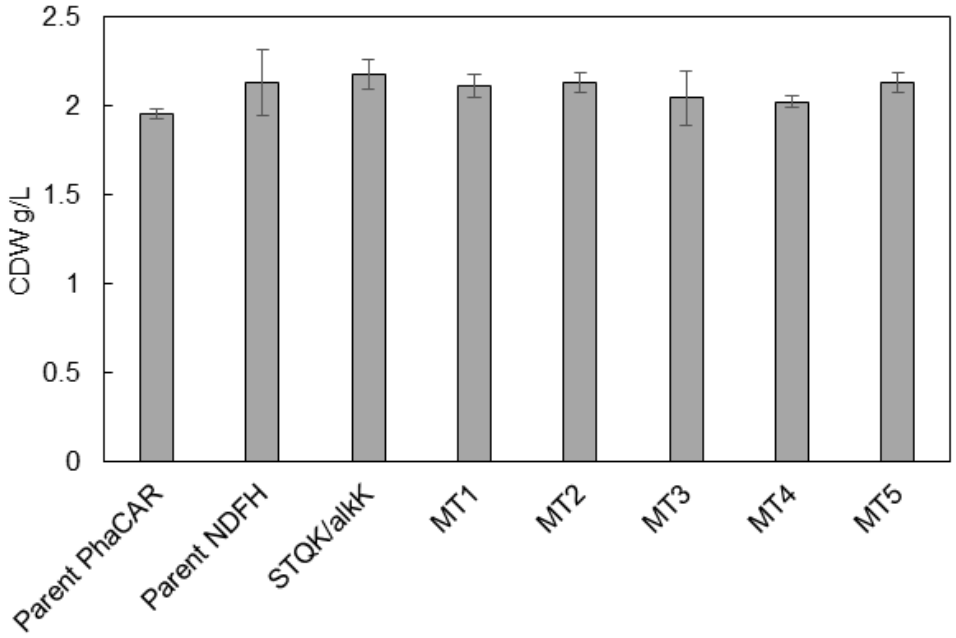

(B)

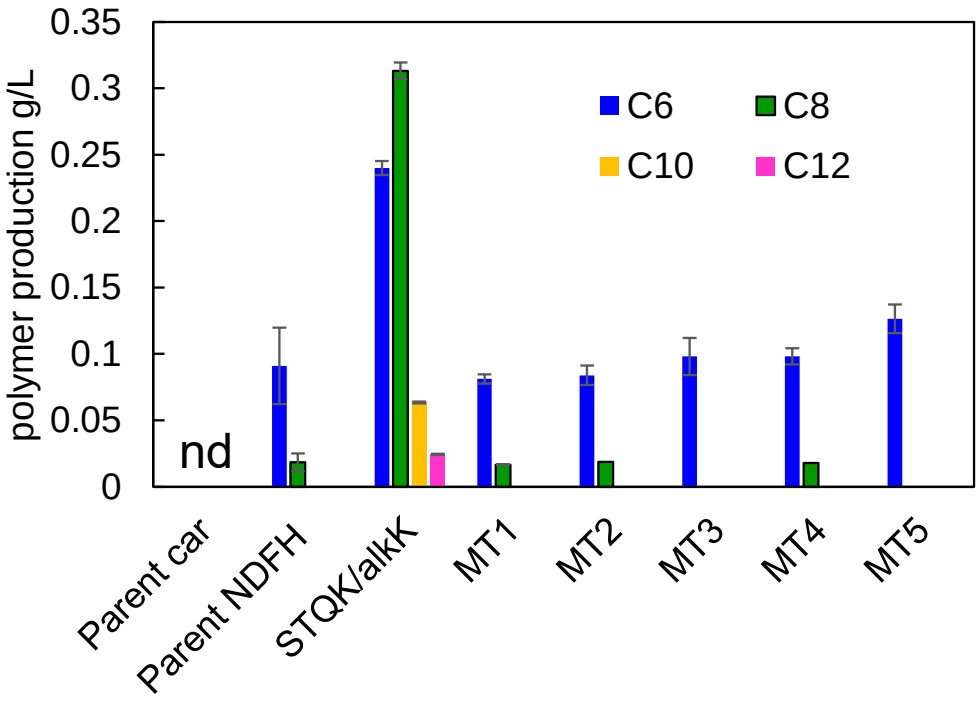

Figure 4-6. (A) Polymer production of selected candidates in liquid culture. The x-axis displays samples used, including original $PhaC_{AR}$ (negative control), parent NDFH, STQK/AlkK (positive control), and five mutants (MT1, MT2, MT3, MT4, MT5) obtained

from the screening stage. Data on polymer production and cell-dried weight are displayed on the Y-axis. Data are presented as mean ± standard deviation of the biological triplicate, nd: not detectable.

Since all the *E. coli* in the cell dried weight figure has grown successfully on the 3HA-Na, it is possible to collect a significant amount of biomass. The distribution of the polymer components is shown in Figure 4-6. As a result, all the mutants exhibited an increase in the accumulation of 3HHx unit However, no increase in the 3HO fraction in polymer was found.

4.3.4. Trial on polymerization of 3HB and 3HA

Based on the initial result at 4.3.3 part, no positive mutant with increased activity toward 3HO-CoA was found. Next strategy is to co-supply 3HB-Na, natural substrate for PHA biosynthesis, with 3HA-Na. This strategy has been expected to improve 3HO incorporation into copolymer. Figure 4-7shows the preliminary results of copolymer containing both 3HB and 3HO units. As a result, 3HO-containing copolymer was produced by all the PhaCs, including the PhaC1STQK/alkK, original $PhaC_{AR}$, and its mutants. The presence of 3HB units may facilitate the incorporate of 3HO units. These findings are consistent with the previous study. [4, 5] The mechanism that 3HB facilitates the incorporation of 3HO is unclear. By co-feeding 3HB monomer and PhaG-3HA into screening system might facilitate screening efficiency

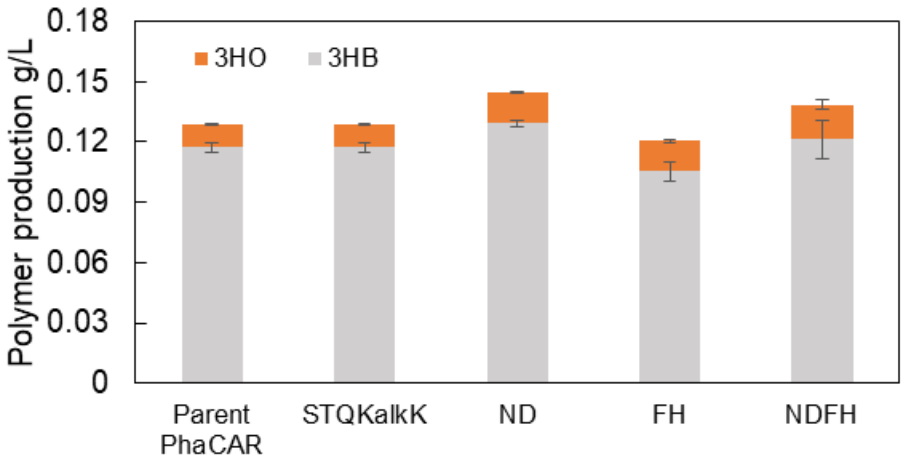

Figure 4-7. Polymer production of P(3HB-*co*-3HA) using parent $PhaC_{AR}$, STQK/alkK, mutants (ND, FH, and NDFH). Data are presented as mean ± standard deviation of the biological triplicate.

4.4. Conclusions

Using random mutagenesis by error-prone PCR technique, I attempted to isolate new beneficial mutants of $PhaC_{AR}$ that exhibit higher activity toward 3HO-CoA. The essential conditions of the screening system on agar plates containing fluorescent dye were established for the directed evolution of $PhaC_{AR}$. Initial attempts at random mutagenesis and screening assays revealed several potential candidates for advantageous mutations. Even though the mutants only showed increased incorporation of 3HHx, the screening system can be a foundation to broad the specific activity of $PhaC_{AR}$ and to produce novel types of MCL-SCL block copolymers.

4.5. References

(1) Taguchi, S.; Doi, Y. Evolution of polyhydroxyalkanoate (PHA) production system by "enzyme evolution": successful case studies of directed evolution. *Macromol Biosci* **2004**, *4* (3), 146-156. DOI: 10.1002/mabi.200300111.

(2) Wang, Q.; Tappel, R. C.; Zhu, C.; Nomura, C. T. Development of a new strategy for production of medium-chain-length polyhydroxyalkanoates by recombinant *Escherichia coli* via inexpensive non-fatty acid feedstocks. *Appl Environ Microbiol* **2012**, *78* (2), 519-527. DOI: 10.1128/aem.07020-11 From NLM.

(3) Jia, Y.; Yuan, W.; Wodzinska, J.; Park, C.; Sinskey, A. J.; Stubbe, J. Mechanistic Studies on Class I Polyhydroxybutyrate (PHB) Synthase from *Ralstonia eutropha*: Class I and III Synthases Share a Similar Catalytic Mechanism. *Biochemistry* **2001**, *40* (4), 1011-1019. DOI: 10.1021/bi002219w.

(4) Taguchi, S.; Matsusaki, H.; Matsumoto, K. i.; Takase, K.; Taguchi, K.; Doi, Y. Biosynthesis of biodegradable polyesters from renewable carbon sources by recombinant bacteria. *Polymer International* **2002**, *51* (10), 899-906. DOI: 10.1002/pi.878.

(5) Matsumoto, K.; Nakae, S.; Taguchi, K.; Matsusaki, H.; Seki, M.; Doi, Y. Biosynthesis of poly(3-hydroxybutyrate-co-3-hydroxyalkanoates) copolymer from sugars by recombinant *Ralstonia eutropha* harboring the phaC1Ps and the phaGPs genes of *Pseudomonas* sp. 61-3. *Biomacromolecules* **2001**, *2* (3), 934-939. DOI: 10.1021/bm0155367.

Chapter 5.

Conclusions

In this study, I performed engineering of a sequence-regulating PHA synthase $PhaC_{AR}$ for expanding the structural diversity of PHA and its block copolymers.

I created a set of mutants by saturation mutagenesis at the 314th position of $PhaC_{AR}$ and the FH mutant was chosen as a beneficial mutant that exhibited enhanced enzyme activity toward 3HHx-CoA. Interestingly, this mutant acquired an ability to synthesize homopolymers P(3HHx) and P(2HB). The greater molecular weight of these homopolymers produced by the class I $PhaC_{AR}$ mutant ($M_w \sim 10^6$) over the previously described class II enzyme PhaC1STQK ($M_w \sim 10^5$) has been an advantage. The spontaneous sequence-regulation ability of $PhaC_{AR}$ to synthesize block copolymer without performing any additional manipulation during cultivation of *E. coli* was maintained by this mutation. By utilizing the function, I presented for the first time a new type of block copolymer P(3HHx)-b-P(2HB), which is composed of MCL segments P(3HHx) and SCL segment P(2HB).

The PDLA-based block copolymers produced by microbial system were achieved using combinational effect of beneficial mutations. In particular, a pairwise mutant NDFH containing N149D and F314H mutations as found to synthesize P(3HHx)-*b*-51 mol% PDLA containing PDLA homopolymer segment. The molecular weight of these block copolymers was10^5 order of magnitude. This was considerable breakthrough given that molecular weight of PDLA homopolymer synthesized by PhaC1STQK has been limited to 10^3 order of magnitude. The mechanism of block copolymer synthesis has remained unelucidated.

I constructed a screening system for directed evolution and it was applied to $PhaC_{AR}$ to acquire activity 3HO-CoA. I optimized two factors, polymer accumulation level and the fluorescence intensity of colonies which influenced the isolation efficiency

of beneficial candidates. This was the first attempt to evolve class I PhaC using only MCL substrates.

Overall, I achieved biosynthesis of novel PHAs, MCL-SCL block copolymers, high-molecular-weight MCL PHA, PDLA-containing polymers, by engineering the polymerizing enzyme $PhaC_{AR}$. Based on these findings, I have greatly expanded the scope of molecular design of PHAs and their block polymers.

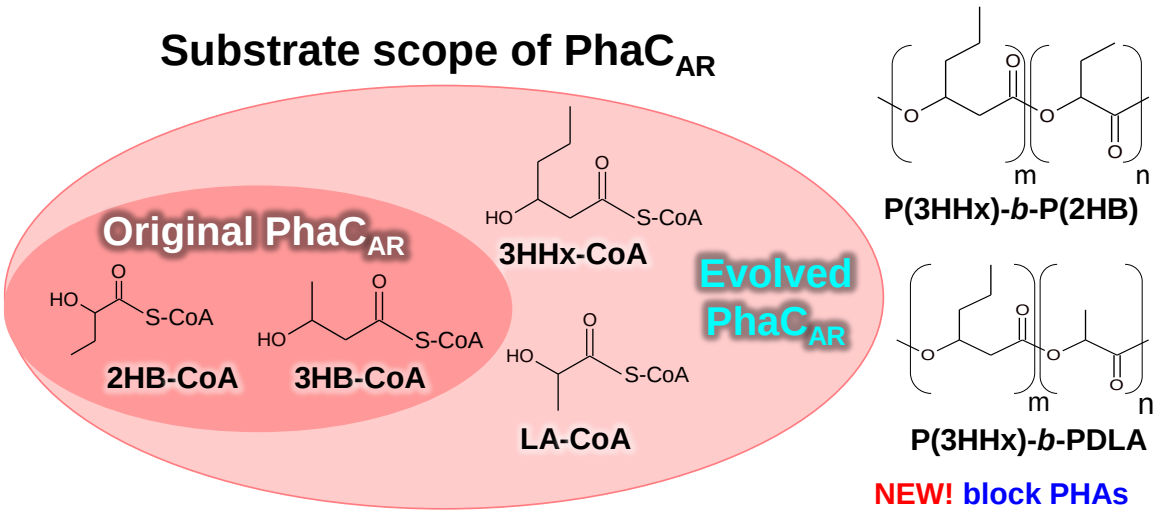

Acknowledgements

I would like to express my deepest gratitude to the following persons who supported and guided me throughout my PhD journey, which has started as the same time as the onset of Covid-19 pandemic. Their assistances play significant roles to the successful completion of this work.

First and foremost, I would like to thank my supervisor, Prof. Ken'ichiro Matsumoto, for his insightful direction, thoughtful recommendations, valuable suggestions, and consistent support all along this research.

Prof. Hiroya Tomita for the guidance, helpful advice, and encouragement through this study. Also, Prof. Hiroshi Kikukawa, Prof. Shin-ichi Hachisuka, for their great comments that improved the dissertation.

The thesis referees at Hokkaido University, Prof. Toshifumi Satoh, Prof. Tohru Dairi, and Prof. Kazuki Sada, for their providing excellent feedbacks and suggestions for enhancing the dissertation.

Ms. Yumi Hosoe and Ms. Rikako Satoh for all the support and teachings in the laboratory which helped me a lot at the beginning of the Ph.D. course. And all my lab mates, especially Ms. Ami Iguchi Ami, Mr. Kengo Yanagawa, and Mr. Wataru Fuji for their friendship, assistance with technology, and enjoyable times.

The great financial assistance of the Japanese Ministry of Education, Culture, Sports, and Technology (MEXT) made it possible to complete the work for this PhD thesis.

Lastly, I would like to thank my family for their understanding and support. Especially, my partner and my daughter for giving me love and encouragements throughout this journey.